

Max-Planck-Institut für Kolloid- und Grenzflächenforschung

---

# **Towards Understanding RAFT Aqueous Heterophase Polymerization**

## **Dissertation**

zur Erlangung des akademischen Grades  
"doctor rerum naturalium"  
(Dr. rer. nat.)  
in der Wissenschaftsdisziplin Kolloidchemie

eingereicht an der  
Mathematisch-Naturwissenschaftlichen Fakultät  
der Universität Potsdam

von  
**Samira Nozari**

Potsdam, im Mai 2005

## Table of contents

<b>1. Introduction</b> .....	<b>3</b>
<b>2. Theory and Background</b> .....	<b>7</b>
2.1. Free radical polymerization .....	7
2.2. Controlled radical polymerization (CRP) .....	10
2.2.1. Stable free radical polymerization (SFRP) .....	12
2.2.2. Atom transfer radical polymerization (ATRP).....	13
2.2.3. Degenerative transfer (DT) .....	14
2.2.4. Reversible addition-fragmentation transfer (RAFT).....	15
2.3. RAFT: the mechanism.....	16
2.4 Aqueous heterophase polymerization .....	24
2.4.1. General description.....	24
2.4.2. Compartmentalization .....	26
2.4.3. Swelling .....	27
2.4.4. Solubility .....	28
2.5. RAFT in aqueous heterophase polymerization .....	29
<b>3. Methods of Characterization</b> .....	<b>31</b>
3.1. Reaction calorimetry.....	31
3.2. Gel permeation chromatography (GPC).....	35
3.3. Dynamic light scattering .....	38
3.4. Ultraviolet/Visible (UV-Vis) spectroscopy .....	41
<b>4. Results and Discussion</b> .....	<b>44</b>
4.1. The Initiators, the RAFT agents, and homogeneous polymerizations .....	46
4.1.1. The initiators .....	46
4.1.2. The RAFT agents.....	48
4.2. RAFT ab-initio emulsion polymerization of styrene .....	51
4.2.1. Rate of polymerization .....	52
4.2.2. AIBN: polymerization rate, colloidal and molecular properties .....	58
4.2.3. The molecular properties obtained with the other initiators.....	62
4.2.4. Coagulum formation and colloidal stability.....	66
4.2.5. Particle size in RAFT ab-initio emulsion polymerization.....	69

---

4.2.6. Number of polymer chains .....	71
4.3. Phase transfer of RAFT agents in heterophase polymerization .....	73
4.3.1. The experimental setup and procedure .....	74
4.3.2. Polymerization of swollen seed particles .....	78
4.3.3. Radical entry into latex particles .....	81
4.3.4. Transport of different RAFT agents.....	82
4.3.5. Carrier for the transport.....	83
4.3.6. An approach for preparation of composite particles.....	85
4.4. Heterophase polymerization of styrene with RAFT at room temperature .	87
4.4.1. The influence of the initiator concentration .....	87
4.4.2. Time-dependent characteristics at room temperature.....	88
4.4.3. The influence of temperature .....	90
<b>5. Conclusion and Outlook .....</b>	<b>93</b>
<b>Appendix .....</b>	<b>I</b>
Appendix I: Categorized Library of Results .....	I
Appendix II: Experimental Section .....	IX
Appendix III: References .....	XVII
Appendix IV: Symbols and Abbreviations.....	XXIV
<b>Acknowledgements .....</b>	<b>XXIX</b>

“It may be that the old astrologers had the truth exactly reversed, when they believed that the stars controlled the destinies of men. The time may come when men control the destinies of stars.”

Arthur C. Clarke

*First on the Moon, 1970*

## 1. Introduction

Human beings either due to their nature or their need to survive have always struggled to take control of events taking place in their surroundings. This endeavor has played an important role in all aspects of human way of life, such as the formation of borders, the structure of societies, and the improvement of the standard of living. Even today, from making every effort to be able to control the amount of milk that a farm cow produces to seeking control over the resources of another country, controlling is everywhere and is done by almost everyone. We, human beings, want everything to function the way that we desire; the plants and animals reproduce the way that we wish; the machines and devices operate the way that we want them; and the materials exhibit the properties that we fancy. Nowadays, the level of seeking control in science is both vast and small. Vast in the sense that it covers all aspects of life and small in the scale of control sought. The new plants and animals have modified genes, the new devices are molecular motors, and the new materials are, for instance, nanotubes, and nanoparticles. These days, scientists are engaged in controlled crystallization, assembly, polymerization, and try to put together atoms, molecules, and particles in a controlled manner to build up complicated structures that exhibit unique and novel properties.

The increasing control that chemists are able to exert over molecular architecture allows for the design and preparation of macromolecular and polymeric systems of unprecedented sophistication. Macromolecules<sup>1</sup> -large molecules consisting of

several repeating units- have a great potential to exhibit new properties when different combinations, numbers and orders of units are employed in their structure. However, the polymerization methods that allow for such a level of structural control are limited not only in numbers but also in the required reaction conditions. For example, anionic polymerization, the method that provides the highest level of control, usually requires reaction temperatures below  $-50^{\circ}\text{C}$  and the absolute elimination of oxygen and water. On the other hand, the most common method of polymerization -also for commercial production of polymers- has been free radical polymerization<sup>2</sup> (FRP) because of its simplicity and tolerance towards all kinds of impurities and auxiliary materials, such as stabilizers, trace amounts of oxygen, and water. Moreover, the range of the monomers that can be polymerized by radical means, the molar mass of the generated polymers, and the range of the reaction temperature are considerably larger than those in other techniques. Therefore, many different processes such as bulk, solution, and emulsion polymerization can be applied for FRP.

However, the limitation of this method is the lack of control over the reactivity of the radicals, which causes the lack of control over the molar mass, molar mass distribution, end-functionalities, and molecular architecture. Taming free radicals is an issue since the early days of radical polymerization. The recent emergence of many so called “living” or “controlled” radical polymerization (CRP) processes has opened a new area in this “old polymerization” method that had witnessed relatively small progress in the years before. Nowadays, various CRP techniques provide simple and robust routes toward the synthesis of well-defined, low-polydispersity polymers, and the fabrication of novel functional materials. Despite the advanced developments of these methods in homogeneous systems, their progress in polymerizations under heterophase conditions has encountered severe difficulties.

The heterophase polymerization, especially in aqueous media, offers invaluable practical advantages over homogeneous polymerizations, such as the absence

of volatile organic compounds, the better control of heat transfer, and the possibility to attain high molar mass polymers with high conversion and a faster rate of polymerization than in homogeneous systems. The product of aqueous heterophase polymerization is environmentally friendly, easy to handle due to its low viscosity, and in many cases, such as coating applications, is almost ready to use. Heterophase polymerization is among the fastest, cheapest, and easiest methods for preparation of colloidal polymeric particles in any scale.

The main reason that the application of CRP methods in heterophase systems is very challenging, is the existence of multiple phases. In a multiphase system, unlike the homogeneous ones, the exact concentration of the reactants at the polymerization loci is unknown and strongly depends on the solubility of the reaction components in each of the phases. This dependency leads to complicated reaction kinetics and needs more care in the selection of the reaction components.

Among several methods of controlled radical polymerization, the most commonly used are “stable free radical polymerization” (SFRP)<sup>3-5</sup>, “atom transfer radical polymerization” (ATRP)<sup>6-8</sup>, and “reversible addition-fragmentation transfer” (RAFT)<sup>9-12</sup> polymerization. The latter is the youngest, the most versatile, the easiest to apply, and the least understood of all the mentioned methods. In addition, when it comes to application of CRP in heterophase system, due to its mechanistic feature, RAFT is the only one that can result in higher molar mass and polymerization rates in comparison with homogeneous systems. Therefore for the investigation of controlled radical polymerization under heterophase condition, the RAFT method was chosen for this thesis.

The aim of this work is to examine the influence of hydrophobicity and hydrophilicity of the reaction components on the polymerization kinetics and the molecular and colloidal properties of the polymer product in controlled radical heterophase polymerization of styrene via RAFT. Styrene is chosen as the

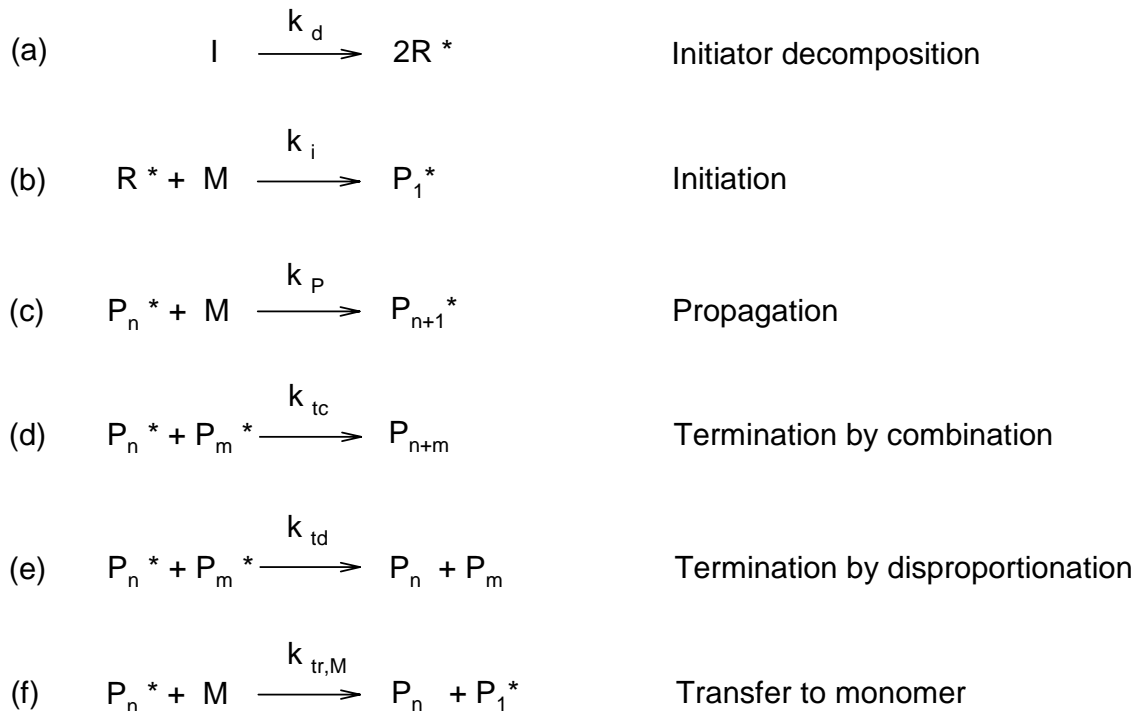
monomer of the polymerization because it is a kind of standard monomer for polymerization and it undergoes less side reactions in aqueous environment than esters.

In the 2nd chapter, the theory and background of FRP, CRP, RAFT in particular, aqueous heterophase polymerization, and the application of RAFT polymerization in aqueous heterophase system are briefly introduced. Chapter 3 provides the theoretical aspects of applied methods of characterization in this work. The experimental results summarized in chapter 4 consist of three parts. The first and main part is dedicated to studying the influence of different types of initiators and RAFT agents with different hydrophobicity under typical aqueous heterophase polymerization conditions in comparison with homogeneous systems. The second part discusses the development of a new and easy method for quantitative assessment of the kinetics of diffusion and transportation of the reaction components under heterophase conditions. The mechanistic information that can be revealed by applying the RAFT technique to aqueous heterophase polymerization at room temperature is elucidated in the third part.

## 2. Theory and Background

### 2.1. Free radical polymerization<sup>13-15</sup>

Free radical polymerization is a chain growth polymerization with a free radical - an unpaired electron at the last carbon atom of the growing chain- as the propagating site. Several kinetic steps are involved in a free radical polymerization: initiation, propagation, termination and transfer reactions (Scheme 1).



**Scheme 1. Free radical polymerization**

The initiation process involves two reactions: the generation of primary radicals by homolytic scission of an initiator when heated, irradiated, or by any other means; and the reaction of the primary radical with a monomer molecule to form a growing radical (Scheme 1 (a) and (b), respectively). The decomposition of the



initiator is the rate determining step since it is slower than the initiation process. Therefore, the rate of initiation ( $R_i$ ) is given as:

**Equation 1** 
$$R_i = 2 f k_d [I]$$

where  $f$  is the factor for initiator efficiency,  $k_d$  is the decomposition rate coefficient, and  $[I]$  is the initiator concentration.

Propagation is the consecutive addition of monomer molecules to the radical site at the end of the chain (Scheme 1(c)). This process repeats very rapidly several times before it terminates. The rate of polymerization or propagation ( $R_p$ ) is depending on concentration of the growing radicals ( $[P^*]$ ) and the monomer ( $[M]$ ) and, it is given as:

**Equation 2** 
$$R_p = k_p [P^*] [M]$$

$k_p$  is the propagation rate coefficient.

Termination of growing chains generally takes place through bimolecular reactions between the active radical centers: by recombination, where a homopolar bond is formed by pairing the single electrons of the free radical sites of the two chains (Scheme 1(d)); or by disproportionation, where a hydrogen atom is transferred from one growing chain to the other (Scheme 1(e)). Therefore, the rate of termination ( $R_t$ ) is usually of second order with respect to the radical concentration as given here:

**Equation 3** 
$$R_t = k_t [P^*]^2$$

$k_t$  is the termination rate coefficient. Thus, a change in radical concentration affects the rate of termination more than the rate of polymerization.

Transfer reactions can take place between a growing radical and a molecule of solvent, initiator, monomer, transfer agent, or even the polymer. In a transfer reaction, the active site at the end of the growing chain is removed but another radical arises from the second molecule. A schematic example for transfer to monomer is given in Scheme 1(f). Consequently, the rate of transfer to monomer ( $R_{tr,M}$ ) would be:

**Equation 4** 
$$R_{tr,M} = k_{tr,M} [P^*] [M]$$

Where  $k_{tr,M}$  is the rate constant of transfer to monomer.

In free radical polymerization the lifetime of the polymer radical is typically in the order of 1-10 seconds, during which initiation, propagation, and termination take place, yielding in a “dead” chain with no end functionality. Such dead chains are formed at every instant and accumulated throughout the course of polymerization that may last several hours in many cases. Thereby, high molar mass polymer chains are expected from early stages of the polymerization. In the absence of transfer reactions the average degree of polymerization is the same as the kinetic chain length. The kinetic chain length ( $\nu$ ) is a measure of the average number of monomer units reacting with an active centre during its lifetime as is described by:

**Equation 5** 
$$\nu = R_p / R_t = k_p^2 [M]^2 / 2 k_t R_p$$

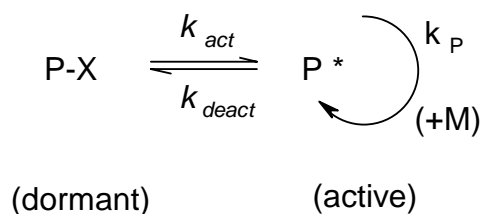
Despite the versatility of the FRP, the extremely high reactivity of the radicals results in a lack of control on the polymerization and characteristics of the polymer product. The molar mass is difficult to predefine as is determined by the complicated combination of many parameters such as polymerization temperature, monomer, solvent, viscosity, radical source, etc. The molar mass distribution is generally broad and can only be influenced to some extent by the use of chain transfer agents and variations in the initiator concentration.

Macroscopic properties of the polymer product which depend on the molecular properties of the polymer can only partly be controlled. FRP as the oldest polymerization technique was already used to prepare block copolymers since 1939<sup>16</sup>; however, there is no direct access to well-defined and more complex architectures such as star-like polymers.

## 2.2. Controlled radical polymerization (CRP)<sup>17</sup>

Different criteria are defined for a polymerization to be characterized as living or controlled. Perhaps the most reasonable definition is given by Fischer<sup>18</sup>. Accordingly, the polymers are called “living” when they preserve their end functionality and they continue to grow by further addition of monomer. The polymerization is “controlled” when with increasing monomer conversion, the number average molar mass ( $M_n$ ) increases linearly and the polydispersity index (PDI) decreases gradually and approaches ~1 at high conversions. Control and livingness are different properties and achieving only one is not necessarily an indication for the presence of the other. From an industrial point of view, livingness is more important of control.

To be able to control the characteristics of the polymer in terms of molar mass, molar mass distribution, architecture, and function, the overall growth time of a polymer molecule must be as long as the overall polymerization time, subdivided to several steps, interrupted by deactivated states. To prevent the irreversible termination of propagating radicals in conventional free radical polymerization, the termination reactions must be suppressed and an effective activation-deactivation cycle has to be established (Scheme 2).



**Scheme 2. Reversible activation (general scheme)**

The dormant (end-capped) chain (P-X) is supposed to be activated to a growing radical (P<sup>\*</sup>) by thermal, photochemical, and/or chemical stimuli. In the presence of monomer (M), P<sup>\*</sup> will undergo propagation until it is deactivated back to P-X. In practically important systems, it usually holds that  $[P^*]/[P-X] < 10^{-5}$ , meaning that a living chain spends most of its polymerization time in the dormant state.

If a living chain experiences the activation-deactivation cycles frequently enough over the whole period of polymerization, all living chains will have a nearly equal chance to grow, yielding a low-polydispersity product. This frequency depends on the concentration of all the species present in the polymerization medium, and on the chemical structure of the dormant chain and the type of stimuli applied to the system. However, CRP is distinguished from termination-free polymerizations like anionic living polymerization by the existence of bimolecular termination, chain transfer, and all other elementary reactions involved in conventional FRP.

The transient lifetime of P<sup>\*</sup>, namely the time interval between an activation and the subsequent deactivation on the same chain, is typically in the range of 0.1-10 ms. The sum of the transient lifetimes of a chain over the whole polymerization period is related to the number average degree of polymerization ( $DP_n$ ) finally achieved. If the radical lifetime in the conventional system is 1s, for example, the sum of transient lifetimes in the corresponding LRP system should be set to be sufficiently smaller than 1s. Otherwise, a large portion of chains in the CRP system will be dead at the end of the run. In other words, if  $DP_n$  of the product from the conventional run is  $10^4$ , that from the CRP run should be sufficiently smaller than  $10^4$ . If the  $DP_n$  of the CRP product is  $10^3$  or  $10^2$ , we may expect that,

respectively, about 10% or 1% of the chains to be dead. A high fraction of living chains is an obvious requisite for preparing polymers with sophisticated structures.

The rate constants of activation  $k_{act}$  and deactivation  $k_{deact}$  given in the general scheme (Scheme 2) are both defined as a pseudo-first-order constant in the unit of  $s^{-1}$ . Every dormant chain is activated once every  $k_{act}^{-1}s$  and deactivated back to the dormant state after a transient lifetime of  $k_{deact}^{-1}s$ , on average. In typical successful CRP,  $k_{act}^{-1} = 10-10^3$  s and  $k_{deact}^{-1} = 0.1-1$  ms. The stationariness (steadiness) of polymerization requires the following equilibrium to hold:

**Equation 6** 
$$k_{act}[P-X] = k_{deact}[P^*]$$

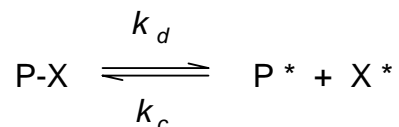
This is a quasi-equilibrium that will actually hold when the rates of activation and deactivation are much larger than those of termination and (conventional) initiation reactions. In a successful CRP this condition is met.

The reversible activation reactions in the most successful CRPs currently known may mechanistically be classified into two types: “reversible termination”, and “reversible transfer” mechanisms. The most common reversible termination mechanisms are stable free radical polymerization (SFRP) and atom transfer radical polymerization (ATRP). The most known reversible transfer polymerization mechanisms are degenerative transfer (DT) and reversible addition-fragmentation chain transfer (RAFT).

### 2.2.1. Stable free radical polymerization (SFRP)

The SFRP follows a dissociation-combination mechanism (Scheme 3), where P-X is thermally or photochemically dissociated into  $P^*$  and  $X^*$ . The stable (persistent) radical is assumed to be stable enough to undergo no reaction other than the combination with  $P^*$  (and other alkyl radicals, if present). Namely,

“ideal” stable free radicals (SFR) do not react between themselves, do not initiate polymerization, and do not undergo disproportionation with  $P^*$ .



**Scheme 3. Dissociation-Combination mechanism**

The rate constants of dissociation  $k_d$  and combination  $k_c$  are related to  $k_{act}$  and  $k_{deact}$  by:

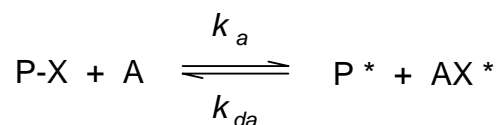
**Equation 7**  $k_{act} = k_d$

**Equation 8**  $k_{deact} = k_c$

The best known examples of SFR are nitroxides such as 2,2,6,6-tetramethylpiperidiny-1-oxyl (TEMPO). This method is the most environmentally friendly regarding the nature of the SFR used. However, despite the recent developments, it is still limited to relatively high reaction temperatures and restricted to certain monomers.

### 2.2.2. Atom transfer radical polymerization (ATRP)

In this mechanism, P-X is activated by a redox reaction with A, and the capping agent is transferred to form a stable species  $AX^*$  (Scheme 4).



**Scheme 4. Atom transfer mechanism**

All currently known successful CRPs in this category use a halogen such as Cl or Br as capping agent X, and a halide complex of transition metal like Cu or Ru as activator A. The rate constants  $k_a$  and  $k_{da}$  defined in Scheme 4 are related to  $k_{act}$  and  $k_{deact}$  by:

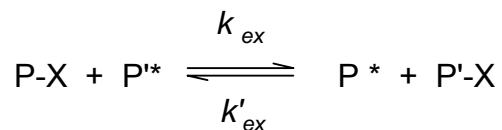
**Equation 9** 
$$k_{act} = k_a [A]$$

**Equation 10** 
$$k_{deact} = k_{da} [AX^*]$$

Compared to SFRP, the equilibrium constant of ATRP is larger by an order of magnitude which indicates a faster polymerization rate. The equilibrium constant is also more easily adjusted by choosing different capping agents and transition metals. The main limitation of this method is its sensitivity to trace amount of oxygen and the employment of relatively high amount of transition metal complex that has to be removed from the final polymer.

### 2.2.3. Degenerative transfer (DT)

In this mechanism, P-X is attacked by the propagating radical P<sup>\*</sup> to form the active species P<sup>\*</sup> and the dormant species P'-X (Scheme 5).



**Scheme 5. Degenerative transfer mechanism**

This is an exchange reaction that takes place directly without forming any kinetically important intermediate. X is an atom or simple molecule. A typical example is the iodide-mediated polymerization, where X is iodine. If the radicals P<sup>\*</sup> and P'<sup>\*</sup> are kinetically identical, follows  $k_{ex} = k'_{ex}$ .and:

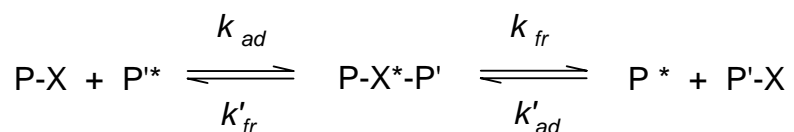
**Equation 11**  $k_{act} = k_{ex} [P^*]$

**Equation 12**  $k_{deact} = k_{ex} [P-X]$

The common degenerative transfer agents have very low transfer rate coefficient to the radicals and are, therefore, of limited applicability.

#### 2.2.4. Reversible addition-fragmentation transfer (RAFT)

In RAFT, the transfer agent X is a group with a double bond that is accessible to the addition of P\*. The exchange reaction occurs via the addition of P\* to P-X, to form the intermediate radical P-X\*-P' followed by fragmentation of P-X\*-P' into P\* and P'-X (Scheme 6).



**Scheme 6. Reversible addition-fragmentation mechanism**

The probability for the equilibrium to proceed forward ( $P_{fr}$ ), which means the successful exchange of X between the dormant chain and the growing radical, is:

**Equation 13**  $P_{fr} = \frac{k_{fr}}{k_{fr} + k'_{fr}}$

Therefore the activation rate constant is:

**Equation 14**  $k_{act} = \frac{k_{fr}}{k_{fr} + k'_{fr}} k_{ad} [P^*]$



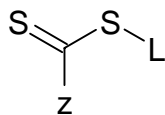
If P and P'\* are identical:

**Equation 15** 
$$k_{act} = \frac{1}{2} k_{ad} [P'^*]$$

RAFT is considered to be the most versatile CRP method regarding the vast range of temperatures, monomer types, and reaction conditions that can be applied. Basically, RAFT agents can just be added to conventional free radical polymerization recipe without changing the reaction conditions. The high tolerance of RAFT polymerization to the presence of impurities, oxygen and water makes it an ideal CRP method to be applied in emulsion polymerization. However, this method also has its own drawbacks, which will be discussed later. Since RAFT is the method of choice in this thesis for investigation of aqueous heterophase system, the following section is dedicated to a more in-depth description of this method and its features and peculiarities.

### 2.3. RAFT: the mechanism

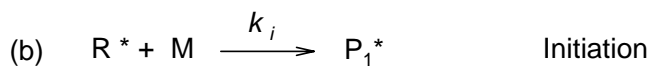
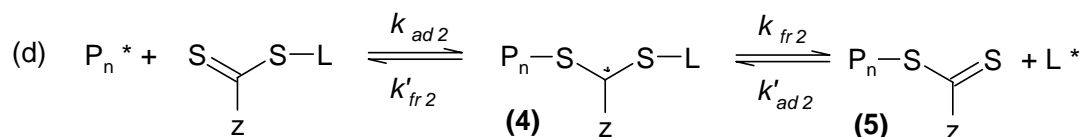
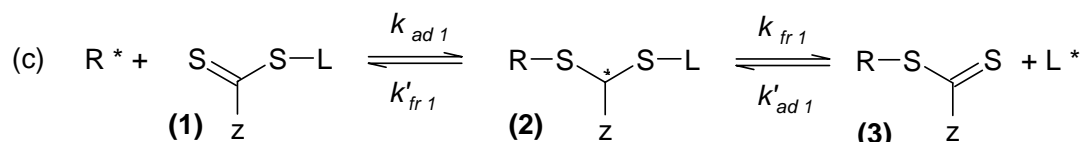
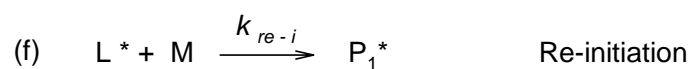
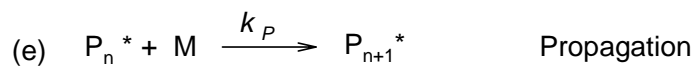
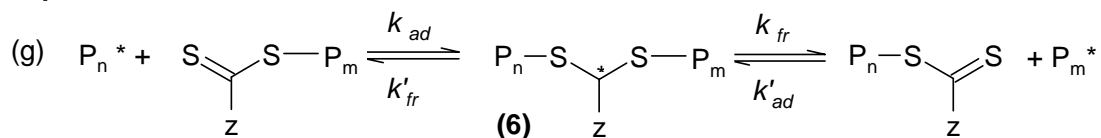
The first species used as RAFT agents were methacrylate macromonomers<sup>19,20</sup>. However, due to their low reactivity, the polymerization had to be carried out under certain conditions (i.e. starved condition with respect to the monomer) in order to exhibit living characteristics<sup>21</sup>. This characteristic disappears when methacrylate is replaced by other monomers such as styrene or acrylates. Therefore, more reactive transfer agents were required to make this process applicable to batch reactions and other monomers. It was found out that dithioesters<sup>9,10</sup>, trithiocarbonates<sup>11,22</sup>, some dithiocarbamates<sup>11,12</sup>, and xanthates<sup>11</sup> are suitable compounds for this purpose. In 1998, a patent by Le et al.<sup>9</sup> described the application of these RAFT agents in both homogeneous and heterogeneous systems for various monomers. Scheme 7 shows the general structure of the RAFT agents.

**Scheme 7**

Numerous RAFT agents are available by varying the structure of the substituents Z and L. The rate of polymerization as well as the polydispersity and molecular weight control obtained under a particular set of reaction conditions depend on the nature of Z and L<sup>10,12,22-34</sup>. The role of Z (the activating group) and L (the leaving group) is discussed together with the mechanism of RAFT polymerization. The mechanism of polymerization in the presence of RAFT agents can be summarized in five main steps (Scheme 8):

- I. Initiation: production of primary radicals during the whole course of polymerization
- II. Pre-equilibrium: addition or transfer of all the RAFT agents to the primary or oligo-radical and liberation of the leaving group from the RAFT agent
- III. Re-initiation by the leaving group
- IV. Main equilibrium and propagation: the dormant chains through the exchange of the dithioester moieties with growing radicals periodically become active and propagate
- V. Termination: this is not eliminated completely in any CRP method.

The necessity for existence of an external source of primary radicals in the RAFT method is one of the major differences of this process compared with reversible termination methods. The activation process needs the existence of free radicals; otherwise, the polymerization will eventually die before reaching full conversion. In this sense, the RAFT polymerization can be considered a kind of telomerization<sup>35</sup> that results in higher molar mass and higher capability for chain extension.

**Initiation****Pre-equilibrium****Propagation and Re-initiation****Equilibrium****Termination****Scheme 8. Schematic presentation of RAFT polymerization**

On the other hand, the introduction of primary radicals throughout the polymerization itself contributes to termination, which reduces the livingness, and contributes to formation of new chains, which increases the polydispersity index (PDI). Therefore, employment of an optimum amount of initiator in RAFT polymerization is very important.

The addition of RAFT agent to the primary or growing radicals (Scheme 8 (c) and (d)) must take place very quickly before the radicals have a chance to propagate too long or to terminate. Therefore, the addition rate constant of the RAFT agent to the primary radicals ( $k_{ad1}$ ) and growing radicals ( $k_{ad2}$ ) must be significantly larger than the propagation rate constant ( $k_p$ ). The addition rate constant strongly depends on the structure of the RAFT agent and especially of the activating group Z. The Z group must activate the C=S double bond toward radical addition. The intermediate species **(2)** and **(4)** must also fragment very quickly in order not to slow down the polymerization rate. The driving force for the pre-equilibrium step to proceed forward is the stability of the departing radical ( $L^*$ ,  $R^*$ , or  $P_n^*$ ) and the strength of the S-C bonds in both **(1)** and **(3)** or **(1)** and **(5)**. Hence, the right choice of the L group is crucial in this regard. The more stable, more electrophilic, more bulky L groups leave the molecules more easily. At the same time, the leaving group must be capable of initiating new chains as well; and a too stable L group will not be capable of doing so. Since every consumed RAFT agent molecule adds one initiating radical to the polymerization system, the total concentration of polymer chains depends on the concentration of the RAFT agent (below).

**Equation 16**                       $[all\ chains] = [RAFTagent] + 2 \cdot f \cdot k_d \cdot [I]$

Consequently, the molecular weight (MW) of the polymer also depends on the concentration of the RAFT agent (Equation 17).

$$\text{Equation 17} \quad MW_{\text{theoretical}} = \frac{[M] \cdot MW_{\text{monomer}}}{[RAFTagent] + 2 \cdot f \cdot k_d \cdot [I] \cdot t} \cdot \%conv + MW_{RAFTagent}$$

The second term in the denominator corresponds to the concentration of primary radicals produced by decomposition of the conventional initiator up to the considered time (t). This amount is usually much smaller than the concentration of the RAFT agent and is often neglected.

After successful consumption of the initial RAFT agents, the main equilibrium will be established during which the dithioester moieties are exchanged between the active and dormant chains. In this way, through the rest of the polymerization period, all the chains have a chance of going through a cycle of activation and deactivation and therefore, all grow at the same time. Here again the Z group plays an important role because it influences the rate of addition of the free growing radicals to the Macro-RAFT agents (dormant chains).

As in any FRP, termination takes place during the whole course of RAFT polymerization. However, it is relatively suppressed because the probability that two radicals meet each other is much lower than in case of similar FRP in the absence of the RAFT agent. Nevertheless, an additional termination reaction is stated to exist particularly in RAFT polymerization. It is claimed that the intermediate radicals ((2), (4), and (6)) undergo reversible or irreversible terminations with other radical species in the reaction system. However, the existence of such reactions is still a matter of extensive discussion<sup>36-40</sup>.

The two stages of pre-equilibrium and main equilibrium are apparent in Figure 1 which summarizes the change in the concentration of various species during a simulated bulk polymerization in the presence of a RAFT agent. This figure shows the full consumption of the RAFT agent and formation of the dormant chains during the pre-equilibrium.

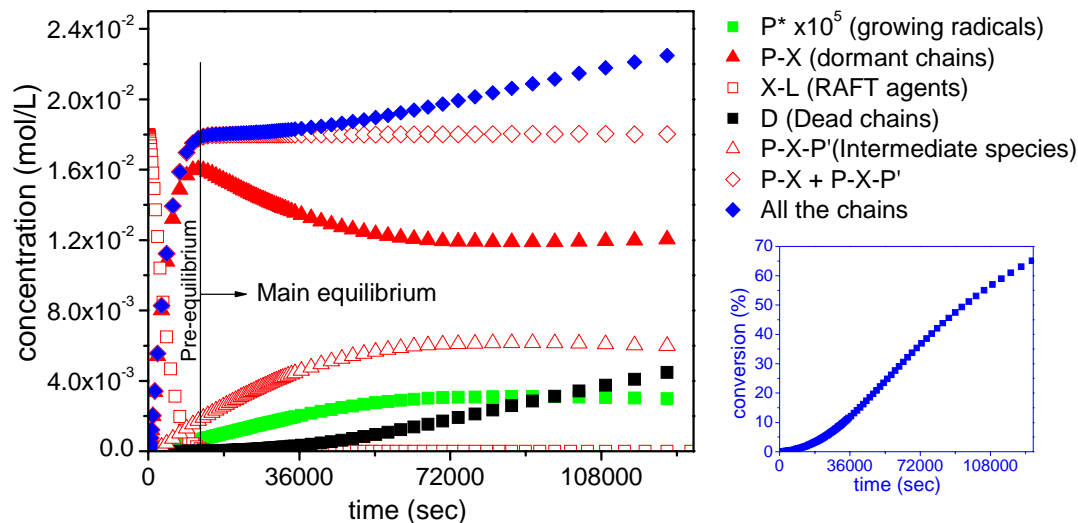


**Figure 1. Concentration change during the bulk polymerization of styrene (simulation results with PREDICI, rate constants from Vana et al<sup>41</sup>) at 60°C initiated with 0.015 mol/L AIBN**

After establishment of the main equilibrium, the total concentration of the intermediate species and dormant chains are constant and equal to the initial concentration of the RAFT agent. The small ratio of the growing chains comparing to the dormant ones is important to note. The total concentration of all the chains is slowly increasing with time due to an increase in the concentration of the dead chains. It is obvious that the dead chains are formed through out the polymerization. This can be contributed to the continual generation of primary radicals due to the initiator decomposition.

A better controlled and living radical polymerization must result in lower concentration of dead chains and smaller PDI values. In addition to right choice of controlling agent, the right ratios of the reactants (i.e initiator, monomer, and RAFT agent) are crucial. Especially in the RAFT process, the origin of control and livingness lies under probabilities. The probability that a growing radical reacts with a monomer, a dormant chain, a primary radical, or another growing radical, strongly depends on the concentration of these species in the reaction

medium during all the stages of the polymerization. For instance, the probability of a reaction between free radicals increases at later stages of the polymerization when the concentration of the monomer is considerably decreasing but the production of the primary radicals continues.

The graphs presented in Figure 2 demonstrate the result of changing the concentration of the RAFT agent on the rate of polymerization, molecular properties of the polymer, and the concentration of the other species. These graphs show that with increasing the RAFT agent concentration, the concentration of the dormant chains (P-X) increases and the concentration of the free radicals (i.e. growing radicals (P\*) and primary radicals (R\*)) and consequently dead chains (D) decreases.

The lower concentration of the free radicals results in lower rates of polymerization (Figure 2 (a)) and the higher concentration of all the polymer chains results in a smaller number average molecular weight ( $M_n$ ) (Figure 2 (e)).

The higher is the concentration of the RAFT agent, the more linear is the  $M_n$  vs. conversion curve, and the smaller is PDI (Figure 2(f)). The molar mass of the dead and dormant chains (Figure 2 (e)) is in the same range so close together that experimental clear separation via GPC is practically impossible. May be MALDI-TOF via end group analysis could allow the discrimination.

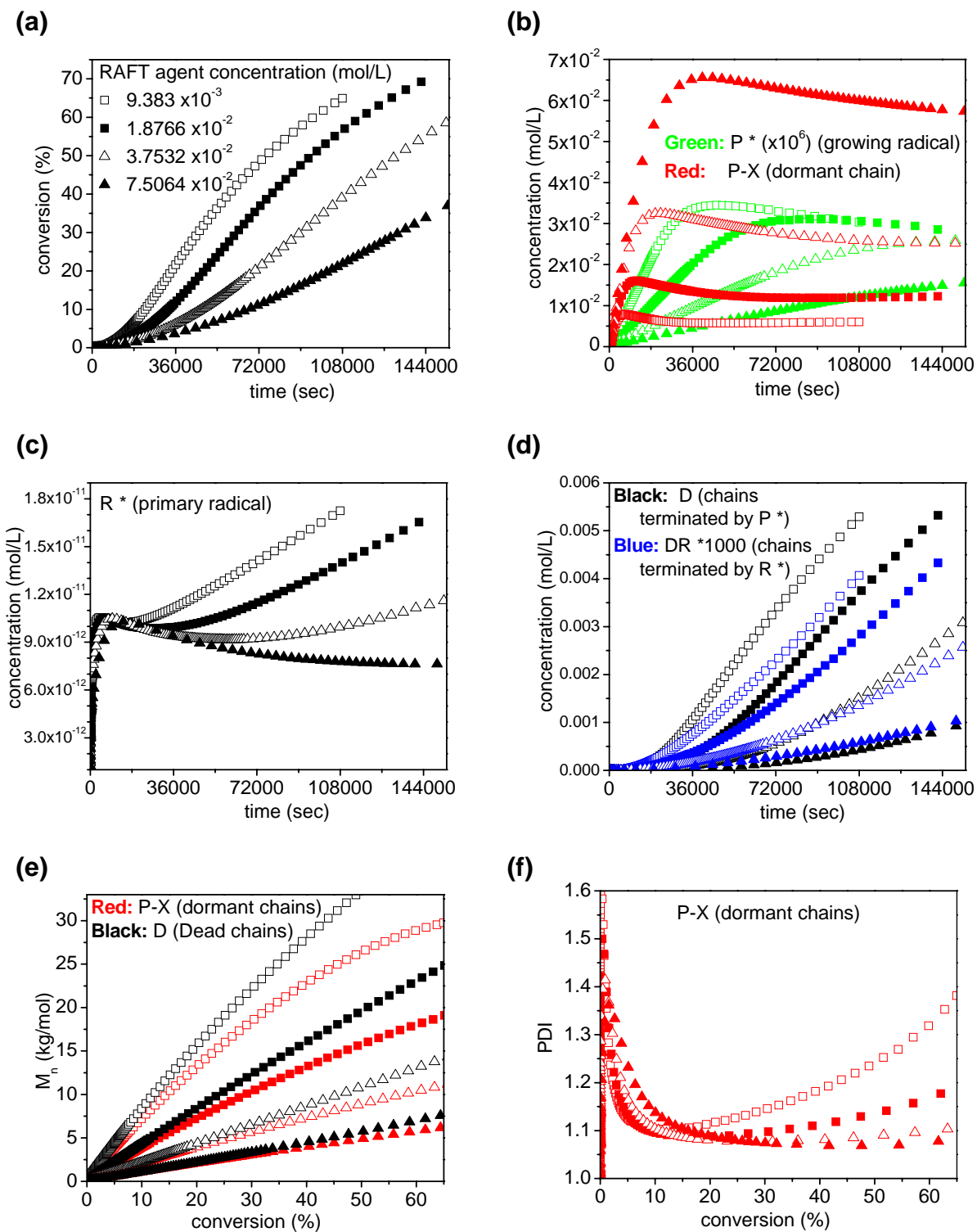


**Figure 2. Bulk polymerization of styrene (simulation results with PREDICI, rate constants from Vana et al<sup>41</sup>) at 60°C initiated with 0.015 mol/L AIBN in presence of various RAFT agent concentrations (The symbols in all graphs represent the same concentrations as in (a)) (a) conversion-time, concentrations of (b) dormant and growing radicals (c) primary radicals and (d) dead chains vs. time, (e)  $M_n$  and (f) PDI vs. conversion**



## 2.4 Aqueous heterophase polymerization<sup>42-45</sup>

### 2.4.1. General description

Aqueous heterophase polymerization is defined as polymerization resulting in the formation of polymer particles in an aqueous continuous phase. The particular term of “emulsion polymerization” is interchangeably used for such a process when the polymerization product is a dispersion of submicron size polymer particles or a so-called “polymer latex”. For an ordinary batch mode of ab-initio emulsion polymerization, a typical reaction mixture consists of one or more types of monomer, surfactant, water, and initiator that are stirred together and heated to the reaction temperature.

The monomer, the main component of the polymerization, usually has only a finite solubility in water and is capable of swelling its polymer. The initiator is generally water-soluble to avoid polymerization in the monomer phase. However, under certain conditions and for specific applications, it is possible to apply oil-soluble initiators as well. The surfactant (also referred to as stabilizer or emulsifier) is used to impart colloidal stability to the latex particles and can be of any kind i.e. ionic, nonionic, or polymeric.

At the beginning of the reaction, the monomer is present in several locations. (a) In the free monomer phase or the monomer reservoir that is usually broken into droplets and dispersed in the aqueous phase by the help of applied shear force. (b) In the aqueous phase, where the monomer is dissolved to its saturation limit. (c) In micelles, in case the concentration of surfactant is above its critical micelle concentration.

Upon the decomposition of the water-soluble initiator and formation of the primary radicals, the initiation will occur in the aqueous phase and the propagation begins. The mechanism for nucleation of polymer particles -like all other mechanisms involving nucleation- is not well understood. However, a

simplified scenario of formation of these particles is as follows. The growing radicals will propagate until they reach a critical chain length or concentration when they are not soluble in water anymore; hence, they aggregate into small primary polymer particles (homogeneous and aggregative nucleation mechanism<sup>46-51</sup>). Depending on the stabilizer concentration, these primary particles might coagulate into larger particles which continue to capture other freshly nucleated primary particles that are formed at later stages. By formation of the polymer particles, one more phase is added to the system and monomers have a new place to go. Of course, this is the case when the polymer swells in its own monomer. On the other hand, as a result of the capture of the aqueous phase radicals by the polymer particles, the main loci of polymerization from the aqueous phase switches to polymer particles. This period of time in which the polymer particles are formed is known as Interval I. During this period, the rate of polymerization increases due to the increase in the number of polymerization loci that are the polymer particles. This period ends when the number of polymer particles does not change anymore.

The next stage of polymerization is known as Interval II or particle growth. This period is characterized by a constant number of particles and the presence of the free monomer phase. The monomer phase continuously supplies the polymer particles with monomer until it is depleted completely.

By disappearance of the monomer phase from the system, the next polymerization stage, Interval III, starts. In this period the polymerization continues and the remaining monomer residue in the particles is consumed. As the monomer concentration in the particles gradually decreases, the polymerization rate decreases as well.

In order to avoid the complications of the nucleation and particle formation period and to control the characteristics of the polymer latex, a commonly used method is to start the polymerization with already prepared “seed” particles loaded with

the monomer. In this way, the polymerization begins from the interval II or III depending on the monomer load. Another method known as “mini-emulsion”<sup>52</sup>, similar to seeded emulsion polymerization, is based on starting the polymerization from stabilized monomer droplets.

### 2.4.2. Compartmentalization

A distinguishing feature of conventional emulsion polymerization is the compartmentalization of propagating radicals, which strongly affects both the reaction rate and molecular weight. When polymerizations are conducted in dispersed systems the propagating radicals are spatially isolated from each other, or compartmentalized inside the polymer particles. This compartmentalization requires the entry of radicals from the aqueous phase. As the particle size increases, the average number of radicals per particle increases as well. The smaller is the particle size, it is more likely that the entry of an aqueous phase radical into the particle with already one propagating radical inside, result in instantaneous termination. For many systems, each particle contains either none or one growing chain at any time. The overall effect of compartmentalization is an increase in reaction rate and a much higher mean molecular weight as compared to bulk polymerization because of the impact of reducing the effective termination rate. The polymerization rate is directly proportional to the average number of radicals per particle ( $\bar{n}$ ) and the number of particles ( $N_p$ ) (Equation 18).

**Equation 18**

$$R_p = k_p \cdot C_{M,P} \cdot \frac{\bar{n} \cdot N_p}{N_A}$$

The Equation 18 shows that the rate of polymerization also depends on the concentration of monomer in the particles ( $C_{M,P}$ ).  $C_{M,P}$  in turn, depends on the stage of the polymerization regarding monomer conversion (i.e. whether or not a free monomer phase exists), and on the capability of the particles to take up

monomer. The latter, i.e. the swelling of the polymer particles, is discussed in the following section.

### 2.4.3. Swelling

Swelling is of special practical importance because the colloidal particles consisting of both polymer and monomer are the main reaction loci<sup>53-55</sup>. Latex particles can only be swollen by monomer to a limited extent defining a characteristic monomer concentration in the particles ( $C_{M,P}$ ) even if the monomer is a solvent for the polymer. The explanation is that the decrease in Gibbs energy which results from mixing the polymer and the monomer is counterbalanced by the increase in Gibbs surface energy because of the increase of the surface area of the swollen particles. Morton et al. deduced a simple equation relating the equilibrium swelling only to the average particle size and the interfacial tension<sup>56</sup>.

**Equation 19**

$$-\frac{2 \cdot V_M \cdot \sigma}{r \cdot R \cdot T} = \ln(1 - \phi_P) + \left(\frac{1}{DP} - \phi_P\right) + \chi \cdot \phi_P^2$$

where ( $V_M$ ) is the molar volume of the monomer, ( $\sigma$ ) the interfacial energy between the swollen particles and the continuous phase, ( $R \cdot T$ ) the thermal energy, ( $r$ ) the radius of the swollen particles, ( $\phi_P$ ) the volume fraction of polymer in the swollen particle, ( $DP$ ) the degree of polymerization, and ( $\chi$ ) the Flory-Huggins polymer-solvent interaction parameter. The monomer concentration in the particles is related to  $\phi_P$  as:

**Equation 20**

$$C_{M,P} = \phi_M \cdot V_M = (1 - \phi_P) \cdot V_M$$

#### 2.4.4. Solubility

The kinetics of any polymerization depends on the concentration of the reactive species. In heterophase polymerization due to the heterogeneity of the system, the reactants distribute among all the phases. This phenomenon largely influences the kinetics of the polymerization. In heterophase polymerization, the solubility of each reactant in each of the phases is therefore, of extreme importance.

Solubility and partitioning of the reactants influences the concentration of the reactants at the loci of polymerization and makes the prediction of the reaction kinetics very challenging. Moreover, the solubility of the reactants influences the mechanism of heterophase polymerization such as nucleation, particle formation, swelling of the particles by their own monomers etc. For example, the solubility of the initiator influences both, the concentration of the primary radicals at the loci of the polymerization, and the solubility of the growing chains via the nature of the end groups. The solubility of the monomer in water influences the critical chain length, concentration, and supersaturation of the oligomeric chains before nucleation. The solvency of the monomer for its own polymer affects the swelling and consequently, the concentration of the monomer in the growing polymer particles. Even the solubility of water in the organic phase is very important. In some cases, as for styrene, the solubility of water in the monomer is higher than the other way around. This trend can assist hydrophilic radicals to enter the monomer phase together with water and start polymerization<sup>45</sup>. All in all, for the design of a heterophase polymerization reaction it is important not only to take into account the solubility and partitioning behavior of all the recipe components, but also the right combination of all of them.

## 2.5. RAFT in aqueous heterophase polymerization<sup>57,58</sup>

One of the motives for the application of CRP in heterophase system is to utilize the advantages of the compartmentalization of growing radicals in the reaction medium (i.e. higher rate and higher molar mass). The consequences of compartmentalization are more pronounced in reversible transfer methods such as RAFT than reversible termination methods due to their mechanistic differences. In RAFT polymerization the entry of free radicals into the polymer particles is an issue and therefore, there is more freedom to tailor the rate of polymerization. Moreover, the mild reaction conditions required for the RAFT polymerization makes it a suitable candidate for applying it to aqueous heterophase system. However, there are also disadvantages that accompany the application of this method to such a system.

The most important issue when applying RAFT to aqueous heterophase polymerization is the partitioning of the RAFT agent between the different phases. A too hydrophilic RAFT agent, especially with a high addition rate constant, would react too quickly with the aqueous phase radicals. Depending on the type of monomer, this might lead to formation of dormant low molecular aqueous phase species and retardation of the nucleation events, and consequently of the polymerization rate<sup>59</sup>. On the other hand, too hydrophobic RAFT agents can also be problematic. In ab-initio emulsion polymerization, if the RAFT agent is too hydrophobic it will be mainly present in the monomer phase. A successful CRP requires that the RAFT agent to transport to the polymer particles. This transportation not only depends on the solubility of the RAFT agent in both the aqueous phase and the monomer, but also on the factors that influence the swelling of the polymer particles by the monomer. Moreover, the transportation can be affected by other factors such as the partitioning of the initiator, and the rate of the addition of RAFT agent to the radicals. For example, in case of oil-soluble initiator, the polymerization starts in the monomer phase and the produced “oligo-RAFT” species would be even more hydrophobic than the initial

RAFT agent. Consequently, the diffusion to the polymer particles is more hindered. Also the swelling of the polymer particles with monomer is reduced as these RAFT-oligomers effectively withhold monomer in the bulk phase.

To avoid the complications for the transport of the RAFT agent to the loci of polymerization, the majority of the research on RAFT in aqueous heterophase system has been carried out in seeded emulsion<sup>60-63</sup> or miniemulsion<sup>64-74</sup> polymerization. Yet, many of these attempts also faced control or stability issues at first<sup>64,66</sup>. More stability and control was achieved by changing the normal conditions, for example, performing the miniemulsion polymerization in continuous stirred tank reactors<sup>68</sup>, applying different types or excess amounts of surfactant<sup>64,66,70</sup>, employing acetone as co-solvent for efficient loading of RAFT agent in the seeded emulsion<sup>61</sup> systems, or of course, employing RAFT agents with different reactivity and hydrophobicity<sup>65,67,69</sup>.

Studies on application of RAFT in ab-initio emulsion polymerization are rather limited. Le et al.<sup>9</sup> reported the first polymerization with RAFT in ab-initio emulsion and acknowledged the importance of an optimum hydrophobicity for the RAFT agent. After initial reports by Kanagasabapathy<sup>75</sup> and Uzulina<sup>59</sup> on slow polymerization rates and more than 40% coagulation, the following works in ab-initio systems were focused on low reactivity RAFT agents<sup>76-79</sup>, surface active RAFT agents<sup>80,81</sup>, self-assembling amphipathic RAFT agents<sup>82,83</sup>, and controlled feed conditions<sup>26,77,82,83</sup>. However there has been no systematic investigation for clarifying the events leading to coagulation, lack of control, and livingness in batch ab-initio emulsion polymerization. The aim of this thesis is to systematically study the influence of hydrophobicity of the reaction components on the polymerization process and the molecular and colloidal properties of the polymer produced.

### 3. Methods of Characterization

This chapter is dedicated to introducing the main methods of characterization used in this thesis. These methods are:

- Reaction calorimetry: to pursue the kinetics of the polymerization
- Gel permeation chromatography: to determine the molecular weight and the molecular weight distribution of the polymer
- Dynamic light scattering: for evaluation of the average particle size
- UV-Vis spectroscopy: to measure the concentration of the light absorbing molecules.

#### 3.1. Reaction calorimetry

Chemical Reactions are associated with changes in internal energies ( $\Delta H_R$ ) of the molecules. This means that energy is required or liberated as a result of the reaction taking place. The form of the energy absorbed or released during a change can vary. It sometimes appears as light or electrical work, but most often it occurs only as heat. When the entire energy change of a reaction involves heat, its amount is called the heat of reaction (Q). By measuring the reaction heat flow ( $\dot{Q}_{chem}$ ), it is possible to determine the extent and rate (r) of any chemical reaction (Equation 21,  $V_R$ : the reaction volume). This method is called “Reaction Calorimetry”.

**Equation 21**

$$\dot{Q}_{chem} = V_R \cdot (-\Delta H_R) \cdot r$$

And since for a given chemical reaction:



**Equation 22**  $Q = f(V, P, T)$

Therefore, in case of a constant pressure ( $P$ ) and volume ( $V$ ), it is possible to measure the rate of the reaction only by tracing the changes in the temperature with time. The basis of the calorimetric measurement is a heat balance of the reactor (Equation 23). Apart from the heat released through a chemical reaction (e.g. polymerization), additional contributions through accumulation ( $\dot{Q}_{accu}$ ), conduction ( $\dot{Q}_{cond}$ ), the loss to the surrounding ( $\dot{Q}_{loss}$ ), and stirring ( $\dot{Q}_{stir}$ ) need to be considered (Figure 3).

**Equation 23**  $\dot{Q}_{chem} = \dot{Q}_{accu} + \dot{Q}_{cond} + \dot{Q}_{loss} - \dot{Q}_{stir}$

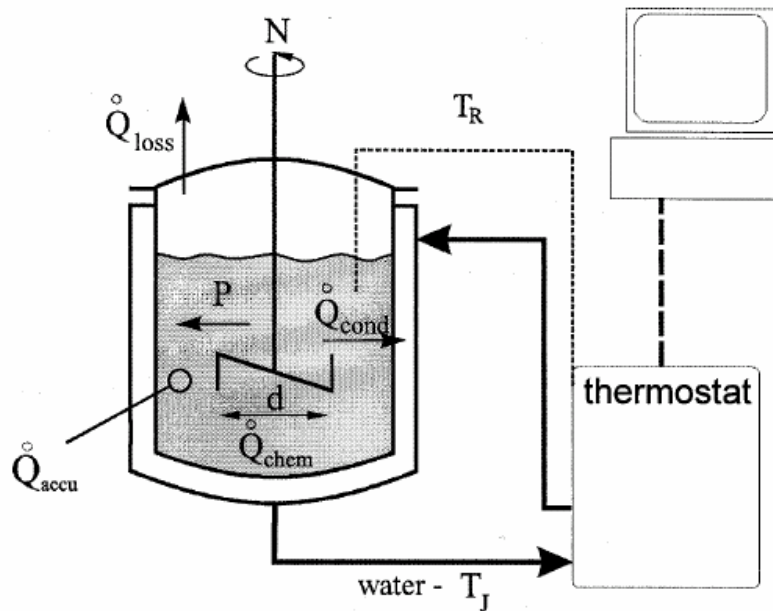


**Figure 3. A calorimetry reactor**

In Equation 23:

**Equation 24**

$$\dot{Q}_{\text{accu}} = C_P \frac{dT_R}{dt}$$

, where  $C_P$  and  $T_R$  are the heat capacity and temperature of the reaction mixture, respectively, and:

**Equation 25**

$$\dot{Q}_{\text{cond}} = U \cdot A \cdot (T_R - T_J)$$

, where  $U$  is the overall heat transfer coefficient, and  $A$  and  $T_J$  are the area and temperature of the reactor's jacket, respectively.  $\dot{Q}_{\text{stir}}$  and  $\dot{Q}_{\text{loss}}$  in most cases are relatively small values and are disregarded in the calculation. Therefore, the reaction heat flow is:

**Equation 26**

$$\dot{Q}_{\text{chem}} = C_P \frac{dT_R}{dt} + U \cdot A \cdot (T_R - T_J)$$

Depending on the purpose of the measurement, the reaction calorimetry can be carried out in different modes: isothermal, and adiabatic. In an adiabatic case the temperature of the jacket is kept the same as the temperature of the reaction mixture in order to evaluate the consequences of the failure of the cooling system for a specific reaction. In this case, the  $\dot{Q}_{\text{cond}}$  will be zero because no conduction takes place between the jacket and the reactor. However, in most cases, it is preferred to perform the measurement in the isothermal mode because it resembles the real reaction condition.

In an isothermal calorimetric run the temperature of the reaction mixture is kept constant. For that reason an occurring heat flow, produced by chemical reactions, must be absorbed to the cooling jacket. Thus, the

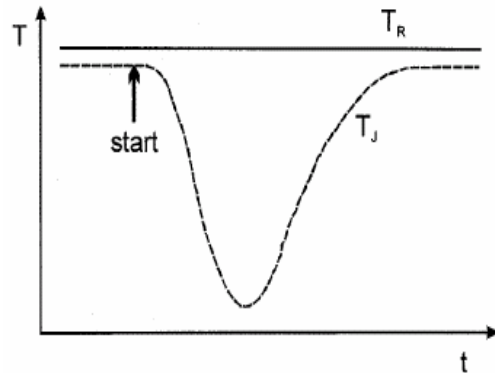


**Figure 4. Isothermal reaction calorimetry**

jacket will immediately be cooled down by the thermostat when reaction starts (Figure 4). Therefore, the reaction heat flow would be equal to the heat flow through conduction:

**Equation 27** 
$$\dot{Q}_{chem} = U \cdot A \cdot (T_R - T_J)$$

Depending on the type of the reactor, the product of the heat exchange area and the overall heat transfer coefficient ( $U \cdot A$ ) are predetermined through calibration. Therefore, measuring the temperature difference between the jacket and the reaction mixture during the whole course of the reaction leads to the values for the heat flow. The calorimetric measurements in this thesis are performed by a precalibrated reaction calorimeter and the data produced by the calorimeter are directly the heat flow.

Bearing in mind that the chemical heat flow is proportional to the rate of the reaction and:

**Equation 28** 
$$r = \frac{dX}{dt}$$

The reaction conversion ( $X$ ) can also be determined:

**Equation 29** 
$$X(t) = \frac{\int_{t_0}^t \dot{Q}_{chem} dt}{\dot{Q}_{chem \cdot total}} = \frac{\int_{t_0}^t \dot{Q}_{chem} dt}{\int_{t_0}^{t_{end}} \dot{Q}_{chem} dt}$$

The results of the calorimetric measurements in this work are presented in Section 4.2.

### 3.2. Gel permeation chromatography (GPC)

Gel permeation chromatography (GPC), also known as size exclusion chromatography (SEC), is considered to be one of the most important methods for the determination of molecular weight (MW) and molecular weight distribution (MWD) of polymers. During this process macromolecules are fractionated according to their hydrodynamic volume. A dilute polymer solution containing a broad molecular weight distribution of polymer chains, oligomers or even unreacted monomers is allowed to flow through a column packed with finely divided solid particles. These particles can be either microporous glass beads or swollen, polymer gel. Smaller molecules can penetrate the pores and hence spend some time in the column before their elution, whereas the larger ones, unable to do the same, are eluted first out of the column. The separation process is illustrated in Figure 5.

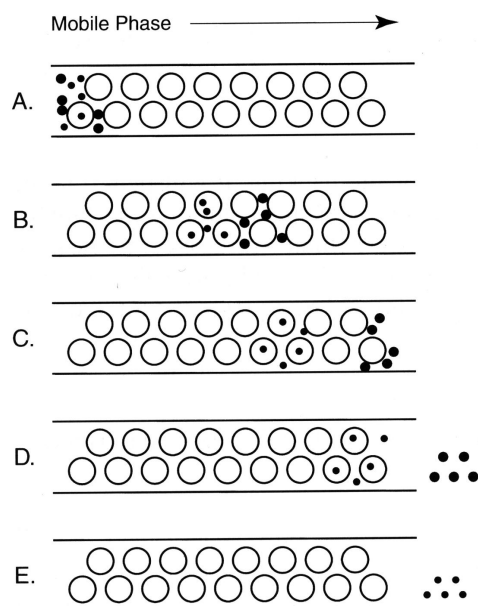


Figure 5. Separation in a GPC column

The polymer concentration in the analyte is measured as a function of time or elution volume ( $V_e$ ). The latter is defined as:

**Equation 30**

$$V_e = V_o + k_{GPC} V_i$$

, where  $V_o$  is the exclusion volume,  $V_i$  the volume inside the pores and  $k_{GPC}$  the distribution coefficient. Differential refractometer (DRI) and/or Ultraviolet/Visible (UV-Vis) absorption systems are the most commonly employed GPC detectors. According to the first method, the difference in the refractive index between the eluted solution and the pure solvent is proportional to the concentration of the polymer chains. In the case where a UV-Vis detector is used, and the polymer is consisted of UV-active monomer units, then by setting the spectrometer to a specific wavelength (e.g. to the aromatic absorption region of a polymer with phenyl rings) the signal will be proportional to the mass. When a polymer chain carries a UV-active end-group, a signal proportional to this group will be detected.

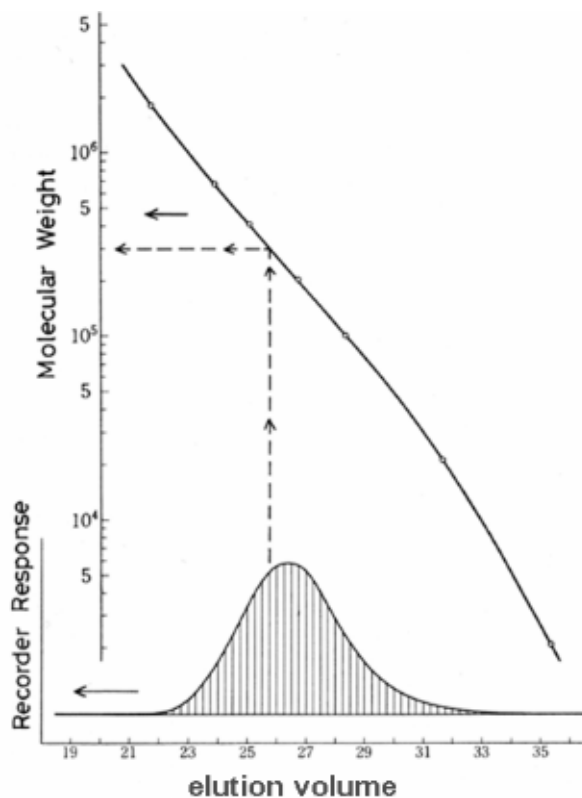


**Figure 6. a typical calibration curve**

GPC is a relative method for determining the molecular weight. This can be achieved only after calibrating the system in terms of the elution volume.

Calibration is performed using fractions of a particular polymer which have been previously well characterized regarding their molecular weight, using absolute methods such as osmometry and light scattering. These samples are known as polymer “standards”. The measured elution volumes are plotted as a function of the molecular weight and form a “calibration curve”. The calibration curve is used for converting the elution volume data to molecular weight. The procedure is demonstrated in Figure 6.

As mentioned previously, usually the signal intensity ( $I_{RI}$ ) in any slice ( $i$ ) of a GPC chromatogram is proportional to the concentration of the eluting chains ( $c_i$ ):

**Equation 31**

$$c_i \sim \frac{(I_{RI})_i}{\sum_j (I_{RI})_j}$$

The expression in the denominator corresponds to the total area of the chromatogram. The molecular weight corresponding to each chromatographic fraction can be determined via the calibration curve. Thus, from the obtained data, number and weight average molecular weight ( $M_n$  and  $M_w$ , respectively) can be calculated among others (Equation 32 and Equation 33) and with them the polydispersity index ( $PDI=M_w/M_n$ ). PDI takes values from  $1 \rightarrow \infty$ . If this ratio is equal to 1 then a situation where all molecules have exactly the same weight (i.e. monodisperse) is achieved.

**Equation 32**

$$\bar{M}_n \equiv \frac{\sum_i c_i}{\sum_i c_i / M_i}$$

**Equation 33**

$$\bar{M}_w \equiv \frac{\sum_i c_i M_i}{\sum_i c_i}$$

### 3.3. Dynamic light scattering

One of the most popular methods in colloid and polymer analysis is the so-called dynamic light scattering (DLS) or quasi-elastic light scattering. This technique enables the determination of the particle size and the particle size distribution in dispersion in a range of 1 – 2000 nm. The method of DLS is based on the survey of the Brownian motion of small particles in diluted solutions.

When a laser irradiates dispersions, the particles (colloidal particles or micelles) become scattering centers, scattering the light in all directions. By constructive and destructive interferences of the emitted secondary waves, characteristics patterns of the light are built, and together with the relative movement of the particles, one originates a fluctuating interferogram. The principle of DLS is based on the Doppler-effect. The frequency of a moving source will be displaced to higher or lower frequencies if it moves away or closer to the receptor. As a result of the Doppler-effect the frequency of the emitted irradiation is displaced, whereas the absolute value of the displacement depends on the speed of the particles. Dispersed particles move under the Brownian motion, thus they have a velocity distribution, which results in a symmetric broadening of the scattered light.

The full width at half maximum ( $\Gamma$ ) of the spectral distribution of light scattering is proportional to the translational diffusion coefficient ( $D$ ). As the colloidal movement of the particle, which takes place in solution, is very slow, the frequency displacement is also extremely small and cannot be observed directly in this frequency range. The spectral broadening of the scattered light cannot be solved experimentally. The scattered light contains all information about the diffusion movement of the particles enabling the determination of the size of the particles. The Wiener-Knitschin Theorem provides a solution for the problem. It says that for an intensity distribution  $I(\omega)$  in the real frequency scale exists a fourier-transformation function  $g(t)$  (time or autocorrelation function) in the reciprocal time scale:

**Equation 34** 
$$I(\omega) = \frac{1}{2\pi} \int_{-\infty}^{+\infty} g(t) e^{i\omega t} dt$$

**Equation 35** 
$$g(t) = \int_{-\infty}^{+\infty} I(\omega) e^{-i\omega t} d\omega$$

, with time  $t$  and frequency  $\omega$ .

The narrower the frequency broadening in the real scale, the wider is the distribution in the reciprocal time scale. The small frequency broadening in the real scale introduces a measurable relaxation in the reciprocal scale. Since the temporal fluctuation of the scattered light intensity  $I(t)$  is measured, the determination of the autocorrelation function of the scattered light intensity  $g_I(q, t)$ , is defined as:

**Equation 36** 
$$g_I(q, t) = \frac{\langle I(q, t_0) \cdot I(q, t) \rangle}{\langle I(t_0) \rangle^2} = \lim_{T \rightarrow \infty} \frac{1}{T} \int_0^T I(t) I(t+t') dt$$

From this equation results a correlation function, which mirrors the relationship between the average intensity for the time  $(t+t')$  and the intensity  $I(t)$ .  $I(t)$  and  $I(t+t')$  are independent of each other for big values of  $t$ . For small values, the correlation function  $g_I$  corresponds to the squared averaged scattered intensity  $\langle I \rangle^2$ . The autocorrelation function  $g_I(q, t)$  is connected with  $g(q, t)$  by the Siegert-relation:

**Equation 37** 
$$g(q, t) = 1 + |g_I(q, t)|^2$$

For monodisperse, spherical particles without interparticle interaction that means high dilution,  $g(t)$  is expressed by a simple exponential function, of which the characteristic time constant is related to the diffusion coefficient  $D$ :

**Equation 38** 
$$g(q, t) = A e^{-q^2 D t}$$



Using the Stokes-Einstein relation one can calculate an average hydrodynamic intensity radius from the diffusion coefficient  $D$ :

**Equation 39** 
$$R_H = \frac{k_B T}{6\pi\eta_0 D}$$

, where  $\eta_0$  is the viscosity of the medium,  $k_B$  the Boltzmann constant and  $T$  the absolute temperature. This relation is the basis of the particle size determination by dynamic light scattering, but it is valid only for spherical monodisperse particles. For polydisperse particles, it is necessary to do a cumulant analysis. The correlation function is then represented by:

**Equation 40** 
$$\ln g(q, t) = \sum_{n=0}^{\infty} \frac{(-1)^n \Gamma_n t^n}{n!}$$

The determination of the cumulant  $\Gamma_n$  is done by the extrapolation of the initial slope of the plot of  $\ln g(q, t)$  versus  $t$ :

**Equation 41** 
$$\Gamma_n = \left( \frac{\partial^n \ln g(q, t)}{\partial t^n} \right)_{t \rightarrow 0}$$

The cumulants are related to the diffusion coefficient  $D$  through the scattering vector  $q$ :

**Equation 42** 
$$D = \frac{\Gamma_1}{q^2}$$

The polydispersity of a sample can be determined through the fitting of the cumulant analysis in a gaussian distribution of the intensity weighted diffusion coefficient. By the quotient of the first and second cumulants, one can obtain the variance  $\mu$  of the gaussian distribution, which represents a square standard

deviation  $\sigma$ . The relation between the best fitting of the logarithmic correlation function and the width of a gaussian distribution is then established by:

**Equation 43** 
$$\mu = \frac{\Delta D}{D} = \frac{\Gamma_2^2}{\Gamma_1} = \sigma^2$$

### 3.4. Ultraviolet/Visible (UV-Vis) spectroscopy

Ultraviolet/Visible (UV-Vis) spectroscopy is a useful method for determination of the identity or concentration of a substance. When light -either visible or ultraviolet- is absorbed by valence (outer) electrons these electrons are promoted from their normal (ground) states to higher energy (excited) states. The energies of the orbitals involved in electronic transition have fixed values. Although the energy is quantized the UV-Vis spectrum has broad peaks due to the existing vibrational and rotational energy levels available to light absorbing materials (Figure 7).

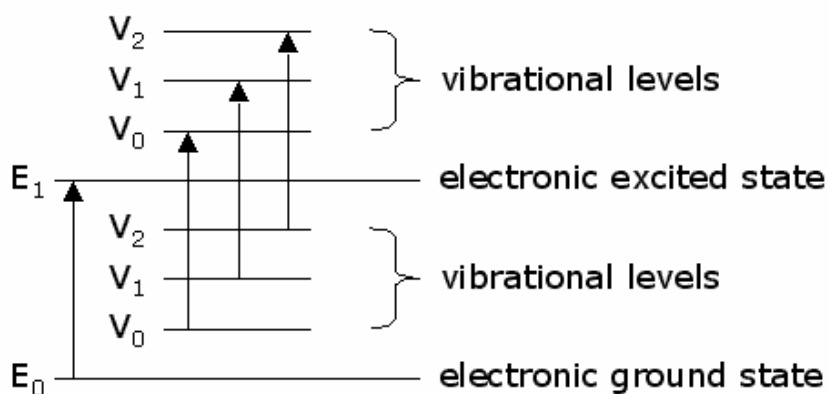


**Figure 7. The energy states of the electrons**

Because light absorption can occur over a wide range, usually the light range from 190 nm to 900 nm is used. Valence electrons are found in three types of electron orbitals: single ( $\sigma$ ) bonding orbitals; double or triple ( $\pi$  bonding orbitals) and non-bonding orbitals (lone pair electrons). Sigma ( $\sigma$ ) bonding orbitals tend to be lower in energy than  $\pi$  bonding orbitals, which in turn are lower in energy

than non-bonding orbitals ( $n$ ). When electromagnetic radiation of the correct frequency is absorbed a transition occurs from one of these orbitals to an empty orbital, usually anti-bonding orbital ( $\sigma^*$  or  $\pi^*$ ). The exact energy differences between the orbitals vary. In organic molecules, double bonds that are next to each other can conjugate (join together and delocalize the electrons over all of the atoms). As a consequence, molecules with many conjugated double bonds can be colored because they absorb energy in the visible as well as the ultraviolet part of the spectrum.

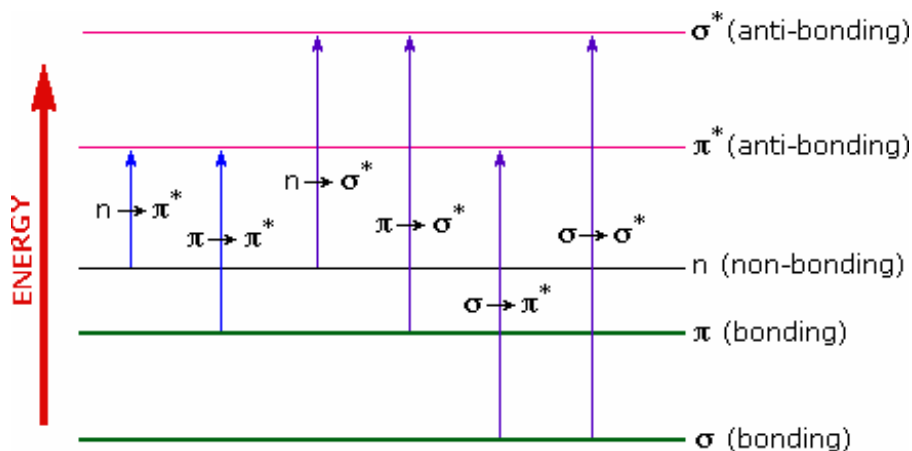


Figure 8. The molecular orbitals

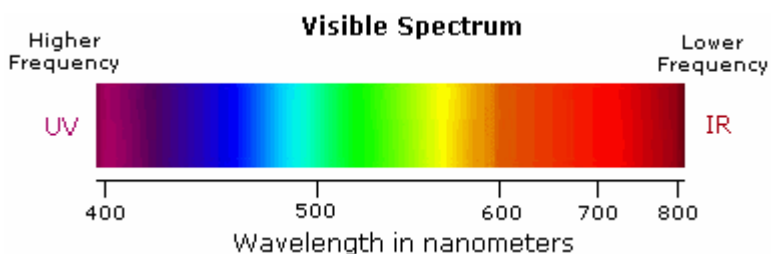


Figure 9. The light spectrum

In a typical measurement, the spectrum of a solution containing the light absorbing substance is measured after or in parallel to a reference cell containing only solvent. The transmitted radiation is detected and the spectrometer records the absorption spectrum by scanning the wavelength of the light passing through the cells.

For most spectra the solution obeys Beer's Law. This states that the light absorbed is proportional to the number of absorbing molecules (i.e. to the concentration of absorbing molecules). This is only true for dilute solutions. A second Law (Lambert's Law) says that the fraction of radiation absorbed is independent of the intensity of the radiation. Combining these two laws gives the Beer-Lambert law:

**Equation 44** 
$$\log \frac{I_0}{I} = \varepsilon \cdot l \cdot c$$

, where  $I_0$  and  $I$  are the intensity of the incident and transmitted radiation, respectively,  $\varepsilon$  is the extinction coefficient,  $l$  is the path length through the absorbing solution, and  $c$  is the concentration of the absorbing species.

If  $\varepsilon$  and  $\lambda_{\max}$  (the wavelength at which maximum absorption occurs) are known for a compound, its concentration can be easily calculated.

“To do the same thing over and over again is not only boredom:  
it is to be controlled by rather than to control what you do.”

Heraclitus  
(535 B.C - 475 B.C.)  
Herakleitos and Diogenes

## 4. Results and Discussion

Prediction of the kinetics of controlled radical polymerization is by far more straight-forward for homogeneous systems such as bulk and solution than for heterogeneous ones like emulsion polymerization. The reason for this difference lies in the multiplicity of the reaction loci in a heterogeneous system. In a homogeneous system, there is only one reaction locus; therefore, the concentrations of the reactants are clearly defined. Contrary, in heterophase polymerization, more specifically, *ab initio* emulsion polymerization, the reaction takes place in all the phases: the monomer phase, the continuous phase, the polymer particles, and at the interface between the particles and the continuous phase. The local concentration of the reactants at the particular locus is not easy to determine as it depends on their solubility and partitioning in the different phases. The kinetics of polymerization in these loci also varies and therefore, the product of polymerization from each locus has different properties. Two main polymeric products are expected from heterophase polymerization: (1) a polymer product originating from the latex particles; (2) a polymer product formed as a result of polymerization in the monomer phase<sup>84</sup>. Provided the coagulation of the latex particles are prevented, the coagulum normally found at the end of the polymerization represents the polymer produced in the monomer phase.

Since the kinetics of polymerization in the monomer phase resembles the one in a bulk system, a lower molecular weight is expected in the coagulum. The relative amounts of these two main products depend on the solubility and

partitioning behavior of the initiating radical. A more hydrophobic initiator in an aqueous heterophase system will result in a higher portion of polymerization in the monomer phase and consequently, more coagulum at the end of the polymerization (except in the systems that polymerization inside stable monomer droplets is desired). Conversely, a more lyophilic primary radical promotes the reactions in the latex phase and thus the amount of latex will be substantially higher than the coagulum.

Therefore, the kinetics of controlled radical heterophase polymerization depends on two main additional parameters in comparison with polymerizations in bulk and solution. The first parameter is the solubility behavior of the initiator or of the primary free radical; and the other parameter is the hydrophobicity of the controlling agent which influences the concentration of the controlling agent in each reaction locus.

The aim of this work is to investigate the influence of the nature of both the initiator and the RAFT agent in *ab-initio* emulsion polymerization. The study comprises four RAFT agents with leaving and activating groups of different solubility in water and four azo- and peroxy-initiators with different partitioning behavior among the various reaction loci.

In Section 4.1, the initiators and RAFT agents employed in this study are introduced and compared when applied to homogeneous polymerizations in bulk and solution. In Section 4.2, the results of batchwise *ab initio* emulsion polymerization of styrene at 80°C are summarized. Section 4.3, presents the development of a novel method for studying the phase transfer and sorption of organic molecules such as RAFT agents. This method provides quantitative evidence for the different solubility of the RAFT agents and their transportation from the monomer phase through the aqueous phase to the polymer particles. Finally, in Section 4.4, the application of the RAFT technique to room

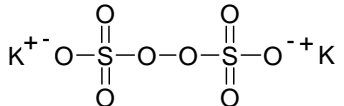
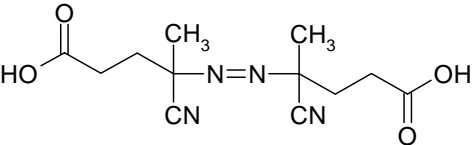
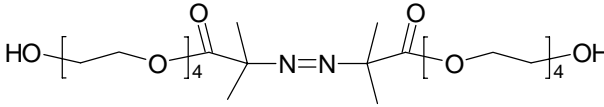
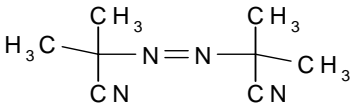
temperature ab-initio emulsion polymerization and its special features are discussed.

#### 4.1. The Initiators, the RAFT agents, and homogeneous polymerizations

##### 4.1.1. The initiators

For the polymerizations in Section 4.3, four types of initiators are employed (Table 1): potassium peroxydisulfate (KPS), 4,4'-azobis (4-cyanopentanoic acid) (ACPA), poly(ethylene glycol)-azo-initiator (PEGA200), and 2,2'-azobis-isobutyronitrile (AIBN). The water solubility of the initiating primary radicals derived from the initiators is expected to vary in the following order: sulfate ion radical (from KPS) > 1,1'-cyano methyl butyric acid with the radical function at the 1-carbon atom (from ACPA) > 2-carbonyl oxy poly(ethylene glycol) with the radical function at the 2-carbon of the propyl group (from PEGA200) > 2-cyano propyl with the radical function on the 2-carbon atom (from AIBN).

**Table 1. The structure of the initiators**

<p><b>(a) KPS</b></p> 	<p><b>(b) ACPA</b></p> 
<p><b>(c) PEGA 200</b></p> 	<p><b>(d) AIBN</b></p> 

KPS is very well soluble in water and has almost no solubility in styrene. For the polymerizations with ACPA, the pH of the continuous phase was adjusted to basic in order to ensure the complete dissolution in the aqueous phase. The situation regarding PEGA200 is more complex as poly(ethylene glycol) is soluble

in both the water and the monomer phase; however, the partition coefficient depends on the temperature<sup>85</sup>. Finally, AIBN dissolves very well in styrene and therefore, in a heterophase system we would expect AIBN to result in extensive polymerization in the monomer phase and produce the highest amount of coagulum among these initiators. KPS and ACPA with the highest solubility in the aqueous phase are expected to result in a minimum amount of coagulum.

**Table 2** the decomposition rate coefficient of various initiators

Initiator	AIBN <sup>86</sup>	ACPA <sup>87</sup>	KPS <sup>88</sup>	PEGA200 <sup>89</sup>
$k_d$	$1.1947 \times 10^{-4}$	$1.1485 \times 10^{-4}$	$8.41 \times 10^{-5}$	$5.8997 \times 10^{-5}$

The decomposition rate coefficient,  $k_d$ , of these initiators at 80°C is summarized in Table 2 and increases in the order: AIBN>ACPA>KPS>PEGA200.

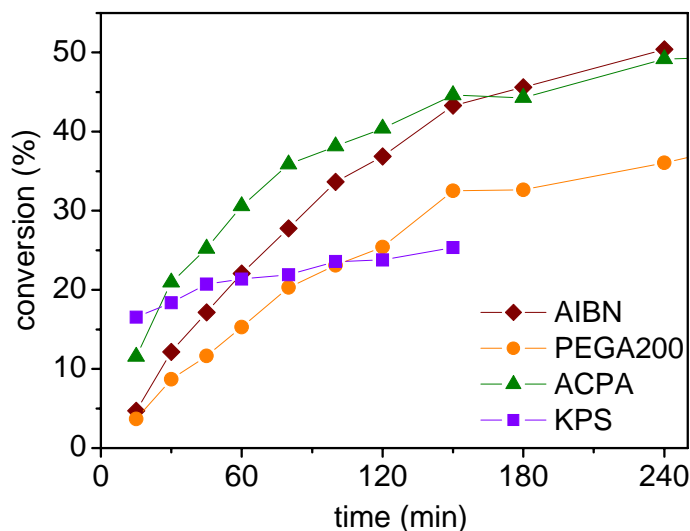


**Figure 10.** Conversion vs. time obtained by gravimetric measurements of samples taken during solution polymerization of styrene in DMF in the absence of RAFT agent

To compare the rate of polymerization initiated with these initiators in a homogeneous media, solution polymerization of styrene in a polar solvent, dimethyl formamide (DMF), was carried out. The advantage of this particular

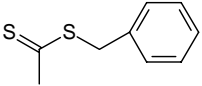
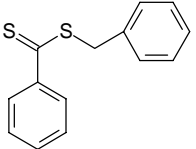
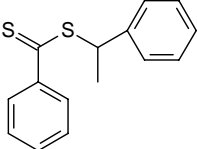
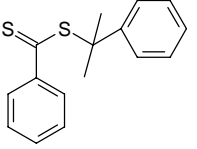


solvent is that styrene, AIBN, PEGA200, and ACPA are easily soluble in DMF. To facilitate the dissolution of KPS in DMF, a complex of KPS with cetyltrimethyl ammoniumbromide (CTAB) was prepared. In this way, the behavior of all the initiators used for the heterophase polymerization could be compared in a homogeneous system.

#### 4.1.2. The RAFT agents

The chemical structure of the employed RAFT agents is given in Table 3. All the RAFT agents chosen are hydrophobic because the hydrophilic RAFT agents at high temperatures and aqueous media are prone to hydrolysis<sup>90</sup>.

**Table 3. The structure of various thiocarbonylthio compounds as RAFT agents**

<p><b>(a) Benzyl dithioacetate (BDA)</b></p> 	<p><b>(b) Benzyl dithiobenzoate (BDB)</b></p> 
<p><b>(c) Phenyl ethyl dithiobenzoate (PhEDB)</b></p> 	<p><b>(d) Cumyl dithiobenzoate (CDB)</b></p> 

The RAFT agents CDB, PhEDB, and BDB can be considered as a homologous series, as all have a phenyl group as their activating (Z) group and their leaving (L) group only differs in the number of methyl groups. Therefore, these RAFT agents are expected to slightly differ in their water solubility in the order of BDB > PhEDB > CDB. Consequently, their L groups that are benzyl, phenylethyl (2-phenylethyl with the radical-function at the 2-carbon of the ethyl group), and cumyl (2-phenylpropyl with the radical-function at the 2-carbon of the propyl group) radical, respectively, are expected to have different water solubility and re-initiation capability. BDA and BDB have the same leaving group but different

activating groups (methyl and benzyl, respectively) with different water solubility (BDA>BDB).

Presently, there are no solubility data available in the literature for these RAFT agents. Therefore, the water solubility of these compounds was roughly estimated using a relation between the water solubility ( $S_W$ ) and octanol-water partition coefficients ( $K_{OW}$ ) as described by Yalkowsky and Banerjee<sup>91</sup>. This procedure requires first, the estimation of the  $K_{OW}$  by fragment constants for each structural component and second, a proper relation between  $S_W$  and  $K_{OW}$ . With the data for calculating  $K_{OW}$  and a  $S_W$ - $K_{OW}$  relation for esters<sup>91</sup>, approximate water solubility values that are obtained for BDA, BDB, PhEDB, and CDB are 14, 1.2, 0.3, and 0.05 mM, respectively. It must be emphasized again that this is a very rough estimation which only confirms the trend of water-solubility of these compounds as BDA>BDB>PhEDB>CDB. Consequently, it is expected that in an aqueous heterophase system, CDB to have the highest concentration in the monomer phase and the lowest in the particle phase. For BDA, the opposite is expected. Bearing in mind, this point is crucial for following the subsequent discussions.

Homogeneous polymerizations in bulk and solution were carried out with the same concentrations and at the same temperature as the heterophase polymerizations to compare the general performance of these RAFT agents in either system. The same trend in the rate of polymerization is observed when changing the RAFT agent in both bulk and solution polymerization (Figure 11).

It is clearly seen that the rate of polymerization for BDB and CDB as RAFT agents is lower than for BDA and PhEDB. Since the ratio of RAFT agent to initiator is not very high (~ 1.25), the rate of polymerization does not decrease significantly. This ratio is chosen for heterophase polymerization, where lower concentration of RAFT agent is sufficient due to the compartmentalization. Even for homogeneous media the data in Figure 12 demonstrate that the

polymerization appears to be controlled, which means the number average molecular weight linearly increases and the PDI decreases with increasing the conversion. There are a couple of important points to note in Figure 12. First, BDA results in higher PDI than other RAFT agents. Second, even in the absence of RAFT agent the number average molecular weight increases almost linearly although the line does not pass the origin and the PDI increases with conversion.

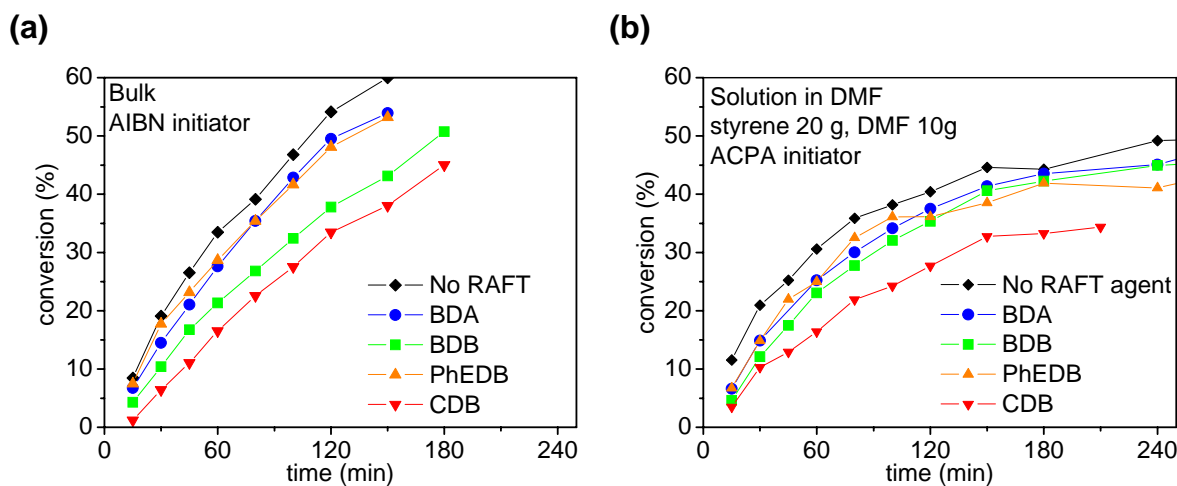


**Figure 11. Conversion-time curve obtained by gravimetric measurements of samples taken during polymerization of styrene in presence of various RAFT agents (a) bulk polymerization initiated with AIBN and (b) solution polymerization in DMF initiated with ACPA**

The reason for higher rate of polymerization in case of BDA comparing with BDB lies in the influence of the activating group. Coote et al.<sup>92</sup> showed through ab-initio molecular orbital calculations that benzyl Z groups by slowing down the rate of fragmentation enhance the retardation of the polymerization rate. Systematic investigations of Chiefari et al.<sup>30</sup> on the influence of the Z group also confirm these results.

The slow rate of polymerization in case of CDB can be the result of the high stability of its leaving group to re-initiate polymerization. This as well could be the reason for observed inhibition period that is reported by several groups for polymerizations carried out in bulk, solution and heterophase systems<sup>26,28,30,31,36,93-</sup>

<sup>95</sup>. It is to note that we did not observe the inhibition effect in our homogeneous polymerizations.

In general the reasons behind the rate retardation in the presence of dithiobenzoates and especially CDB has been the matter of some debates<sup>39,96,97</sup>. It might be that the fragmentation rate coefficient is fast and the reason for the rate retardation is the irreversible cross-termination of the intermediate species<sup>95</sup> or that the fragmentation rate coefficient is slow<sup>93</sup>. The high level ab-initio calculations of the addition-fragmentation equilibrium constants supports the latter<sup>37</sup>.

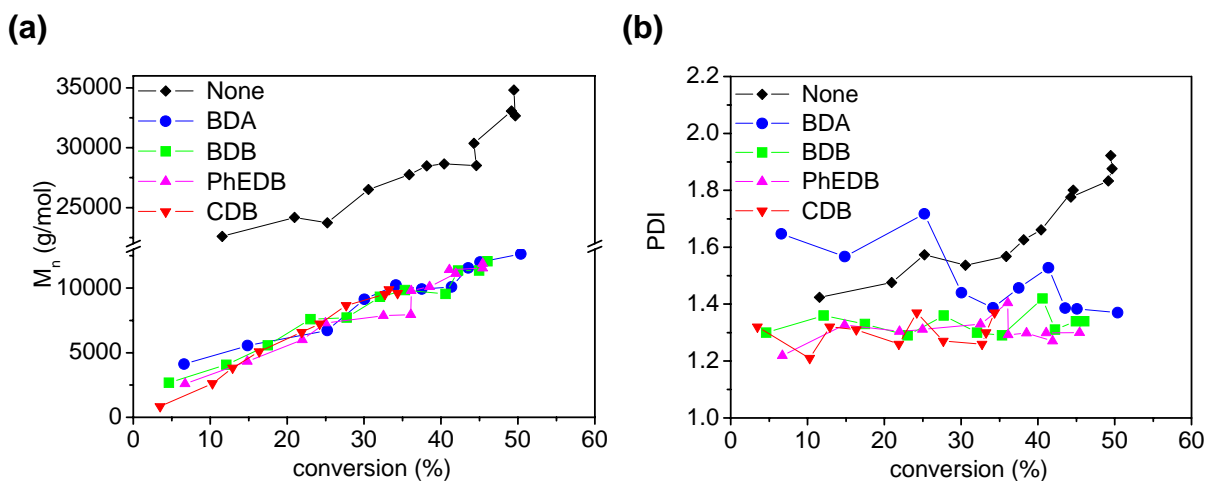


**Figure 12. Evolution of (a) the number average molecular weight and (b) the polydispersity index, during solution polymerization of styrene in DMF initiated with ACPA and in the presence of various RAFT agents**

## 4.2. RAFT ab-initio emulsion polymerization of styrene

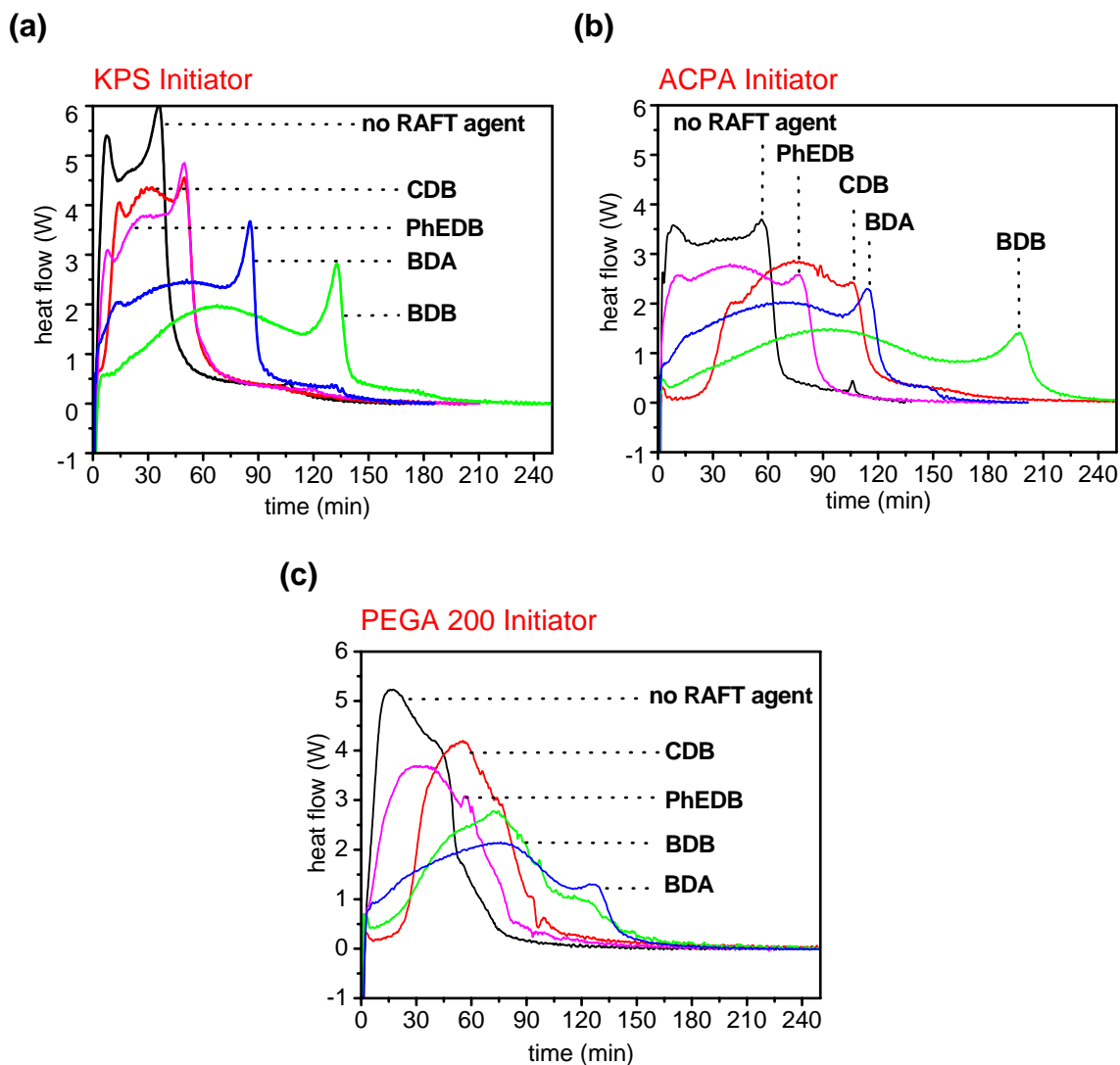
A complete set of data has been elaborated comprising rate of polymerization, evolution of the average particle size, molecular weight, and molecular weight distribution for ab initio emulsion polymerization of styrene. Only a few typical examples are presented in the following discussion. However, a categorized library of graphs is supplied in the Appendix I for further reference.

Note, for ab-initio emulsion polymerization, the polymer particles are the main reaction loci. They are formed during the nucleation period which is governed by reactions in the aqueous phase. Then after swelling with monomer and RAFT agent the controlled polymerization takes place inside the particles.

#### 4.2.1. Rate of polymerization

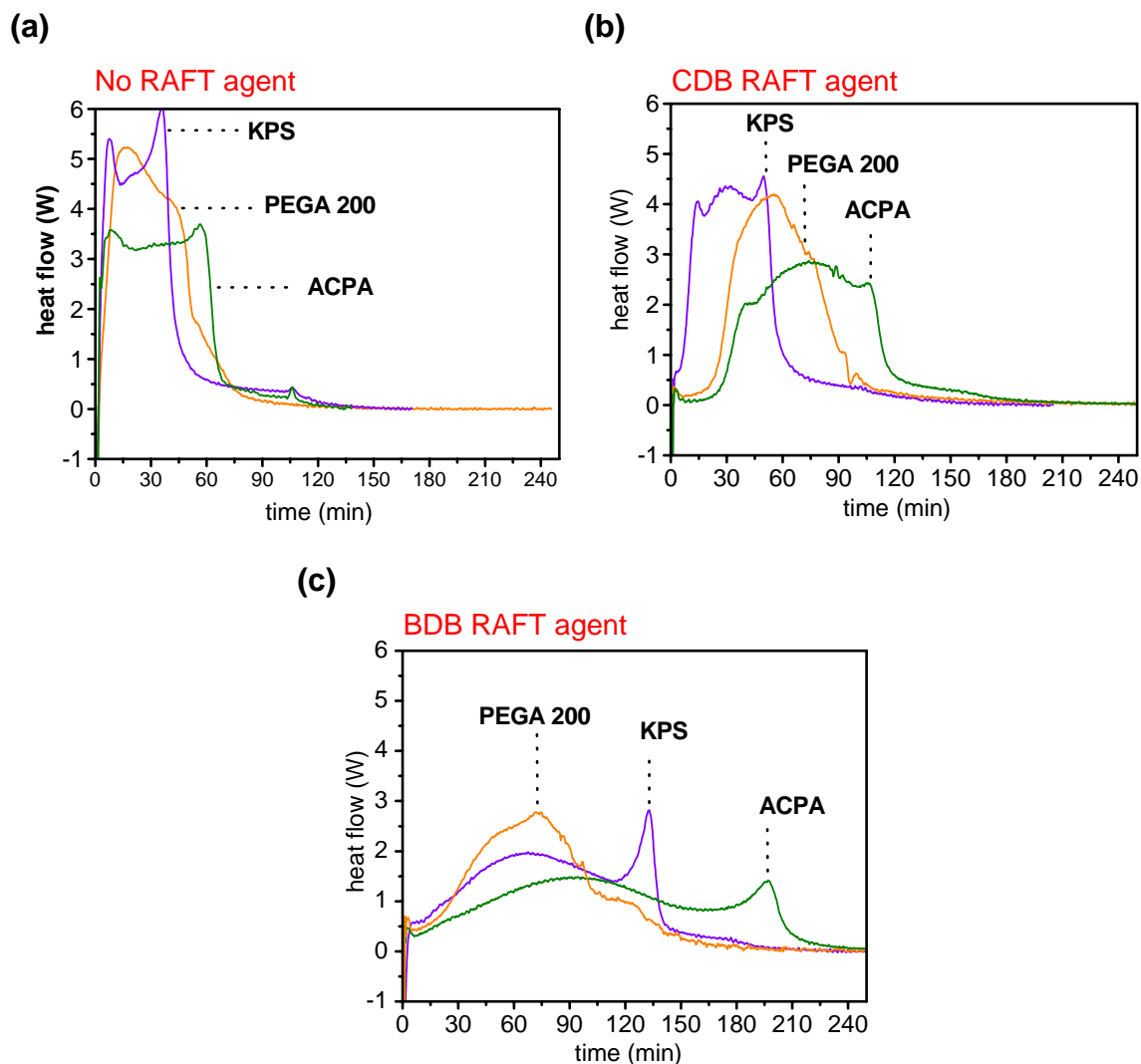
In this section, the influence of the type of RAFT agent and initiator on the rate of ab-initio emulsion polymerization of styrene is discussed. Reaction calorimetry was used as a powerful tool for providing information on the rate of polymerization in emulsion<sup>98</sup>. The polymerizations initiated with AIBN were halted after resulting in massive coagulation in the calorimeter reactor. As it is illustrated by the data assembled in Figure 13, the nature of the RAFT agent does indeed have a strong influence on the polymerization rate for a given initiator. It seems that the rate of polymerization decreases only slightly for more hydrophobic RAFT agents such as CDB and PhEDB, and substantially, in case of the less hydrophobic RAFT agents, BDB and BDA. The order observed here is not the same as the one observed in homogeneous media; therefore, it is reasonable to attribute this to the peculiarities of an aqueous heterophase system. Since a higher concentration of RAFT agent results in a lower rate of polymerization, the data in Figure 13 are an indirect measure of the RAFT agent concentration at the main reaction loci, i.e. the latex particles. Obviously, the less hydrophobic RAFT agents have a higher probability to enter the latex particles.

Figure 13 also demonstrates that the general shape of the rate profile is basically determined by the nature of the initiator. However, in ab-initio emulsion polymerization, the order in which the rate of polymerization changes for different initiators (Figure 14(a)) is not the same as in a homogeneous system (Figure 10) and the decomposition rate coefficient of the initiators is of a minor importance here. This result emphasizes the important role of the reactions in the continuous aqueous phase and the radical entry into the particles.



**Figure 13.** The reaction rate profiles as obtained directly by reaction calorimetry of ab-initio emulsion polymerization of styrene at 80°C in the presence of various RAFT agents initiated with (a) KPS (b) ACPA (c) PEGA200

Furthermore, there seems to be a more complex interaction between the free radical initiators and RAFT agents in aqueous heterophase polymerizations. Figure 14(b)-(c) display an example of this complexity, where depending on the type of the RAFT agent, the initiators show a different order regarding the rate of polymerization.



**Figure 14.** Reaction rate profiles as obtained directly by reaction calorimetry of ab-initio emulsion polymerization of styrene at 80°C with various initiators and in presence of RAFT agents: (a) none (b) CDB (c) BDB

An inhibition period is observed when CDB is used as RAFT agent in ab initio emulsion polymerization (Figure 14(b)). Since we did not observe this effect in bulk and solution polymerization with similar concentration ratios (Figure 11), we can attribute it to the particular conditions that can cause inhibition in heterophase system. Perhaps the stable cumyl leaving group before undergoing re-initiation can exit the monomer phase and quench initiator radicals in the aqueous phase. Inhibition or retardation was frequently observed with CDB<sup>26,28,30,31,36,93-95</sup> and the reason is still a matter of controversial discussion. A

satisfying explanation requires detailed investigations of the initial stage which are beyond the scope of this thesis.

Reaction calorimetry is one of the most accurate methods for following the rate of polymerization because it allows the acquisition of detailed information on the rate of polymerization in all the phases without disturbing the course of the reaction concerning the chemical composition of the reactants and the temperature. However, this method has its own drawbacks: It does not allow sampling during the polymerization; the metal used in the reactor's structure might interact with certain reaction components which can influence the reaction rate<sup>99</sup>; and also immediately after addition of the initiator solution the heat flow is affected and therefore a lower monomer conversion is represented by the heat flow if the polymerization is very fast.

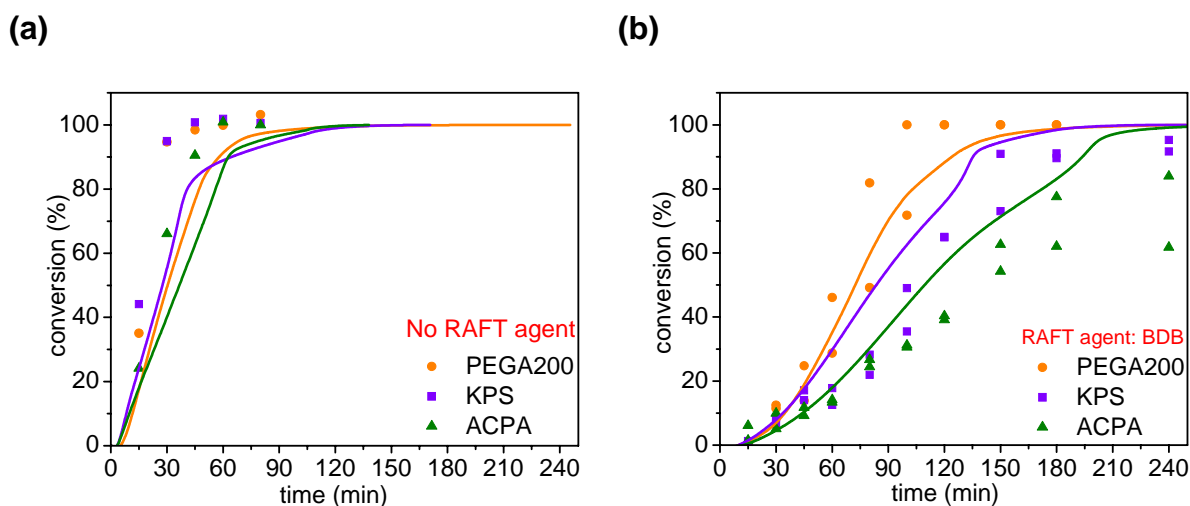


**Figure 15. Conversion-time plots for ab-initio emulsion polymerization of styrene at 80°C with various initiators in presence of RAFT agents: (a) none (b) BDB, (Solid lines): integration of rate profiles from reaction calorimetry, (symbols): gravimetric measurement of samples taken during the polymerization**

Therefore, all the polymerizations performed in the calorimeter were repeated several times in reactors completely made of glass. Samples were taken at certain times during the polymerization and characterized by means of gravimetry, DLS, and GPC for their solids content, particle size and molar mass



distribution, respectively. It is to note that the gravimetric measurements also involve some errors: The conditions of the polymerization and the composition of the reactants are disturbed the more samples are taken; While at early stages of the heterophase polymerization the samples represent all the phases, at higher conversions, especially when coagulum is formed, the product of the polymerization in the monomer phase is not represented; And also at higher conversions, due to the formation of a polymer film during the heating that prevents complete evaporation of the volatiles, the gravimetric measurements result in higher values for conversion and faster rates.

Generally it was observed that the data from both calorimetric and gravimetric measurements correspond better, the slower is the rate of polymerization. Examples are shown in Figure 15 for the fastest polymerizations with no RAFT agent and the slowest with RAFT agent BDB. It is clearly seen that in the absence of RAFT agent when the polymerization is fast, the gravimetric values are higher.

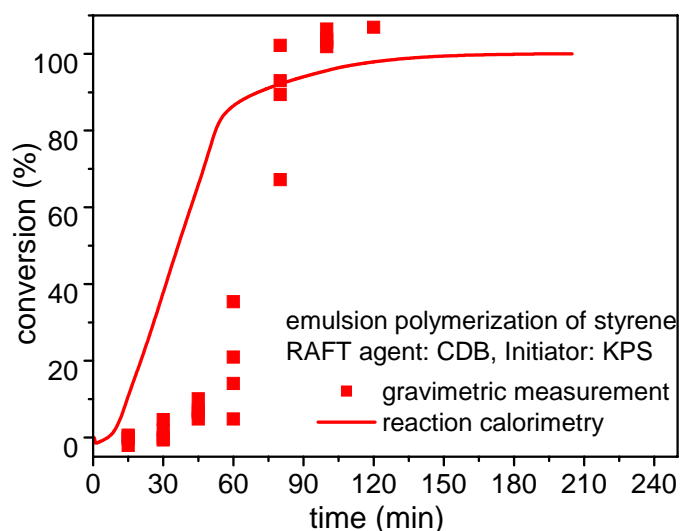


**Figure 16. Conversion-time plots for ab-initio emulsion polymerization of styrene at 80°C initiated with KPS and in presence of CDB, (solid lines): integration of rate profiles from reaction calorimetry, (symbols): gravimetric measurement of samples taken during the polymerization**

An example of specific interactions between the reactants and the reactor's metal parts is demonstrated in Figure 16. The strong initial retardation period observed for CDB in all-glass reactors and also in the calorimeter for other initiators, is not very pronounced for KPS in the calorimeter. Possibly, a redox reaction between the metal parts and KPS leads to an enhanced radical flux as observed also by Tauer et al<sup>100</sup>.

To facilitate the comparison, the slopes of the linear part of the conversion-time plots (10-80% conversion) are considered as average rate (Figure 17). This figure clearly shows that the trend in which the rate of polymerization changes with varying the RAFT agent for each type of initiator is very similar in both methods. It is also obvious that the values obtained from the gravimetric measurements are larger. Another point to notice in both graphs is that the lowest rates in case of water soluble initiators are observed for BDB and not for BDA. Only for PEGA200 the deceleration of the rate of polymerization correlates inversely with the water solubility of the RAFT agents.

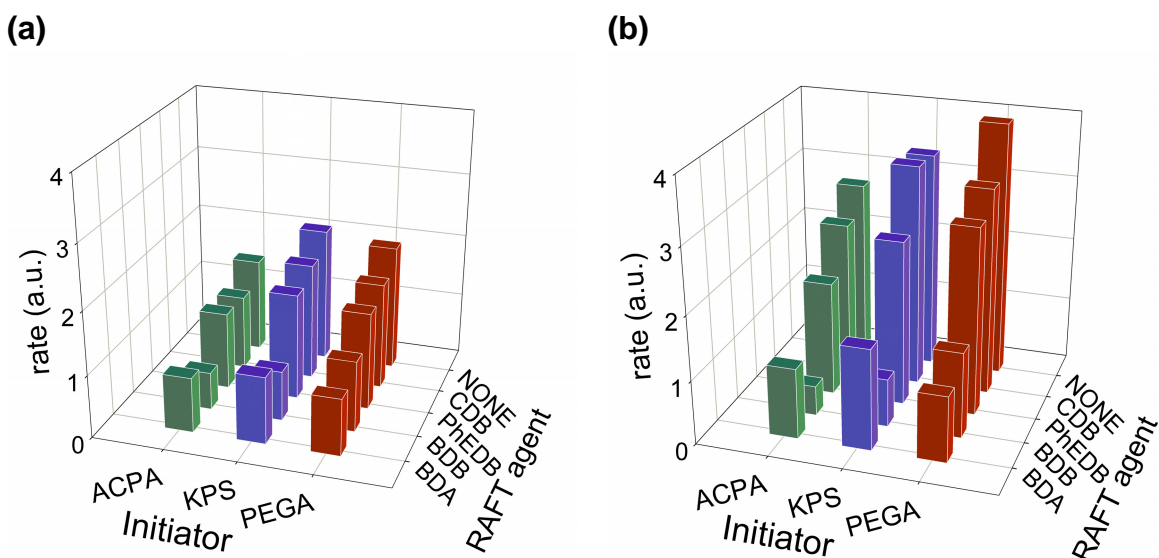


**Figure 17. Average polymerization rates\* for ab initio emulsion polymerization of styrene at 80°C with various RAFT agent-initiator combinations obtained from: (a) reaction calorimetry, and (b) gravimetric measurements**

\* Average values for the slopes of conversion-time curves between 10 and 80% conversion

#### 4.2.2. AIBN: polymerization rate, colloidal and molecular properties

Emulsion polymerizations initiated with AIBN resulted in massive coagulation. The high interaction of this coagulum with the metal parts of the calorimeter reactor hindered the calorimetric evaluation. The results of time dependent investigation in an all-glass reactor in the absence of RAFT agent (Table 4) shows a sudden drop in the solids content between a polymerization times of 180-240 min. The GPC analysis of these samples exhibited a steep jump in the number average molecular weight at the same point of time. At the end of polymerization more than 50% of the polymer formed was a coagulum around the stirrer. The number average molecular weight of the coagulum was similar to the samples taken before the sudden change. These results indicate that until about 60% conversion the polymerization mainly takes place inside the monomer phase. When the free monomer phase disappears, the coagulum becomes more and more solid and “precipitates” from the dispersion and the main polymerization locus shifts to the polymer particles.

**Table 4. Evolution of molecular and colloidal properties during the ab initio emulsion polymerization of styrene at 80°C initiated with AIBN and in the absence of RAFT agent**

Sampling time	Solids Content* (%)	Particle Size (nm)	M <sub>n</sub> (g/mol)	PDI
15 min	0.75	-	35480	1.813
30 min	3.04	99.4	40540	2.011
45 min	5.28	119.4	42580	2.234
60 min	6.40	132.6	42260	2.158
80 min	6.85	149.1	45380	2.282
100 min	8.50	160.7	45010	1.973
120 min	9.28	174.1	56560	2.575
150 min	11.76	186.5	60240	2.423
180 min	12.60	198.0	60840	2.523
240 min	6.64	234.1	189100	2.568
300 min	5.86	251.1	198400	3.060
coagulum	10.16 (g)	-	64770	2.410

\* in a recipe with 80g water, 20g styrene, 4g aqueous solution of SDS (5 wt. %), and 56mg AIBN

Consequently, the overall molecular weight distribution (MWD) during the polymerization represents the polymers formed in the different polymerization loci (Figure 18(a)), the low molecular weight part inside the bulky monomer phase and the high molecular weight part inside the latex particles. This scenario does not change in the presence of RAFT agents as the polymerization rates (Figure 18(b)), especially at the beginning of the polymerization, resemble the polymerization rates in bulk with the same initiator (Figure 11(a)).

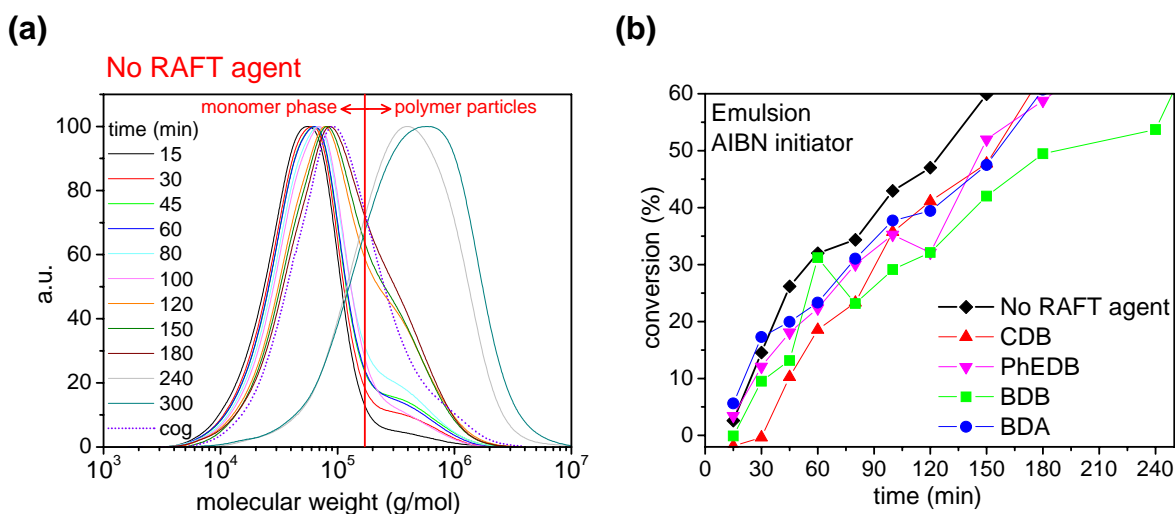


**Figure 18. Emulsion polymerization of styrene initiated with AIBN at 80°C (a) evolution of molar mass distribution in the presence of no RAFT agent. (b) conversion-time data in presence of various RAFT agents**

Figure 19(a) exemplarily displays the separation of the reaction mixture in two phases in the absence of stirring. The different color of both the upper monomer phase in Figure 19(a) and the remained solid polymer from both phases after drying (Figure 19(b)) proves the higher concentration of the RAFT agent in the monomer phase. After the conversion reaches above 60 %, the remaining RAFT agent is caught in the coagulum (Figure 19(c)).

Also, the GPC data in Figure 20 reveal the existence of two reaction loci as indicated by the distinct bimodality of the MWD. The lower molar mass peaks in both graphs represent the polymer formed in the monomer phase whereas the

higher molar mass product is formed in the polymer particles. In the final stages of polymerization when the viscous monomer phase coagulates and completely separates from the latex phase, only the high molecular weight polymer remains in the latex. The low molecular weight fractions show an increase with conversion as required for controlled polymerization, the high molecular weight fraction shows no change with conversion and hence, nearly no control. This result proves the importance of the concentration at the reaction locus for heterophase polymerization as discussed above. The MWD of the coagulum at the end of the polymerization shows that it is mainly composed of polymer formed under quasi-bulk polymerization condition. Only a very minor part originates from coagulated polymer particles.

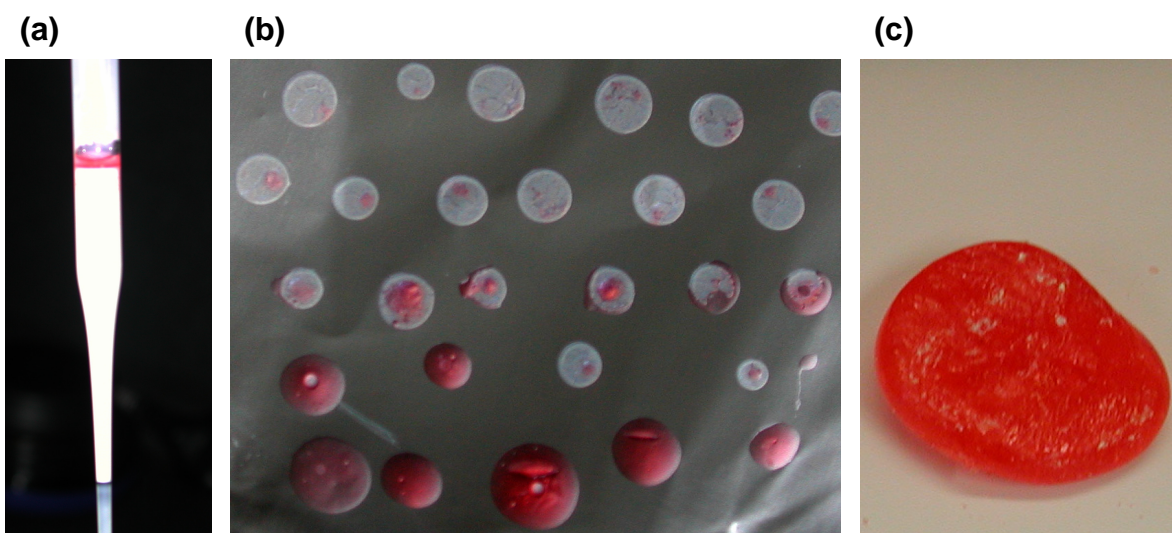


**Figure 19.** Ab initio polymerization of styrene initiated with AIBN in presence of RAFT agent PhEDB after 3 hours (a) separation of the phases in the sampling pipette (b) the solid polymer after drying (c) the coagulum

Moreover, the data in Figure 20(a) and (b) reveal an influence of the nature of the RAFT agent, particularly its hydrophobicity. The more hydrophobic RAFT agent CDB is less present in the polymer particles. Therefore, it has been mainly effective for controlling the polymerization in the monomer phase. In contrast, the less hydrophobic RAFT agent BDA reaches the polymer particles more easily, and thus control is observed in either phase.

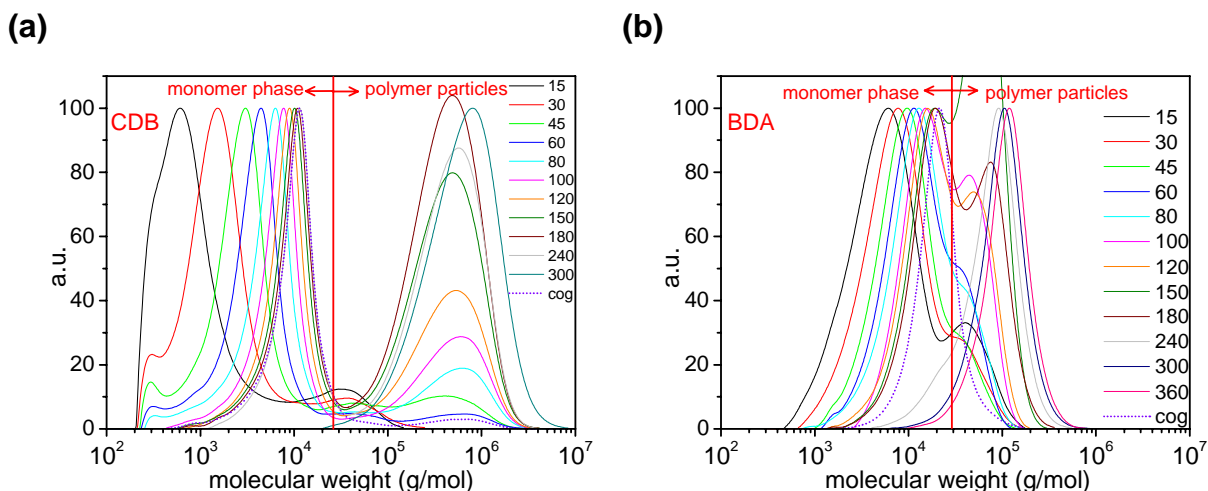


**Figure 20.** The evolution of molar mass distribution during the emulsion polymerization of styrene initiated with AIBN at 80°C in presence of RAFT agents (a) CDB and (b) BDA

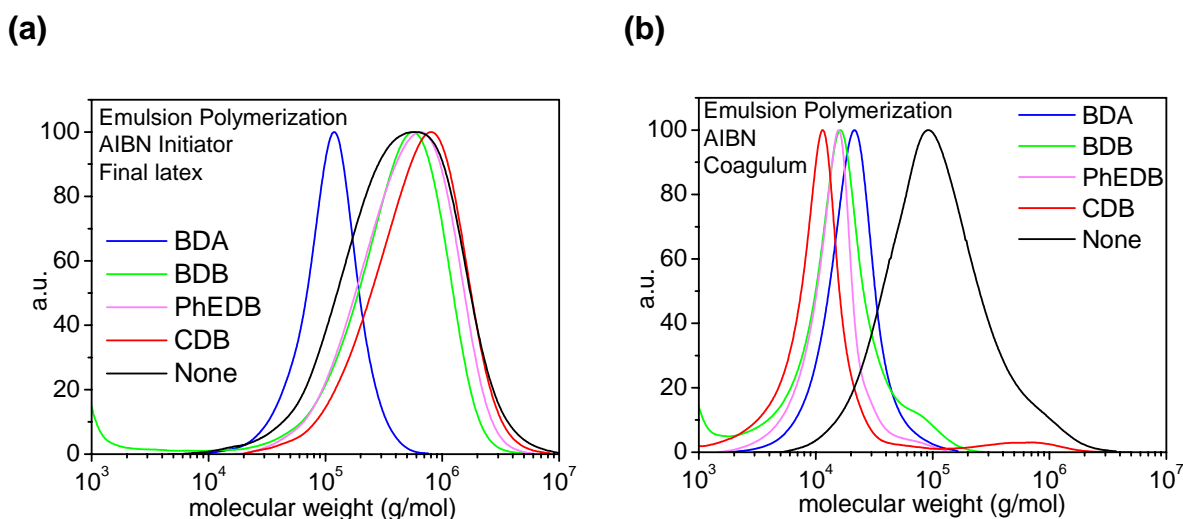


**Figure 21.** The molar mass distribution of (a) the final latex and (b) the coagulum from the ab initio emulsion polymerization of styrene at 80°C initiated with AIBN in the presence of various RAFT agents

The MWD of final latexes and the coagulum collected at the end of all polymerizations with AIBN is summarized in Figure 21. It can be seen that the less hydrophobic the RAFT agent, the final latex has a narrower MWD and a lower molar mass. For the coagulum the opposite is found. This is a clear evidence for the importance of the role of hydrophobicity and hydrophilicity of the RAFT agent in aqueous heterophase polymerization. A quantitative study on

transportation kinetics of RAFT agents from the monomer phase to polymer particles is discussed in Section 4.3.4.

### 4.2.3. The molecular properties obtained with the other initiators

Replacing AIBN with more hydrophilic initiators changes the conditions during the heterophase polymerization. The use of hydrophilic initiators (generally lyophilic initiators) reduces the portion of polymerization in the monomer phase and shifts the polymerization almost completely to the polymer particles. This has considerable consequences regarding the MWD also in the presence of RAFT agents. For example, comparing the MWD evolution during the polymerizations in the presence of the most hydrophobic RAFT agent CDB, initiated with AIBN, PEGA200, and KPS (Figure 20(a), and Figure 22(a)-(b), respectively) clearly exhibits the influence of the shift of reaction loci. Other examples are shown for BDB with PEGA200 and KPS in Figure 23 and for BDA with AIBN, PEGA200, and KPS in Figure 20(b) and Figure 24(a)-(b), respectively.

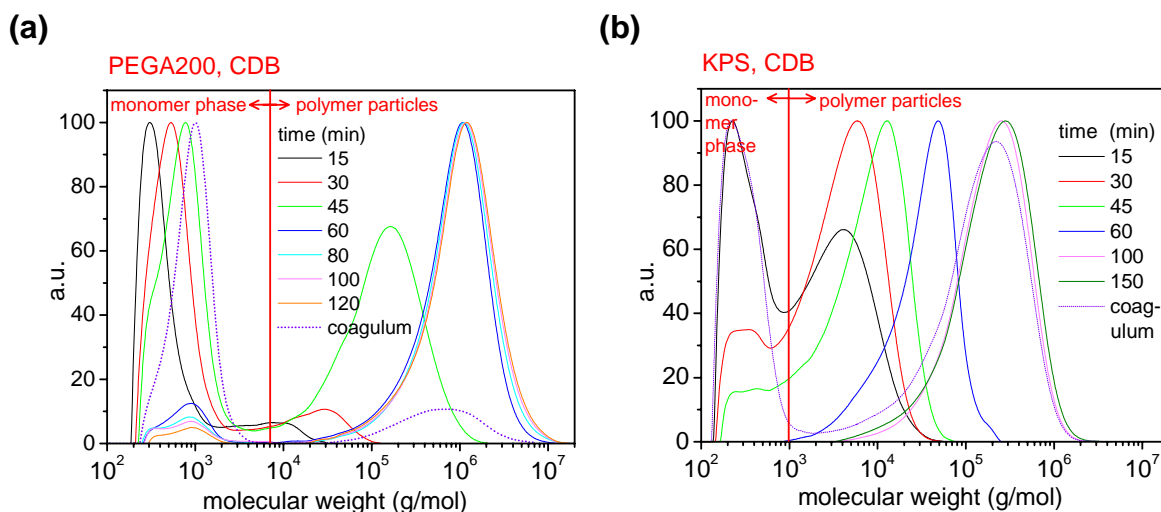


**Figure 22.** The evolution of molecular weight distribution during ab initio emulsion polymerization of styrene at 80°C in the presence of CDB as RAFT agents and initiated with (a) PEGA200 (b) KPS



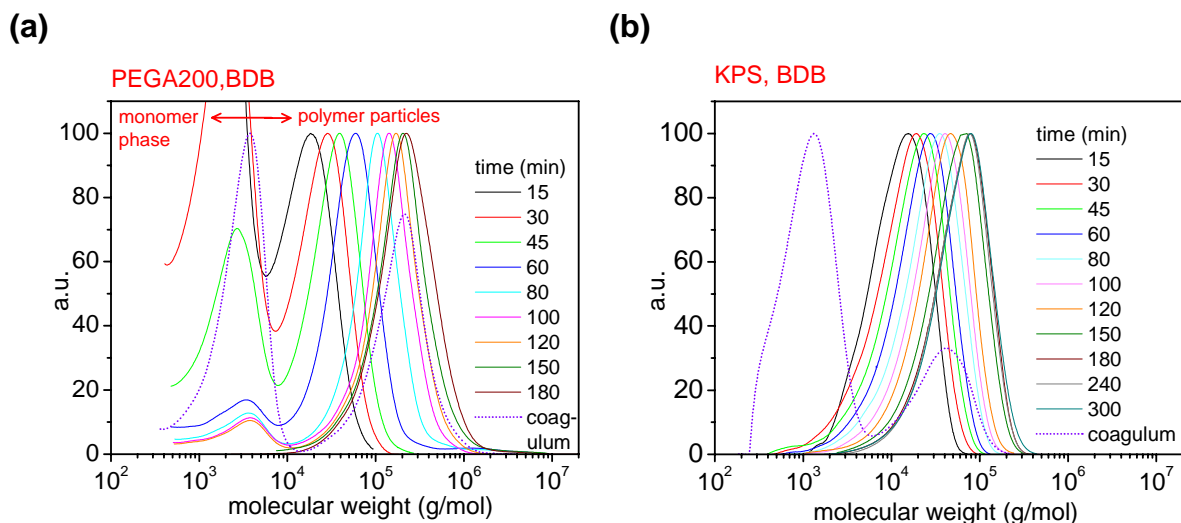


**Figure 23.** The evolution of molecular weight distribution during *ab initio* emulsion polymerization of styrene at 80°C in the presence of BDB as RAFT agents and initiated with (a) PEGA200 (b) KPS

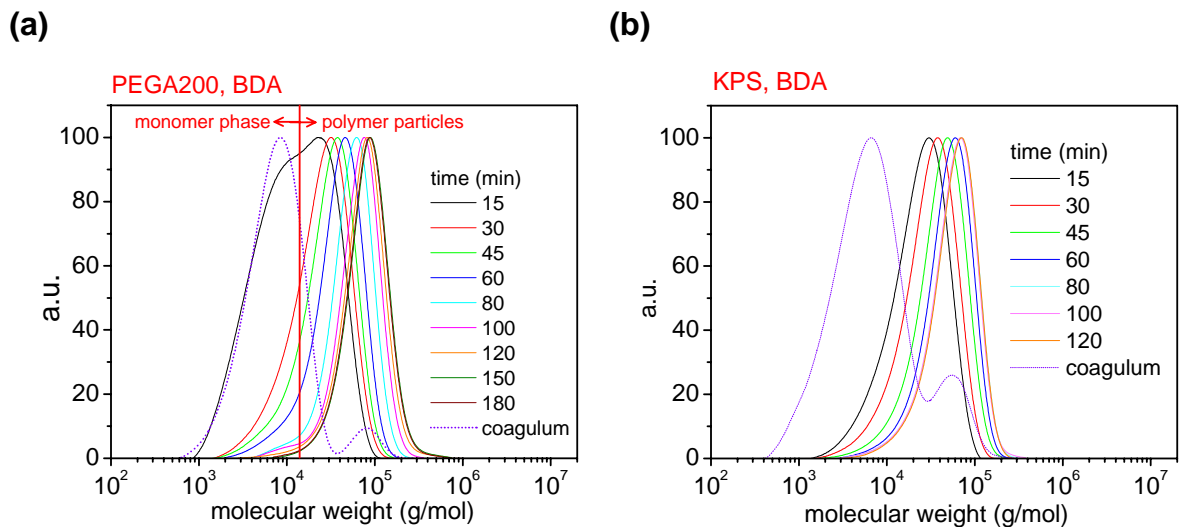


**Figure 24.** The evolution of molecular weight distribution during *ab initio* emulsion polymerization of styrene at 80°C in the presence of BDA as RAFT agents and initiated with (a) PEGA200 (b) KPS

All of these data clearly show that a high portion of controlled polymerization inside the monomer phase prevents control in the latex particle phase. In other words, the hydrophilicity of the initiator mainly determines the degree of control inside the latex particles with generally hydrophobic RAFT agents as investigated



here. For more hydrophobic initiators such as PEGA200 the degree of control inside the latex particles is determined by the relative hydrophilicity of the RAFT agent. The hydrophilicity of the RAFT agent determines the transport from monomer phase to the particles and hence its availability there. The more hydrophilic is the initiator the smaller is the number of initiating radicals in the monomer phase, consequently, the RAFT agent in the monomer phase has a higher chance to exit and travel to the polymer particles before being consumed by the radicals. This effect leads to a higher presence of the RAFT agent in the polymer particles and consequently, higher control of MWD in the latex phase.

Other experimental results that must be examined to verify the control of a radical polymerization are the polydispersity index and the linearity of the molar mass-conversion plot. The number average molecular weight ( $M_n$ ) must linearly increase with conversion and simultaneously, the PDI must decrease.

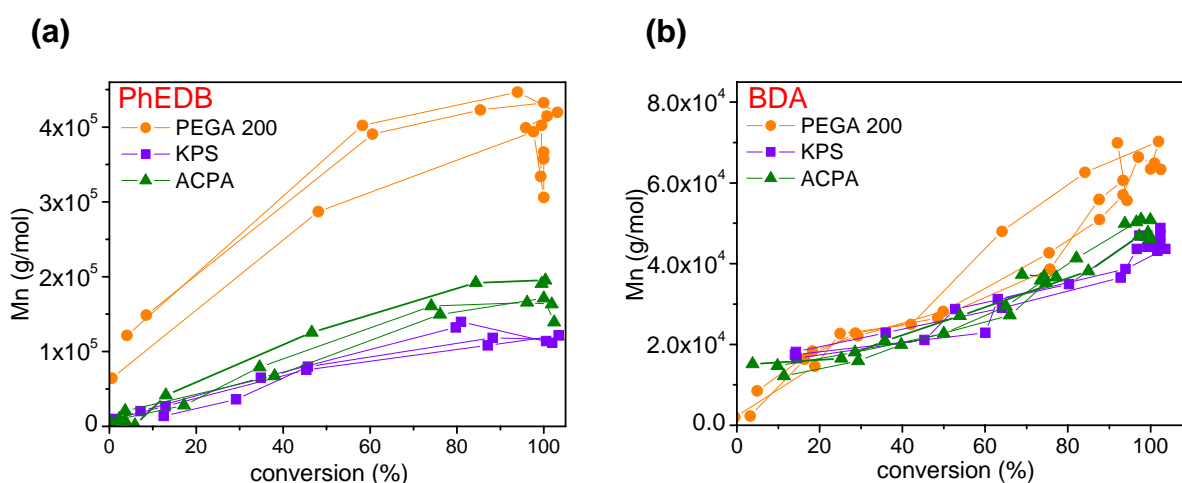


**Figure 25. The evolution of number average molecular weight during the ab initio emulsion polymerization of styrene at 80°C with various initiators and in the presence of RAFT agents (a) PhEDB (b) BDA**

Figure 25 shows an example  $M_n$  (obtained only from the polymer latex) increasing with conversion for both hydrophobic and hydrophilic RAFT agents. However, it is striking that towards the end of polymerization the  $M_n$  considerably decreases for systems where control has been less efficient (more hydrophobic

RAFT agent, here PhEDB). This is a feature usually observed in conventional polymerization in which towards the end of polymerization with considerable reduction in monomer concentration, the production of new radicals is more dominant than propagation. This results in the formation of a population of small radicals which lowers the number average molecular weight. For ab-initio emulsion polymerization of styrene, this effect is mainly observed for more hydrophobic RAFT agents and more hydrophobic initiators (Figure 25(b)).

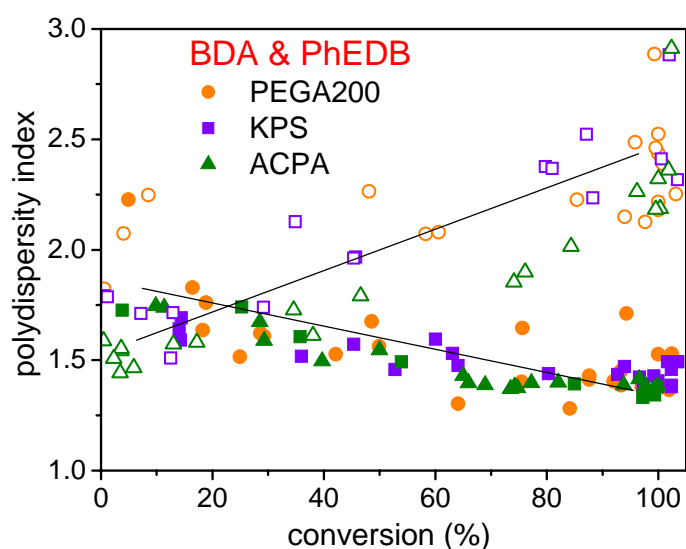


**Figure 26.** Evolution of the molecular weight distribution during the ab initio emulsion polymerization of styrene at 80°C with various initiators and in the presence of RAFT agents PhEDB (empty symbols), and BDA (full symbols), the lines are visual guides.

The polydispersity index does decrease with conversion only in the presence of more hydrophilic RAFT agents (here BDA in Figure 26). However, for the more hydrophobic RAFT agent, here PhEDB, the polydispersity grows with increasing conversion. This is interesting because in a homogeneous system with similar reaction conditions PhEDB controls the polymerization better than BDA (Figure 12). Of course, the peculiarity of the aqueous heterophase system is responsible for this difference. As demonstrated by computer simulation in section 2.3, this property depends on the concentration of the RAFT agent. Clearly in the

example shown, the concentration of the RAFT agent at the polymerization loci (polymer particles) is not high enough to efficiently control the polymerization. As the slope of PDI-conversion plot decreases for more hydrophilic RAFT agents, it is fair to attribute it to the higher capability of the RAFT agents to enter the particles via diffusion through aqueous phase.

#### 4.2.4. Coagulum formation and colloidal stability

Colloidal stability is a serious issue in any controlled radical polymerization. Coagulation is an undesired side effect also in RAFT system and for commercial applications it must be avoided. In general there are two reasons for coagulum formation in ab-initio heterophase polymerization: Colloidal instability of the dispersed phase, and substantial polymerization inside the free monomer phase. Colloidal stability should not be a serious issue as effective stabilizers are available to prevent it. As mentioned before, the coagulum in the considered system is the result of polymerization in the monomer phase and it is formed when the viscosity in the monomer phase increases.

**(a) at the beginning**



**(b) in the middle**



**(c) at the end**



**Figure 27. The formation of the coagulum during the ab-initio emulsion polymerization of styrene initiated with PEGA 200 in the presence of PhEDB**

The images in Figure 27 and Figure 28 give a visual impression of the formation of the coagulum during the ab initio emulsion polymerization of styrene in the presence of RAFT agent PhEDB. Note the difference in the appearance for both initiators at the end of polymerization. For PEGA200, the latex phase is colored

whereas for KPS the latex appears white and only the coagulum is deeply colored.

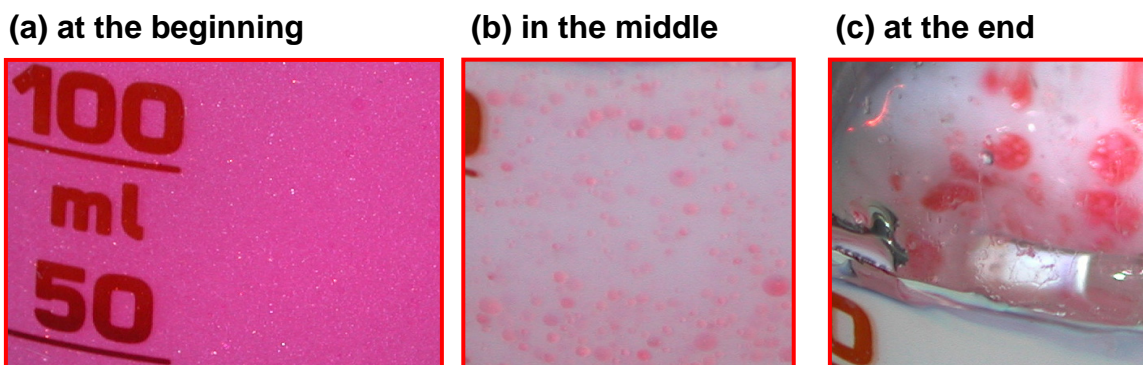


**Figure 28.** The formation of the coagulum during the ab-initio emulsion polymerization of styrene initiated with KPS in the presence of PhEDB

The quantitative analysis of the formed coagulum provides helpful information for verification of the proposed mechanisms. The results of this analysis are summarized in Figure 29.

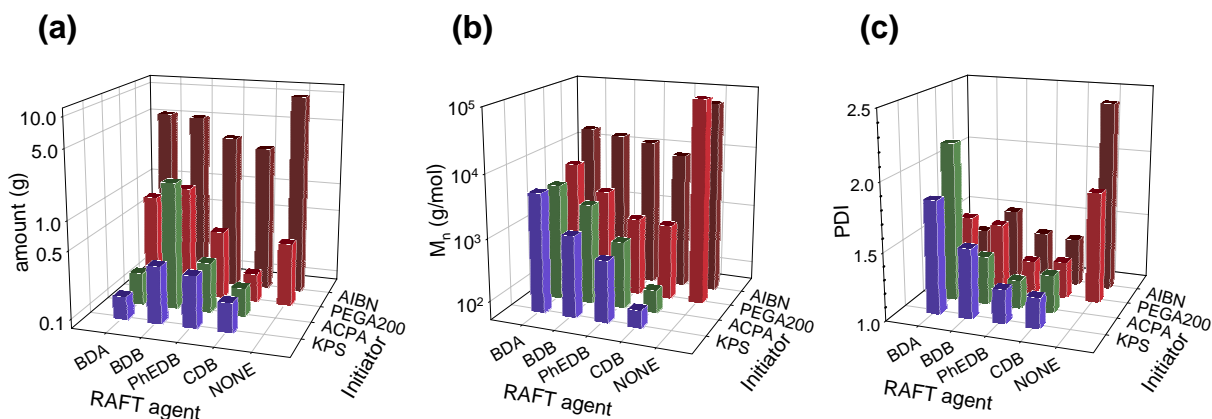


**Figure 29.** The coagulum formed during the ab initio emulsion polymerization of styrene in presence of various initiators and RAFT agents (a) the total amount in gram (b) the number average molecular weight (c) the polydispersity index (PDI)

In general, the amount of coagulum increases with increasing hydrophobicity of the initiator (Figure 29(a)). Regarding the RAFT agents the situation is not so clear. For the more hydrophilic initiators BDB leads to the higher amount of coagulation. In any case, the amount of coagulum is the lowest for CDB, the

most hydrophobic RAFT agent. These results might be understood considering that:

1. RAFT agents lower the rate of polymerization at the reaction locus.
2. The more hydrophilic the RAFT agent, the higher its concentration in the particle phase and the less in the monomer phase.
3. The lower the relative amount of RAFT agent, the relatively higher is the rate of polymerization in the corresponding phase.
4. Higher amounts of coagulum are formed for lower amounts of RAFT agents in the monomer phase.

When less hydrophobic RAFT agent is used, the rate of polymerization is lower in the polymer particles and higher in the monomer phase; therefore, higher amount of polymer forms in the monomer phase. When comparing the amount of coagulum formed in case of the three RAFT agents, CDB, PhEDB, and BDB, we clearly see that the trend is as expected. To explain why BDB, which is more hydrophobic than BDA, results in higher amount of coagulum, one has to recall the results depicted in Figure 11 and Figure 17, which compare the overall rates of polymerizations for different RAFT agents under homogeneous and heterogeneous conditions. BDB causes a lower rate in either case. This difference is expected to be due to the influence of their different activating groups, which means that benzyl activates the transfer reaction more than methyl group.

The data in Figure 29(b) show a smaller number average molecular weight of the coagulum for more hydrophilic initiators and more hydrophobic RAFT agents, which is reasonable with respect to the above discussion on the amount of coagulum.

Figure 29(c) demonstrates that the polydispersity index of the polymer formed in the monomer phase increases the less hydrophilic is the RAFT agent. This

confirms again that the less hydrophobic RAFT agents are present in the monomer phase in relatively lower amounts. Consequently, there is less control on molar mass distribution leading to a higher PDI. The influence of initiator is related to the hydrophobicity of the RAFT agent. In case of more hydrophobic RAFT agent, the relation is straightforward. The more hydrophilic initiator has a lower concentration in the monomer phase. This results in an increase in the ratio of RAFT agent to initiator concentration and consequently, higher control and lower PDI. However, a competitive situation might be reached for both hydrophilic RAFT agents and hydrophilic initiators. The concentration ratio of RAFT agent to initiator may either increase or decrease and consequently, the PDI can increase or decrease as well. An example of this effect is the higher PDI of polymerization with KPS than of ACPA when BDB is used as RAFT agent. Another example is the higher PDI obtained for the ACPA/BDA combination than for PEGA200/BDA.

In summary, the optimum polymerization system with the least amount of coagulum and highest degree of control would be the combination of KPS/BDA, which are the most hydrophilic initiator and the most hydrophilic RAFT agent.

#### **4.2.5. Particle size in RAFT ab-initio emulsion polymerization**

There is also a distinct influence of the nature of the RAFT agent on the average particle size of the final latexes as depicted in Figure 30(a). Interestingly, for each initiator the average particle size changes with the same pattern as the RAFT agent varies. It seems that the dithiobenzoate compounds employed in these polymerizations (i.e. CDB, PhEDB, and BDB) have an influence on the colloidal properties of the latex by decreasing the particle diameter significantly. BDA has almost no effect on the average particle size. Among the many parameters influencing the particle size, the ones that are varying in our polymerizations are the number and length of polymer chains, the surface activity of the chain ends, the final conversions, and the hydrophobicity of the organic additives (influencing

the particle swelling). Among these parameters, the final conversion is excluded since the particle size difference is the case throughout the polymerization. Each of the remaining parameters by itself also cannot be responsible for this pattern of change because it does not match the way that these parameters are varying in the system. However, a competitive relation of all these parameters might be possible.

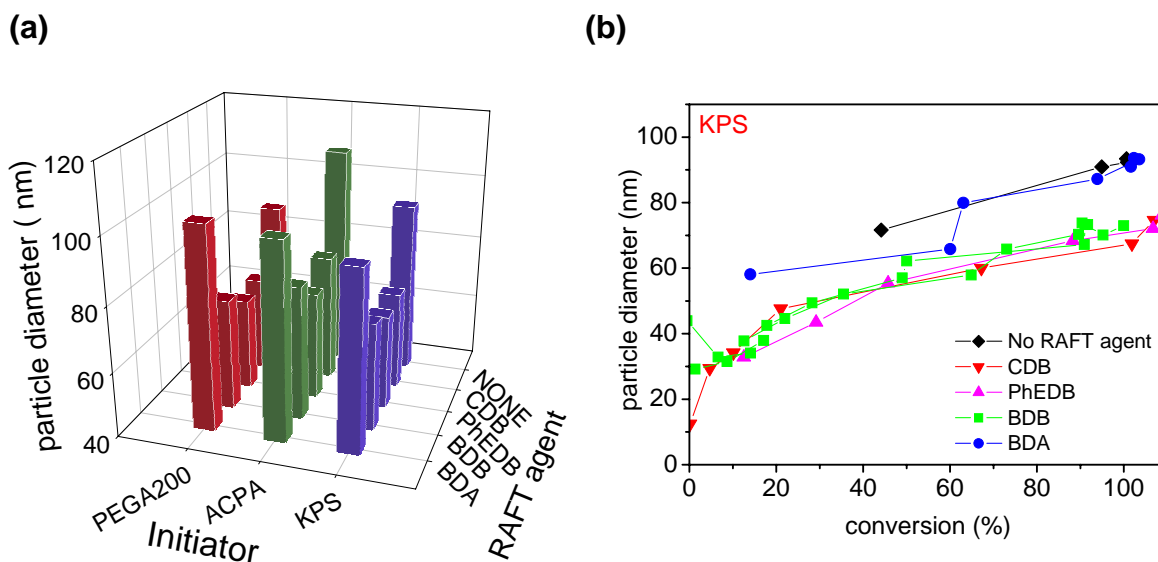


**Figure 30.** *Ab initio* emulsion polymerization of styrene at 80°C in presence of various RAFT agents (a) the final particle diameter after the polymerization initiated with various initiators (b) the evolution of the particle size during the polymerization initiated with KPS

It is an inherent feature of heterophase polymerization that the polymerization kinetics and also the rate of polymerization depend on the average particle size. Generally, the polymerization at given solids content is faster the smaller the average particle size. The data summarized in Figure 31 demonstrate that this is the case for the polymerizations considered here although the relation is expectedly influenced by the nature of the RAFT agent. For example polymerizations with CDB and BDB result in similar particle sizes but different rates, while BDA and BDB lead to different particle sizes but similar average polymerization rates.

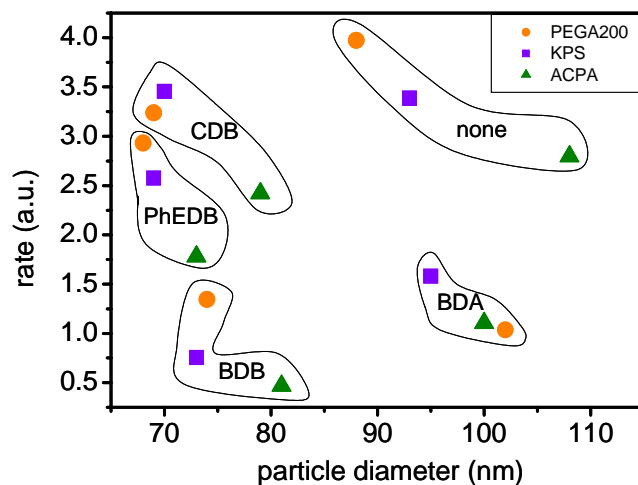


**Figure 31.** The average rate of polymerization versus average particle diameter for polystyrene latexes prepared by ab initio emulsion polymerization in the presence of various RAFT agent and initiators

#### 4.2.6. Number of polymer chains

The number of chains for solution and emulsion polymerizations in the presence of RAFT agent BDA is calculated, using the number average molecular weight and the conversion values (Figure 32). The number of chains in the absence of RAFT agent increases continuously during the polymerization, whereas it stays almost constant after an initial period in the presence of RAFT agents. This is a clear proof for the existence of a pre-equilibrium and an equilibrium period in polymerization with RAFT agents. In case of solution polymerization, not only the number of polymer chains is higher than in emulsion polymerization but also the duration of the pre-equilibrium is significantly shorter.

The pre-equilibrium period - the consumption of initial RAFT agent -for polymerizations in solution and emulsion extends to about 15 - 25% and 50 - 55% conversion, respectively. The latter corresponds to the stage where the free monomer phase usually disappears and means that as long as the free monomer phase exist, the RAFT agent has a chance to enter the particles. Therefore, it is



important for an effective control in aqueous heterophase polymerization that the RAFT agent is not consumed in the monomer phase but only in the dispersed particle phase.

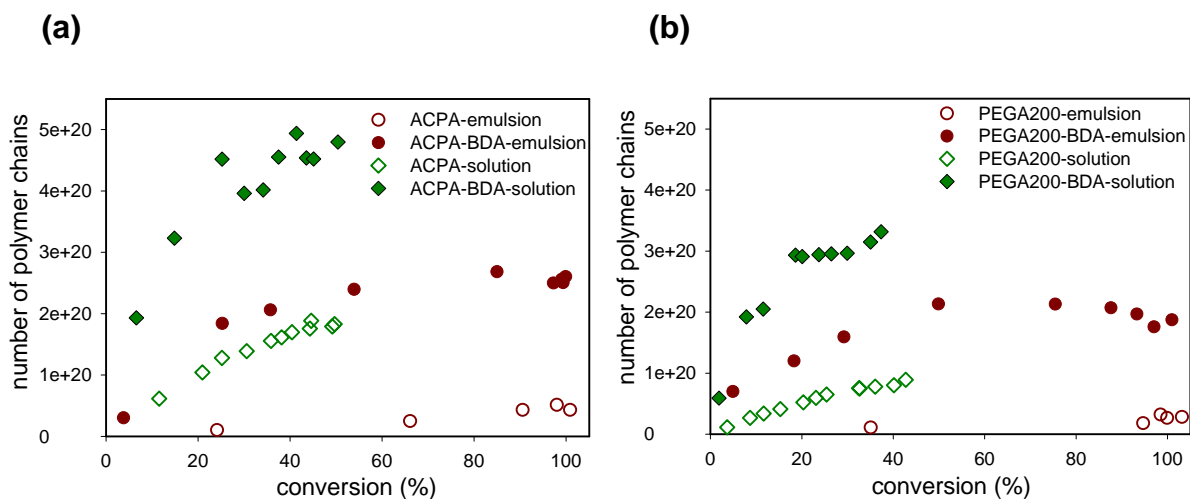


**Figure 32.** The number of polymer chains produced during the polymerization of styrene in emulsion and solution and in the presence and absence of RAFT agent BDA initiated with (a) ACPA and (b) PEGA200

### 4.3. Phase transfer of RAFT agents in heterophase polymerization

All the results presented so far prove that the hydrophobicity of the RAFT agent and hence, its distribution among the phases, plays a key role. The water solubility of the RAFT agents considered should be in the order CDB < PhEDB < BDB < BDA. However, no experimental data on the solubility, partitioning, or hydrophobicity of these RAFT agents are available. Such experimental data would be helpful not only to verify the assumed order of hydrophobicity and the proposed mechanisms, but also for modeling these systems. It was attempted to measure the partition coefficient of these RAFT agents between water and styrene. For this purpose, UV-Vis spectroscopy was presumed to be a proper technique to trace the RAFT agent in different phases because of the absorption in the visible band stemming from  $n \rightarrow \pi^*$  forbidden transition of their C=S group.

A primary set of experiments showed that these RAFT agents have none or negligible solubility in water. These experiments were carried out in a cuvette by placing solutions with a known concentration of RAFT agent in styrene on top of pure water and measuring the absorbance over a large visible range (300-800 nm) every 10 min. Even though the optical path through the water phase was long (50 mm), no absorbance could be detected. Replacing the pure water with a surfactant solution did not enhance the absorbance. Measuring the absorbance through the monomer phase indicated an increasing of the RAFT agent concentration with time which can be due to a faster diffusion of styrene into the water phase but is not an indication of diffusion of the RAFT agent into water.

These results were puzzling since the polymerization data (Section 4.3) clearly show that all of the RAFT agents are able to enter the particles. An observation made during the RAFT polymerization in another project<sup>101</sup> -where after nucleation a coloration of the particles was noticed- led to the following conclusion. An experimental simulation of typical conditions during a heterophase polymerization as similar and as simple as possible in the absence

of polymerization was thought to be a good approach to verify the expected differences between the RAFT agents. This approach is based on the use of proper seed latex instead of pure water or surfactant solution. A novel experimental set-up was designed for this purpose. Since this method is new and the details are crucial for the subsequent discussion, the next section describes this experimental setup before the results are discussed.

#### **4.3.1. The experimental setup and procedure**

As demonstrated in Figure 33, the set-up consists of a double jacketed reactor, especially built with an extra neck on the side for placing a special port for UV-vis immersion probe. The probe is inert to the reaction media and is connected to a vis spectrometer with optical fibers. The reactor is also equipped with a mechanical stirrer, condenser, and cooling and heating thermostats.

Special polystyrene nanoparticles were used to mimic the polymer particles that form during the initial period of ab-initio emulsion polymerization. These seed particles have a very small size to provide the possibility of having higher particle content while causing very low turbidity in water. The combination of the small size and low concentration of the particles is important for a sufficiently high monomer uptake and sufficiently low turbidity. For measuring the absorbed light, due to the chemical structure of the RAFT agent, the turbidity should be minimized. Turbidity is caused by scattering of light and is a function of the size and concentration of the particles, the wavelength of light, and other factors.

The monomer phase consisted of the solution of RAFT agent in styrene and it was slowly placed on top of the aqueous dispersion of the polymer nanoparticles. The amount of monomer solution was chosen to be below the swelling capacity of the particles to ensure the complete uptake. This is to make certain that the RAFT agent has to go to the particles and that no solution remain on top of the seed latex.

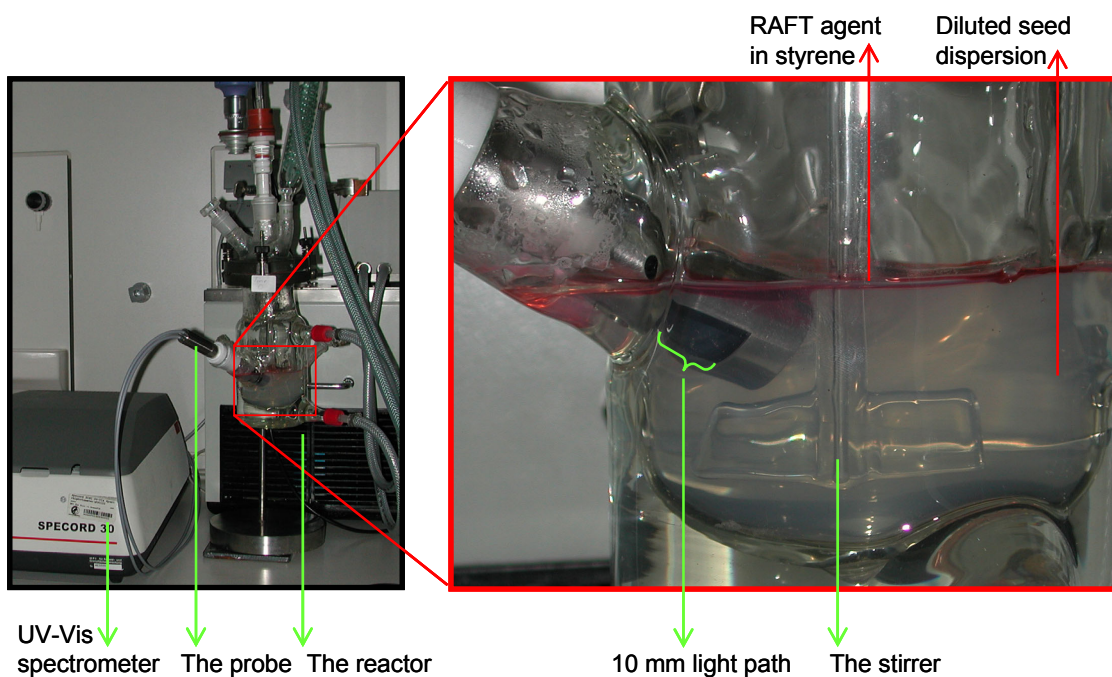
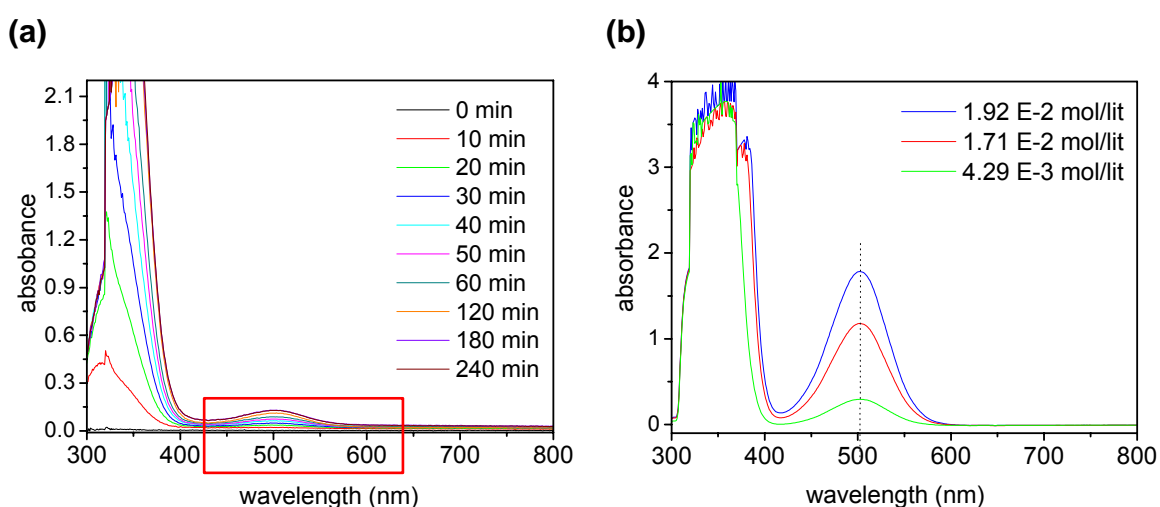


**Figure 33.** Details of the experimental set-up for in-line UV-vis measurement for tracing transportation of RAFT agent into the polymer latex

Before adding the RAFT agent solution, the dispersion was heated to 70°C and the absorbance baseline was measured after thermal equilibration. This baseline is to eliminate the initial turbidity caused by the particles. The chosen temperature is considered to be realistic for emulsion polymerization but is lower than the polymerization temperature in section 4.2 to minimize the possibility of thermal initiation over the relatively long measurement time. Very slow stirring (50 rpm) ensured sufficient mixing of the particles without dispersing the organic phase. The influence of the stirring on the absorbance of light was checked and was found out to have no effect on the absorbance. The absorbance was measured in the visible light range (300 to 800 nm wavelength) every few minutes upon addition of the monomer layer on top of the dispersion.

This method proved to be effective because the detection of the RAFT agent diffusing into the dispersion was possible and the absorbance increased with time. As an example, Figure 34(a) shows the appearance of the maximum

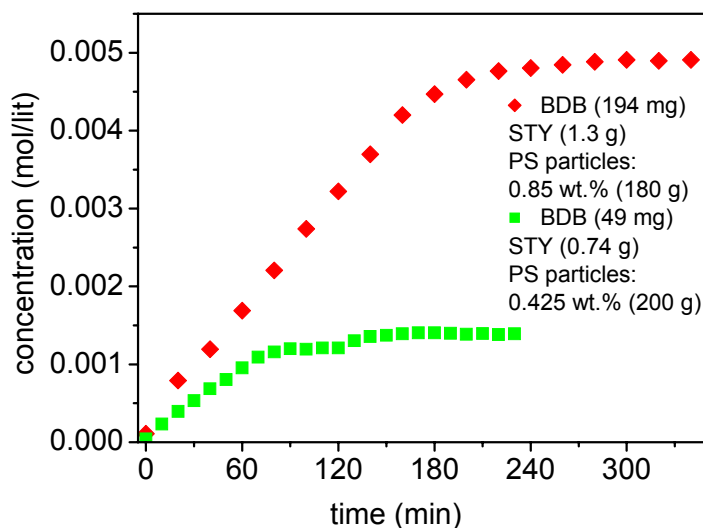
absorbance peaks in the dispersion at the same location observed for the maximum absorbance of the same RAFT agent in pure styrene at different concentrations (Figure 34(b)). The presence of polystyrene nanoparticles proved to be crucial because in a control experiment under same conditions but without particles, no absorbance corresponding to the RAFT agent occurred. Therefore, we can conclude that the RAFT agent together with the monomer is diffused into the polymer particles.



**Figure 34. The light absorbance of RAFT agent BDB (a) dispersion of polystyrene nanoparticles in water at different times (the area in the square is enlarged in Figure 36) (b) in pure styrene at different concentrations**

The maximum value of the absorbance was converted to concentration using the extinction coefficient measured for different concentrations of the RAFT agents in pure styrene. This is necessary because it is not possible to measure the extinction coefficient of the RAFT agent in polystyrene dispersion. This way of calculation is the closest estimation because the RAFT agent is believed to be only present in the dispersed organic phase. The conversion to concentration is necessary because different RAFT agents have different extinction coefficients and therefore, only the intensity of the maximum absorbance is not sufficient for comparing them. While this method of estimation might not be very accurate for providing absolute values it is definitely suitable for comparative studies and also

provides good estimates for the concentration variation of the organic molecules in the polymer dispersion.



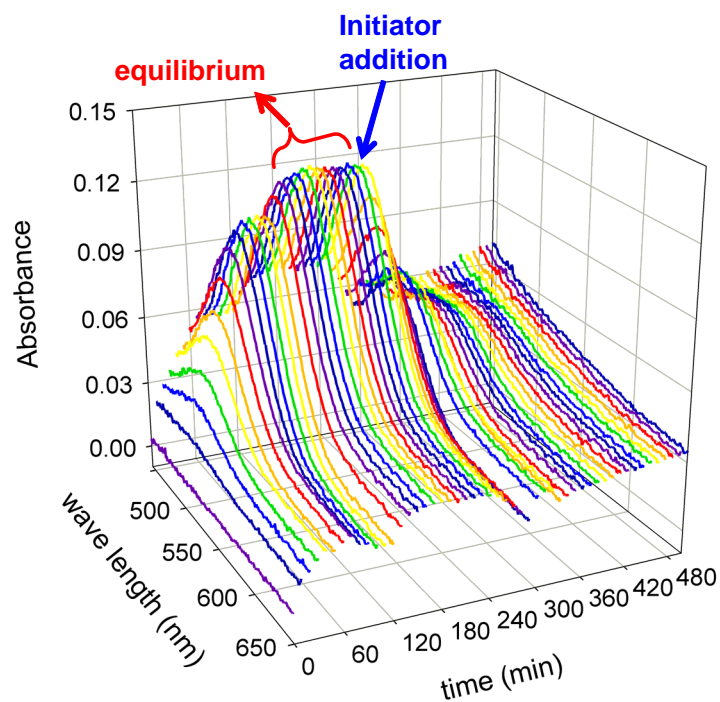
**Figure 35. Concentration development of RAFT agent BDB in dispersion of polystyrene nanoparticles for different initial concentrations of polymer particles and RAFT agent**

Figure 35 shows an example of the concentration-time relation obtained by this method when different concentrations of RAFT agent BDB and polystyrene nanoparticles are employed. Evidently, the concentration of the RAFT agent in the polymer dispersion increases until it reaches an equilibrium. The influence of the particle concentration on the sorption rate and time is also obvious. This figure very well demonstrates the sensitivity of this method for following the concentration alterations in the dispersed media even at very low concentrations. As the data provided for the lower concentration are sufficient for our comparative study, they were chosen as the standard condition for the rest of the measurements. For reasons of research efficiency, this made it possible to reduce the measurement time as well as to save RAFT agents and polymer particles. Moreover, lower concentrations of both particles and monomer lower the turbidity effect caused by the swelling and growth of the particles during the

measurement (in addition to the initial turbidity at the beginning of the experiments).

### 4.3.2. Polymerization of swollen seed particles

The experimental setup also allows following the polymerization online after the complete uptake of the RAFT agent in styrene solution. After addition of KPS, the absorbance started to decrease with time. All the stages of the whole process, which are sorption, swelling, equilibrium, and polymerization, are illustrated in Figure 36.



**Figure 36.** The light absorbance of RAFT agent BDB in dispersion of polystyrene nanoparticles in water at different times

Figure 37 displays the visual observation of this effect. Figure 37(a) and (b) show the dispersion at the beginning of the experiment and after reaching the equilibrium, respectively. Figure 37(c) shows the dispersion after completed polymerization. It illustrates the complete color loss few hours after the initiator

addition. Since the color arises from the dithioester group, the loss of color indicates that this group has disappeared. This figure also shows the increase in turbidity at the end of polymerization.

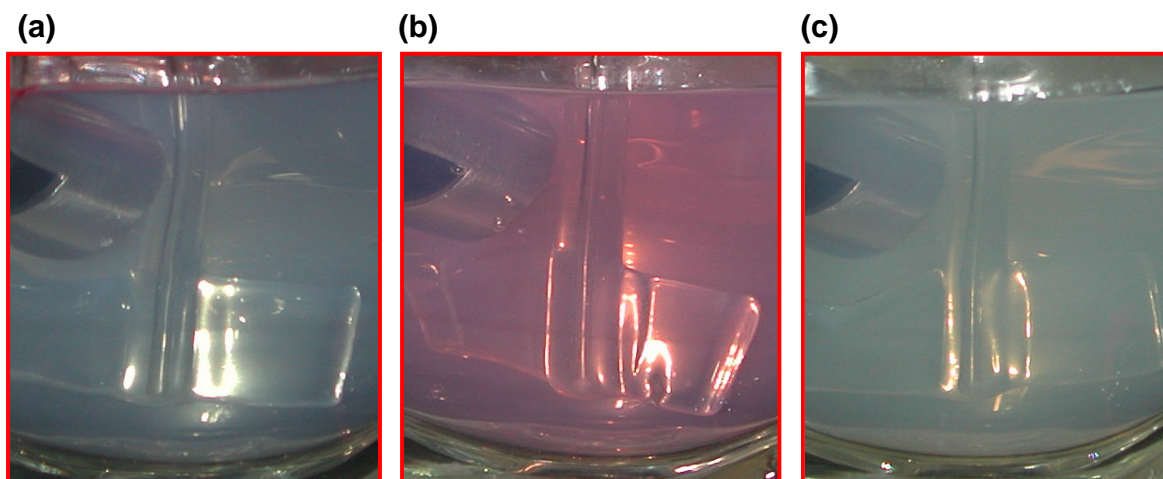


**Figure 37.** The presence of RAFT agent BDB in the polystyrene nanoparticle dispersion (a) at the beginning (b) after reaching the equilibrium and (c) few hours after the addition of KPS initiator

In order to check whether this decoloration is caused by the polymerization reaction or a side oxidation reaction, two additional experiments were carried out. In the first one, KPS was replaced by the water soluble nonionic radical initiator VA086 (structure given in Figure 38) and styrene by ethyl benzene. In the second experiment, only styrene was replaced by ethyl benzene. As it can be seen in Figure 39 in the first experiment, the color was maintained even many hours after addition of VA086.

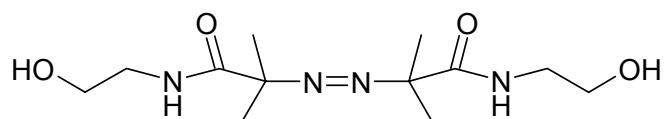


**Figure 38** the chemical structure of initiator VA086



This result indicates that the decoloration is not caused by the polymerization reaction but very likely by the action of persulfate or persulfate radicals via side oxidation reaction.

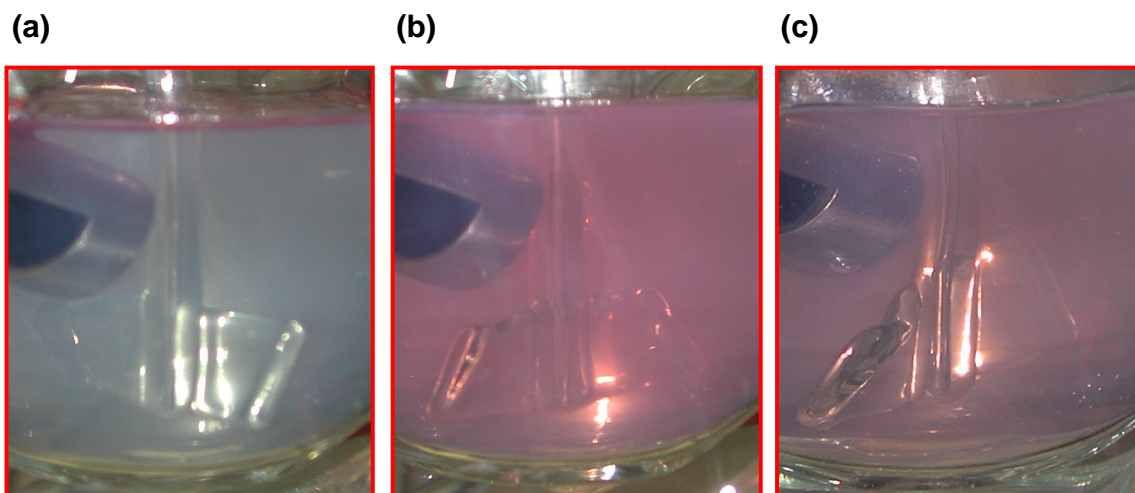


Figure 39. Diffusion of RAFT agent BDB dissolved in ethyl benzene into the polystyrene nanoparticle dispersion (a) at the beginning (b) after reaching the equilibrium (c) few hours after adding the initiator VA086

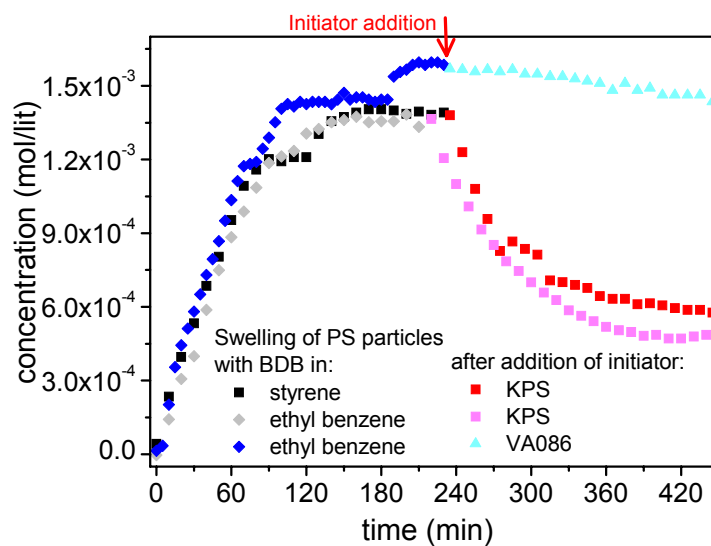


Figure 40. The concentration-time development of RAFT agent BDB in the polystyrene nanoparticle dispersion before and after addition of initiators KPS and VA086

This conclusion is supported by the results of the second experiment where styrene was replaced by ethyl benzene and exactly the same color loss was observed (Figure 40). The RAFT agent concentration-time plots for all three experiments (Figure 40) clearly show the discussed effect and additionally the reproducibility of the experimental method.

These results are basically confirmed by the data of the polymerizations in the all-glas reactors (section 4.3.4.) where with KPS at the end of the polymerization, the latex appears white with reddish colored pieces of coagulum floating around. Contrary, for PEGA200 (decomposed into carbon free readicals) both the latex and the coagulum are reddish colored.

The discoloration does not mean that there is no control at all. Obviously, at higher conversions there is a competition between the controlled chain growth via the RAFT equilibrium and the destruction of the RAFT agent groups by side oxidation reactions. As the average radical concentration per latex particle is low, also a lower concentration of the RAFT agent should be enough for an effective control (compartmentalization effect).

Moreover, these results allow drawing important conclusions regarding the entry mechanism of radicals into the latex particles during heterophase polymerization which will be discussed briefly in the following section.

### **4.3.3. Radical entry into latex particles**

As the polymer particles are the main locus of polymerization during any kind of heterophase polymerization, the entry of radicals in the case of lyophilic initiators is of crucial importance and a matter of ongoing discussion since decades. Ugelstad and coworkers<sup>102</sup> assume that the initiator decomposition or the initiation reaction determines entry and hence it is most likely that primary initiator radicals enter the particles. Another approach is based on the assumption that

radicals grow in the continuous phase until they become surface active before they can enter the particles<sup>103</sup>. Until today no direct experimental proof was given to support one or the other assumption.

Fortunately, the experimental results presented in the former section allow a clear and unambiguous proof on which species enter the particles. These results show that either initiator or primary initiator radicals enter the particles. This statement is based on the following experimental facts:

1. The discoloration is only observed for potassium peroxydisulfate as initiator.
2. The presence of a monomer such as styrene has no influence on the observed effect.
3. Both the peroxydisulfate dianion and the sulfate ion radical are strong oxidizing agents<sup>104</sup> and might be responsible for the side oxidation reaction destroying the RAFT agent.
4. The oxidation power of carbon radicals is obviously not high enough to degrade the RAFT agent as proven by the experiments with primary carbon radicals.

The conclusion of these experiments is of paramount importance for the mechanism of emulsion polymerization as the reasonable assumption that primary radicals enter the latex particles and that surface active of growing radicals is no prerequisite for radical entry is experimentally verified. These conclusions have been confirmed by similar results of another project<sup>101</sup>, in a series of seeded polymerization with various kinds of monomers.

#### **4.3.4. Transport of different RAFT agents**

These measurements were repeated for other RAFT agents as well. The results summarized in Figure 41 show that indeed these RAFT agents diffuse into the dispersion with different rates. As expected this rate is higher in the order of

BDA>BDB>PhEDB=CDB. The abrupt changes during the equilibrium are supposedly artifacts caused by sudden electronic changes in the recording devices. The order observed and also the small difference for CDB and PhEDB matches perfectly with the experimental results and explanations given in Section 4.2. As demonstrated by computer simulations in Section 2.3, higher control and livingness in polymerization is achieved with higher concentrations of the RAFT agent. It can be seen in Figure 41 that 30 minutes after adding the RAFT agent solutions, the concentration for BDA in the polymer particles is at least twice as high as that for BDB and four times higher than that for both PhEDB and CDB.

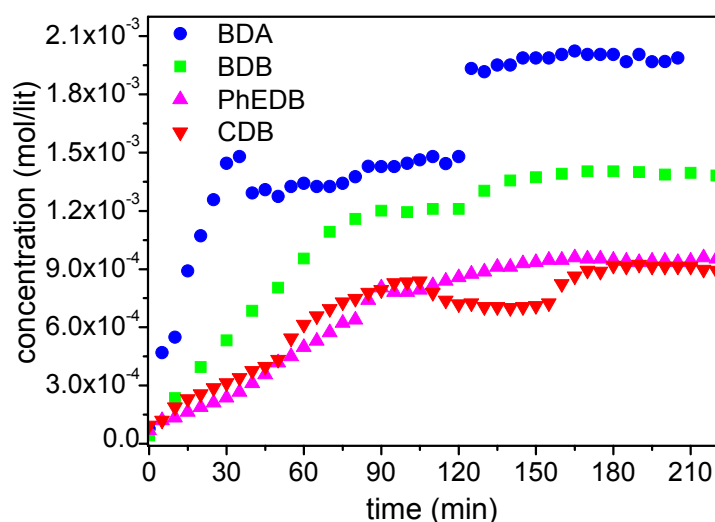


Figure 41. The change in the concentration of various RAFT agents in the dispersion of polystyrene nanoparticles in water at different times

#### 4.3.5. Carrier for the transport

Methyl methacrylate (MMA) is a good solvent for BDB. Moreover, it has higher water solubility than styrene. However, when the same measurement with BDB was carried out with MMA instead of styrene, the rate of its transportation into the particles was significantly slower (illustrated in Figure 42). An explanation might be that MMA is too hydrophilic to transport the RAFT agents as effective as

the other solvents. This means that a complex relation between all of the participating components influences the rate of sorption. This effect leads us to assume that under any given conditions, several parameters play an important role for sorption of hydrophobic organic molecules such as RAFT agents into the polymer particles:

- The hydrophobic organic molecule needs to be soluble in the carrier.
- The carrier must be a solvent for the polymer particle.
- The hydrophobic organic molecule needs a less hydrophobic carrier than itself to be transported into the particles.
- The carrier must have an optimum solubility in the aqueous phase

All in all, the sorption process is the on the one hand, cooperative and on the other hand, competitive. Cooperative action is the support of the transport of the more hydrophobic component by its carrier. The competitive action is given by solubility of both of them in the continuous and dispersed phase.

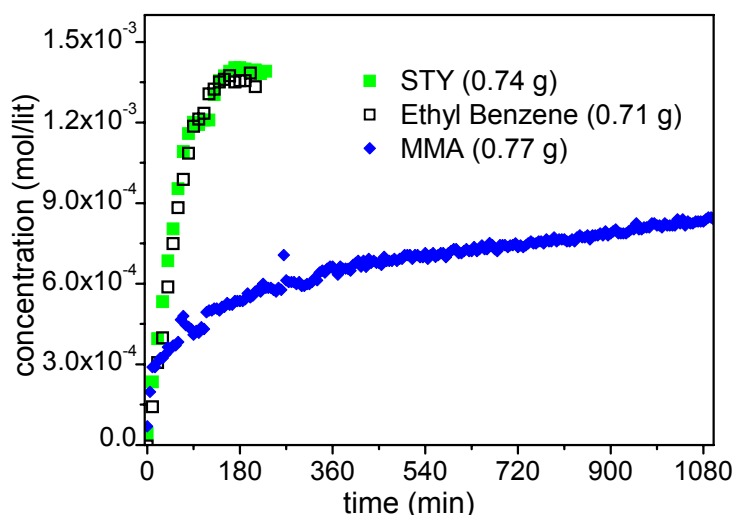


**Figure 42.** The change in the concentration of RAFT agent BDB in the dispersion of polystyrene nanoparticles in water at different times when it is dissolved in different solvents

#### 4.3.6. An approach for preparation of composite particles

If the above-mentioned conditions are fulfilled even extremely hydrophobic molecules can be transferred into the polymer particles. Examples are given for the dye Sudan IV and pentacene. Pentacene is a very hydrophobic and stiff fluorescent molecule (Figure 43) and, as estimated by Yalkowsky and Banerjee<sup>105</sup>, it has only a solubility of about  $10^{-11}$  M in water. Its solubility in organic solvents is also very limited.

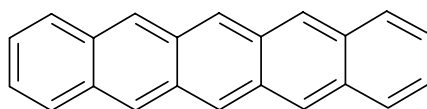


Figure 43 structure of pentacene molecule

Therefore, a saturated solution of pentacene in ethyl benzene has a considerably lower molar concentration comparing to the standard concentrations used for RAFT agent solutions. However, by placing the saturated pentacene solution in ethyl benzene on top of polystyrene latex accompanying with gentle mixing and heating, it was observed that the polymer latex took up all the solution. This was confirmed with fluorescence analysis (Figure 44).

Sudan IV has a higher solubility in ethyl benzene. Therefore, it was possible to prepare a solution with similar concentration to those of the RAFT agents. Upon placing this solution on top of the polystyrene latex, its uptake by the particles started very quickly as it could be observed by the red coloration of the latex. After 20 hours, all the ethyl benzene had been sucked up completely by the particles and a dried layer of Sudan IV crystals remained on top of the polymer dispersion.

These results confirm that sorption of the particular components of mixtures is an interplay of cooperative and competitive action of components. The proper uptake of hydrophobic organic molecules such as Sudan IV and pentacene is

only possible by applying appropriate solutions. This finding opens a variety of possibilities to modify latex particles with even extremely hydrophobic additives.

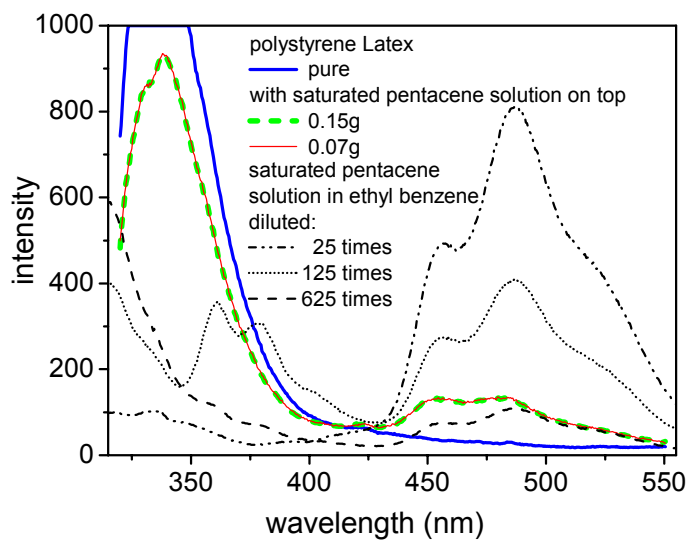


**Figure 44. Fluorescence spectrum of pentacene in ethyl benzene measured in solution and polystyrene latex**

#### **4.4. Heterophase polymerization of styrene with RAFT at room temperature**

Recently, it was found out that radical heterophase polymerization of styrene takes place in micellar aqueous media at room temperature in the presence of non-redox initiators<sup>100</sup>. The initiators varied from extremely water-soluble KPS to very oil-soluble BPO and AIBN. Furthermore, the presence of high amount of surfactant was a requirement for polymerization in such a system and the conversion rate depended on the total surface area. All of these lead to the conclusion that the decomposition of the initiator is promoted by interfacial energy, however, the detailed mechanism is not known yet.

The employment of the RAFT agent to such a system could be advantageous to further understanding of both the RAFT process and the ab-initio heterophase polymerization under such a particular condition. This is the first attempt to our knowledge on the RAFT polymerization in room temperature under heterophase conditions. The earlier works in homogeneous systems at ambient temperatures are reported by Quinn et al.<sup>106</sup> for polymerization of methyl acrylate and excess amount of AIBN initiator, and by Barner et al.<sup>107</sup> and Barner kowolik et al.<sup>108</sup> by means of gamma irradiation of styrene. In this chapter the results of ab-initio heterophase polymerization of styrene with BDA as RAFT agent are discussed.

##### **4.4.1. The influence of the initiator concentration**

As mentioned before, for a successful CRP with RAFT, the ratio of RAFT agent to initiator is very important and the number of RAFT agent molecules must exceed the number of primary radicals. Besides, every consumed RAFT agent and primary radical is responsible for formation of a new chain. A very high concentration of both initiator and the RAFT agent results in extremely low molar mass polymers. The initiator concentration used in the original work<sup>100</sup> is very high and there is not yet a systematic investigation of its influence. In order to



find an optimum initiator concentration for further perusing of this kind of polymerization in the presence of BDA, the effect of different initiator concentrations in the absence of RAFT agent was investigated. KPS and AIBN as hydrophilic and hydrophobic initiator, respectively, were chosen for the following study.

Figure 45 indicates an unusual relationship between the initiator concentration and the conversion. Obviously, the initiator concentration must be above a certain threshold to induce polymerization and there are only minor differences between both initiators regarding the index yield for a given concentration. Taking these results into consideration, the second highest initiator concentration was chosen for further investigations on RAFT-mediated polymerizations.

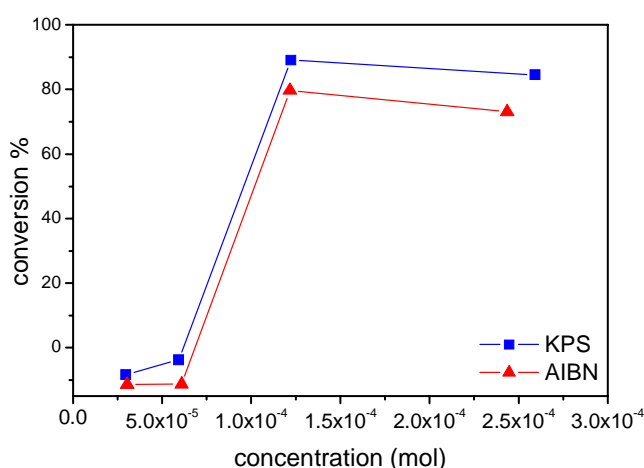


**Figure 45.** The conversion-concentration relation for the ab-initio heterophase polymerization of styrene at room temperature for 24 hours in the presence of KPS and AIBN as initiator

#### 4.4.2. Time-dependent characteristics at room temperature

Despite the scatter of the experimental data, the fact that polymers are produced during the polymerization in the absence of RAFT agent indicates the generation of primary radicals and their subsequent propagation at room temperature. The

extreme retardation in the presence of BDA, as seen in Figure 46 (a) indicates that the addition of RAFT agent to the radicals even at such low temperature is considerably faster than the rate of propagation. It appears that a very slow fragmentation is responsible for the retardation and therefore, the fragmentation is rate determining

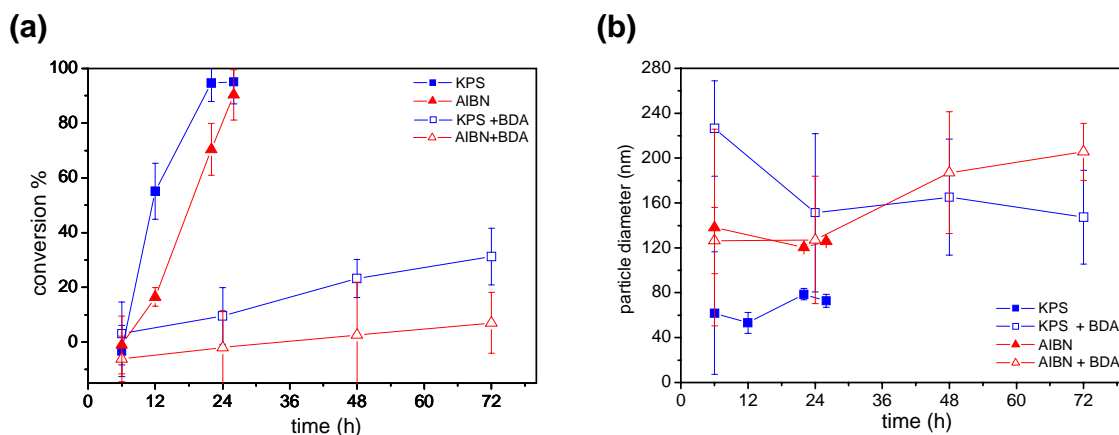


**Figure 46.** Ab initio heterophase polymerization of styrene at room temperature in the presence and absence of RAFT agent BDA and initiated with KPS or AIBN (a) average conversion vs. time (b) average particle diameter vs. time (averages are taken over six polymerization repeats)

The observed retardation is possibly not caused by the irreversible termination of intermediate species, since the observed increase of molecular weight as depicted in Figure 47 confirms that the RAFT process does take place, i.e. the propagation of radicals between cycles of activation and deactivation. The GPC data in Figure 48 show that without BDA the molecular weights are much higher and do not change with the reaction time.

The particle size as shown in Figure 46 (b) is larger in the presence of BDA. Although the reason for this is not yet fully understood it might be attributable to the significant increase in the number of chains.

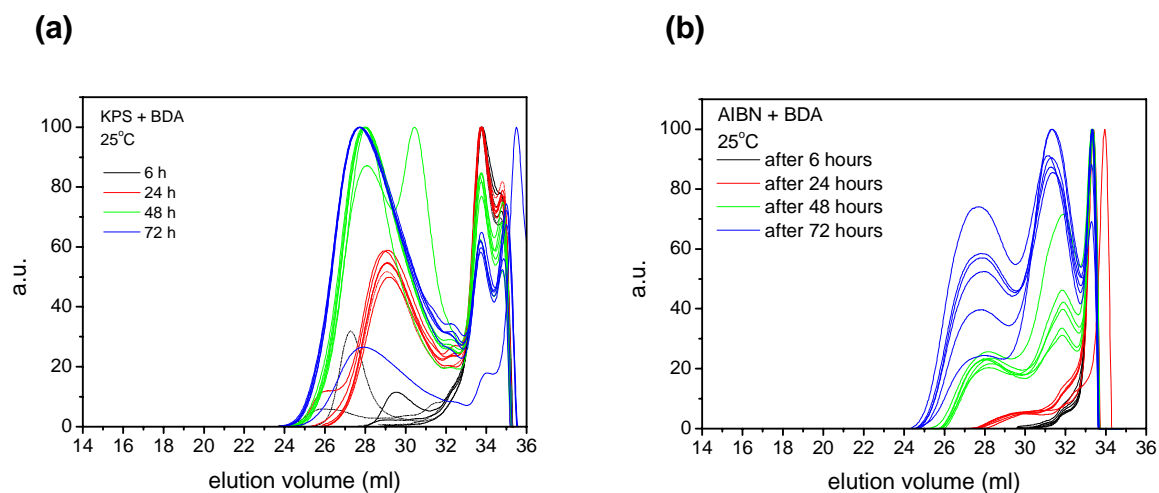


**Figure 47.** The molar mass distribution for ab initio heterophase polymerization of styrene at room temperature in the presence of RAFT agent BDA initiated with (a) KPS and (b) AIBN, after 6, 24, 48, and 72 hours

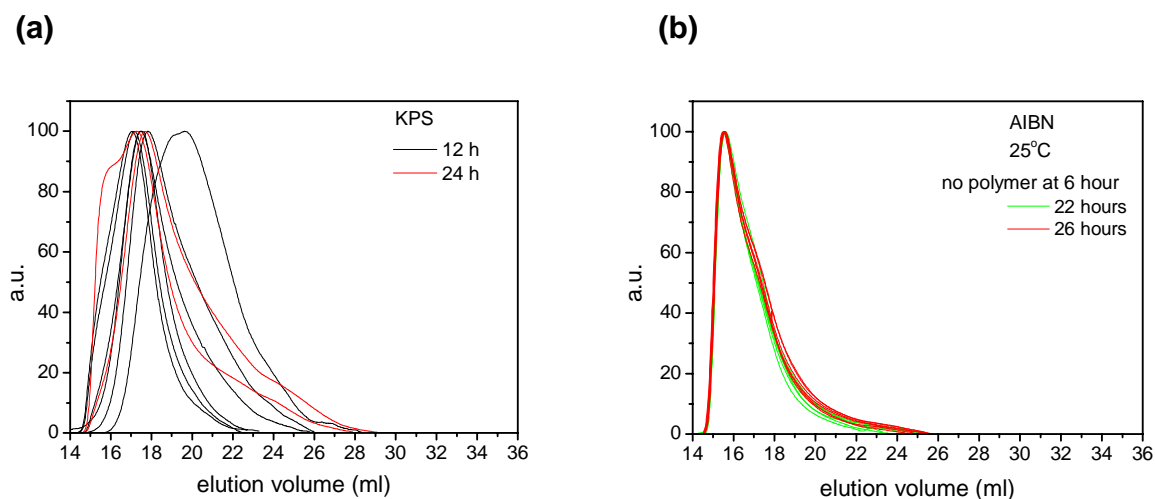


**Figure 48.** The molar mass distribution for ab initio heterophase polymerization of styrene at room temperature in the absence of RAFT agent and initiated with (a) KPS after 12 and 24 hours and (b) AIBN after 22 and 26 hours (there was no polymer after 6 hours)

#### 4.4.3. The influence of temperature

If the origin of retardation especially at low temperature is slow fragmentation, then with increasing temperature we should observe faster polymerization and higher molecular weights. Investigation of the samples taken at given times from

polymerizations carried out at different temperatures, shows both effects are really observed as proven by the data given in Figure 49 and Figure 51.

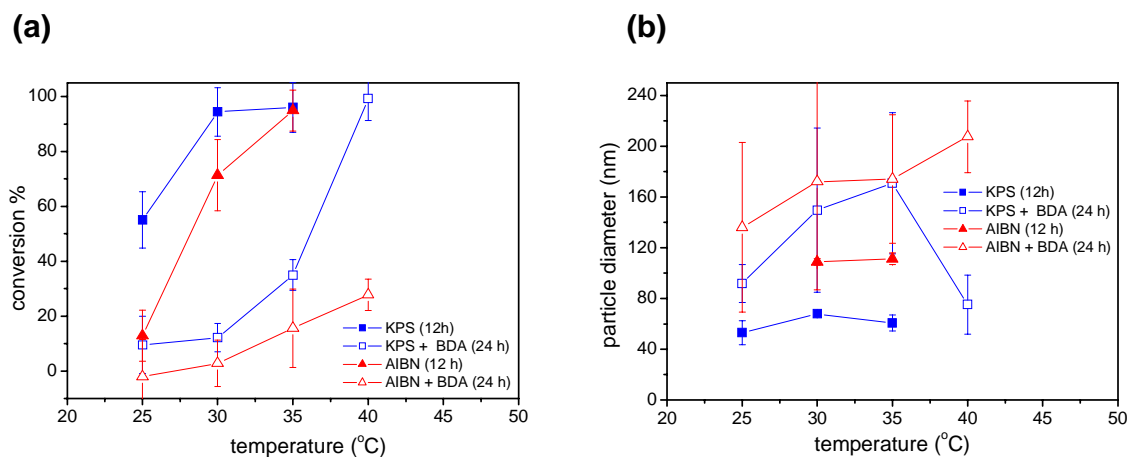


**Figure 49.** Ab initio heterophase polymerization of styrene at different temperatures in the presence and absence of RAFT agent BDA and initiated with KPS or AIBN after 12 hours (a) conversion-temperature (b) particle diameter-temperature (averages are taken over six polymerization repeats)

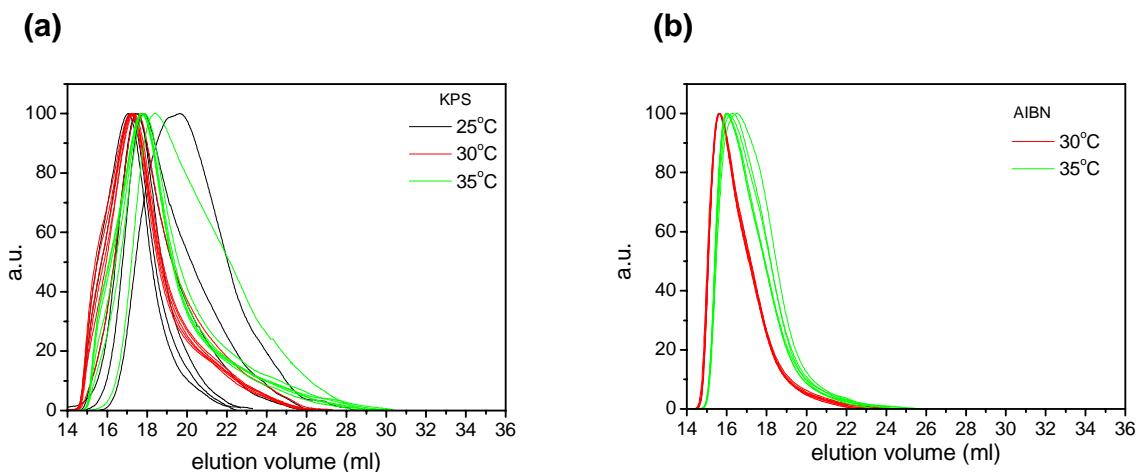


**Figure 50.** The molar mass distribution for ab initio heterophase polymerization of styrene at different temperatures in the absence of RAFT agent and initiated with (a) KPS and (b) AIBN, after 12 hours

The conversion ( $X$ ) – temperature ( $T$ ) dependence (Figure 49(a)) for both initiators shows an interesting effect as in the absence of BDA  $dX/dT$  is decreasing whereas it is increasing in the presence of BDA with increasing

temperature. Again the average particle size is larger for the runs with BDA over the whole temperature range (Figure 49(b)).

The molecular weight distributions shown in Figure 50 indicate that in the absence of the RAFT agent the molecular weight is slightly shifted to smaller values as one might expect, especially in case of AIBN. Contrary, the average molecular weight for the polymerizations in the presence of BDA increases in both cases (Figure 51(a) and (b)) with increasing temperature. Also this effect is expected for at least two reasons. First, the conversion increases with temperature and second, also the fragmentation rate might increase. The multimodality of the molar mass distribution in presence of the RAFT agent, especially with AIBN as initiator, is a sign of occurrence of polymerization in different reaction loci, i.e. the polymer particles and the monomer phase.

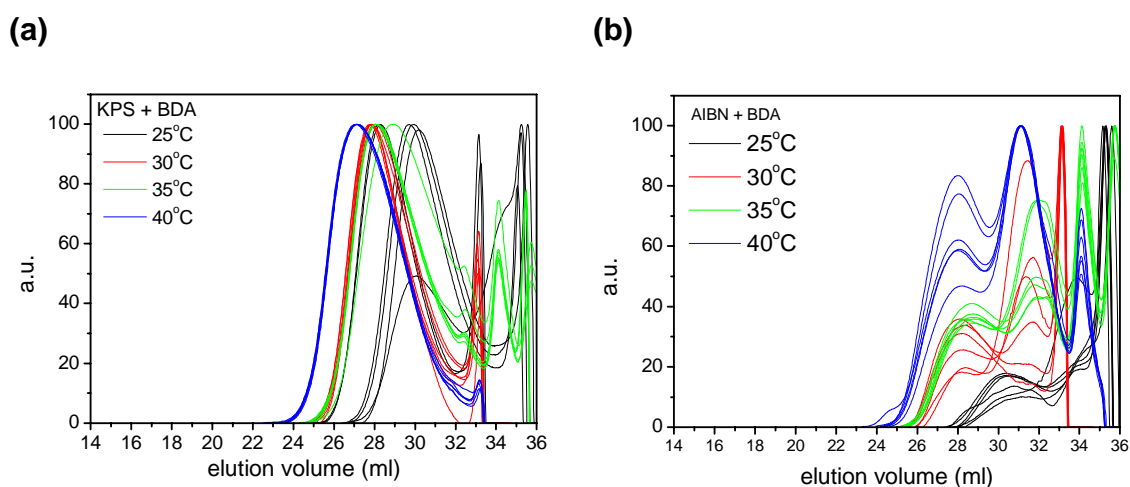


**Figure 51.** The molar mass distribution for *ab initio* heterophase polymerization of styrene at different temperatures in the presence of RAFT agent BDA and initiated with (a) KPS and (b) AIBN, after 12 hours

## 5. Conclusion and Outlook

This thesis is a comprehensive study on the role of hydrophilicity and hydrophobicity of different reaction components - namely the initiator and the controlling agent - on the characteristics of controlled radical polymerization of styrene in aqueous heterophase system via reversible addition-fragmentation chain transfer (RAFT).

In the first part of this work, the influence of various initiators and RAFT agents with varying water solubility on the reaction rate of ab-initio emulsion polymerization was studied by means of reaction calorimetry<sup>109</sup>. These results revealed the strong influence of the type and combination of the RAFT agent and initiator on the polymerization rate and its profile as well as on the molecular and colloidal characteristics of the final polymer latex. Time-dependent investigations in all-glass reactors allowed attaining more information on the evolution of the characteristic data such as average molecular weight, molecular weight distribution, and average particle size. Comparison of these results with similar polymerizations performed in homogeneous media revealed the importance of the peculiarities of the heterophase system such as compartmentalization, swelling, and phase transfer. These results illustrated the important role of the water solubility of the initiator in determining the main loci of polymerization and the crucial role of the hydrophobicity of the RAFT agent for efficient transportation to the polymer particles. In summary, these experimental data demonstrate that for an optimum control during ab-initio batch heterophase polymerization of styrene with RAFT, the RAFT agent must have a certain hydrophilicity as it is given for BDA and the initiator must be water soluble in order to minimize reactions in the monomer phase.

In the second part of this work an analytical method was developed for the quantitative measurements of the sorption of the RAFT agents to the polymer particles. This method is based on the absorption of the visible light by the RAFT

agent or any other organic molecule under study. Polymer nanoparticles, temperature, and stirring are employed to simulate the conditions of a typical aqueous heterophase polymerization system. The results of this study suggested the order of BDA>BDB>PhEDB=CDB for the rate of transportation of the RAFT agents to the particles. These results confirmed the role of the hydrophilicity of the RAFT agent on the effectiveness of the control due to its fast transportation to the polymer particles during the initial period of polymerization after particle nucleation. As the presence of the polymer particles were essential for the transportation of the RAFT agents into the polymer dispersion, it is concluded that in an ab initio emulsion polymerization the transport of the hydrophobic RAFT agent only takes place after the nucleation and formation of the polymer particles. Therefore, as the swelling theory suggests, while the polymerization proceeds and the particles grow the rate of the transportation of the RAFT agent increases with conversion until the free monomer phase disappears.

The degradation of the RAFT agent by addition of KPS initiator revealed unambiguous evidence on the mechanism of entry in heterophase polymerization. These results showed that even extremely hydrophilic primary radicals, such as sulfate ion radical stemming from the KPS initiator, can enter the polymer particles without necessarily having propagated and reached a certain chain length. Moreover, these results recommend the employment of azo-initiators instead of persulfates for the application in seeded heterophase polymerization with RAFT agents.

The significant slower rate of transportation of the RAFT agent to the polymer particles when its solvent (styrene) was replaced with a more hydrophilic monomer (methyl methacrylate) lead to the conclusion that a complicated cooperative and competitive interplay of solubility parameters and interaction parameter with the particles exist, determining an effective transportation of the organic molecules to the polymer particles through the aqueous phase. The choice of proper solutions of even the most hydrophobic organic molecules can

provide the opportunity of their sorption into the polymer particles. Examples to support this idea were given by loading the extremely stiff fluorescent molecule, pentacene, and very hydrophobic dye, Sudan IV, into the polymer particles.

Finally, the first application of RAFT at room temperature heterophase polymerization is reported. These results show that the RAFT process is effective at ambient temperature; however, the rate of fragmentation is significantly slower. The elevation of the reaction temperature in the presence of the RAFT agent resulted in faster polymerization and higher molar mass, suggesting that the fragmentation rate coefficient and its dependence on the temperature is responsible for the observed retardation.

All in all, these results provide some insight on the mechanisms involved in the aqueous heterophase polymerization, especially in controlled radical polymerization via RAFT. Moreover, the results allow –at the moment still theoretical- designing of an optimized procedure for controlled aqueous heterophase polymerization via RAFT. The method of choice would be a seed polymerization. Before starting the monomer feed, the seed particles should be swollen with a RAFT agent-monomer solution. The optimum free radical initiator should be a water soluble initiator decomposing into carbon radicals.

The investigation for further understanding of RAFT-mediated aqueous heterophase system may involve studying the influence of the RAFT agent's structure on the colloidal stability of the polymer particles since the majority of the end groups are provided by the RAFT agent's leaving group. Since a very important application of the controlled radical polymerization is the capability to produce well-defined block-copolymers, the future work can aim at the development of optimum feeding techniques for the preparation of colloidal particles with sophisticated composite structures through controlled radical polymerization in the heterophase system. Development of new nanoscale colloidal particles with distinct colloidal, molecular, and surface structures



contributes to the present generation of novel materials whose properties are well under our control.

## Appendix

### Appendix I: Categorized Library of Results

A complete dataset is made available for the ab initio emulsion polymerization of styrene at 80°C initiated with four types of initiators and in the presence of four types of RAFT agents. In chapter 4.2 only examples of these data were selected for discussion. Here, for further reference, a categorized set of graphs demonstrates the influence of varying the type of initiator and RAFT agent on the rate of polymerization, molecular weight, molecular weight distribution and the particle size during the whole course of the polymerization. The results of polymerizations initiated with AIBN are presented separately in section I.4.B. Here is how the results are presented:

#### I.1. Rate of polymerization

I.1.A. Organized for each type of initiator

I.1.B. Organized for each type of RAFT agent

#### I.2. Number average molecular weight, polydispersity, particle size

I.2.A. Organized for each type of initiator

I.2.B. Organized for each type of RAFT agent

#### I.3. Evolution of molecular weight distributions

#### I.4. AIBN

I.4.A. Molecular weight distributions

I.4.B. conversion-time and particle size-conversion plots for different RAFT agents

## I.1. Rate of polymerization

### I.1.A. Organized for each type of initiator

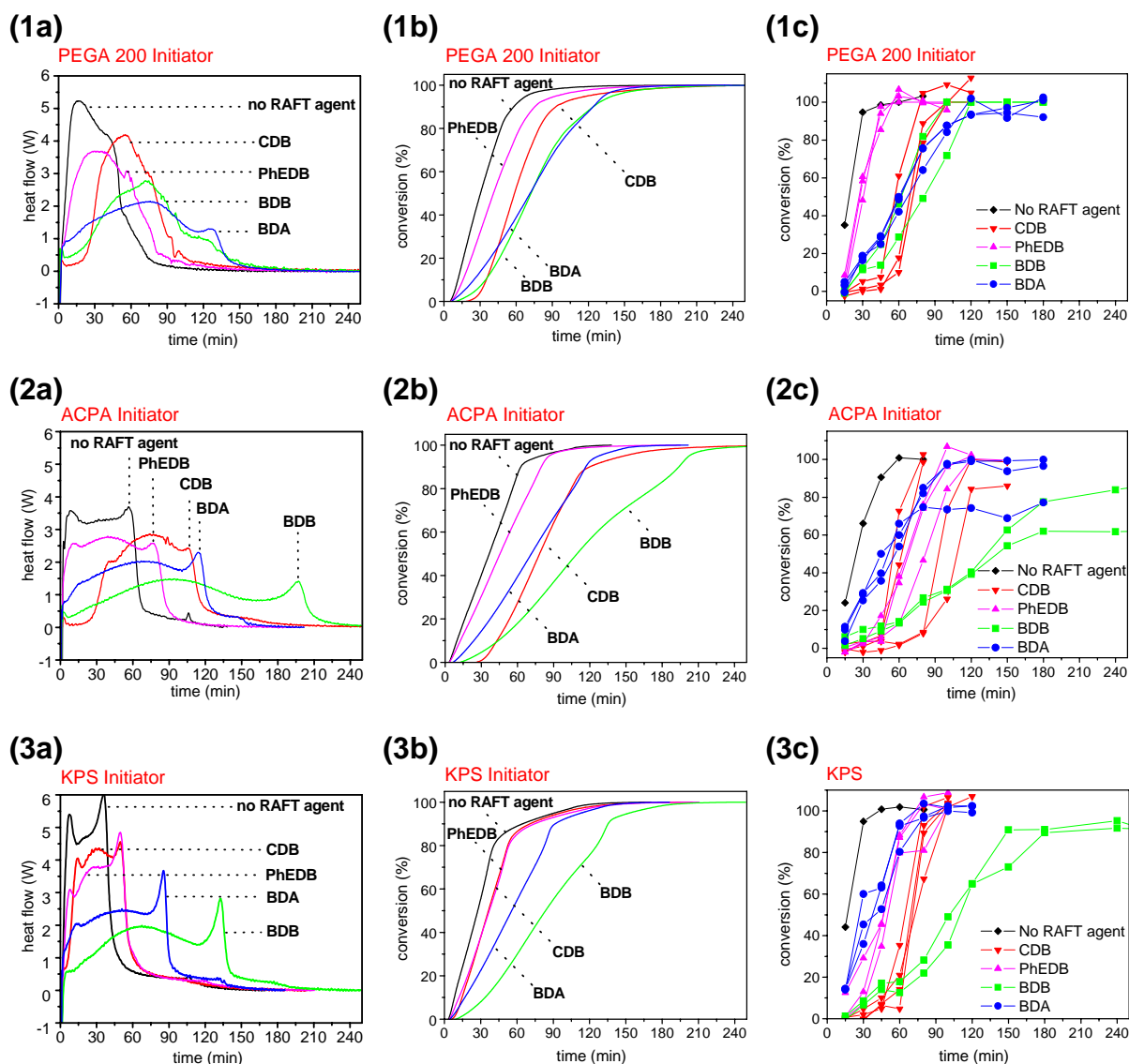


Figure 1. Ab-initio emulsion polymerization of styrene at 80°C in presence of various RAFT agents and initiated with (1) PEGA 200 (2) ACPA (3) KPS, (a) reaction rate profiles as obtained directly by reaction calorimetry, (b) conversion-time plots integrated from gravimetric measurements of the samples taken during polymerization in all-glass reactor

## I.1.B. Organized for each type of RAFT agent

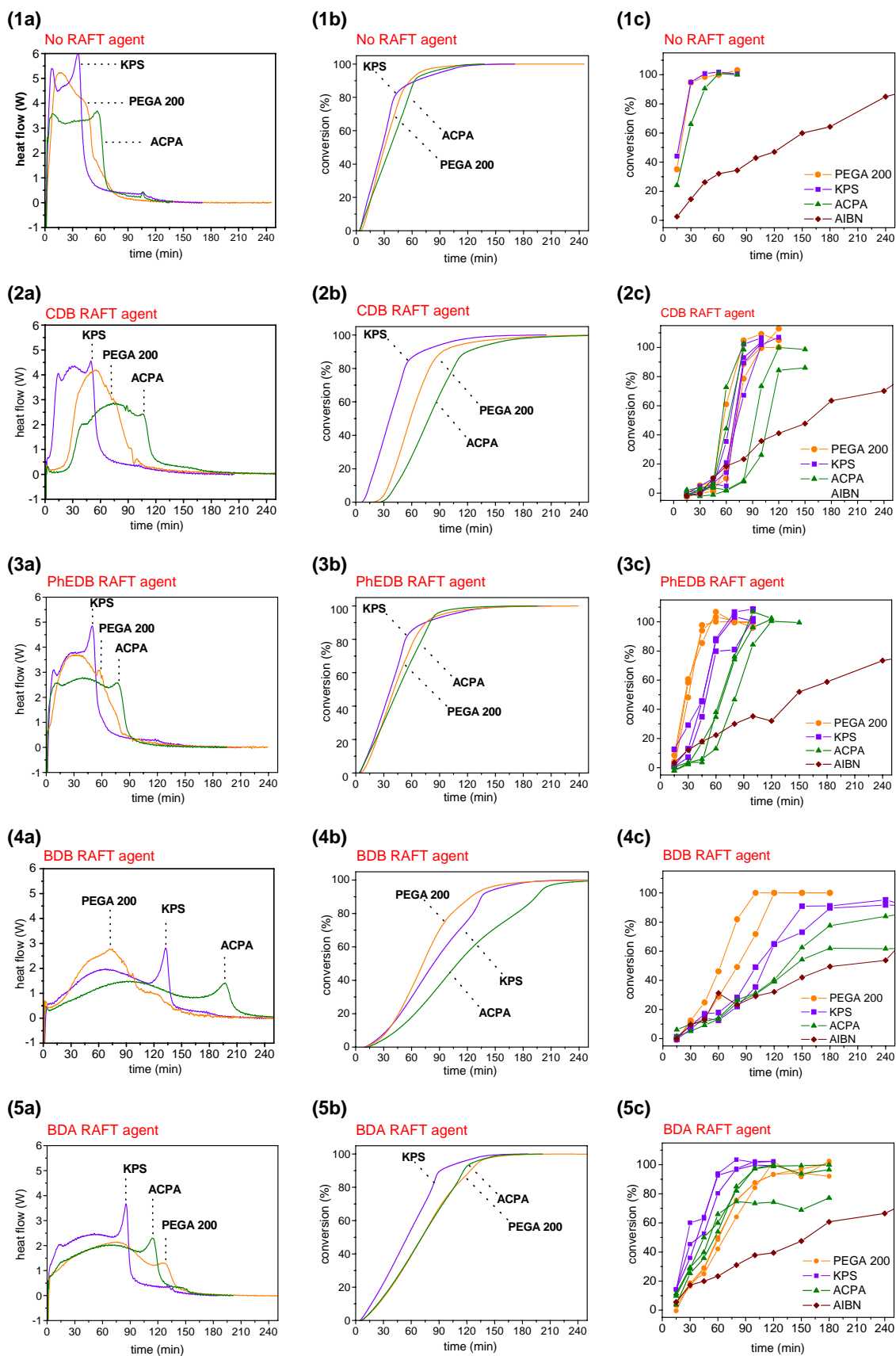
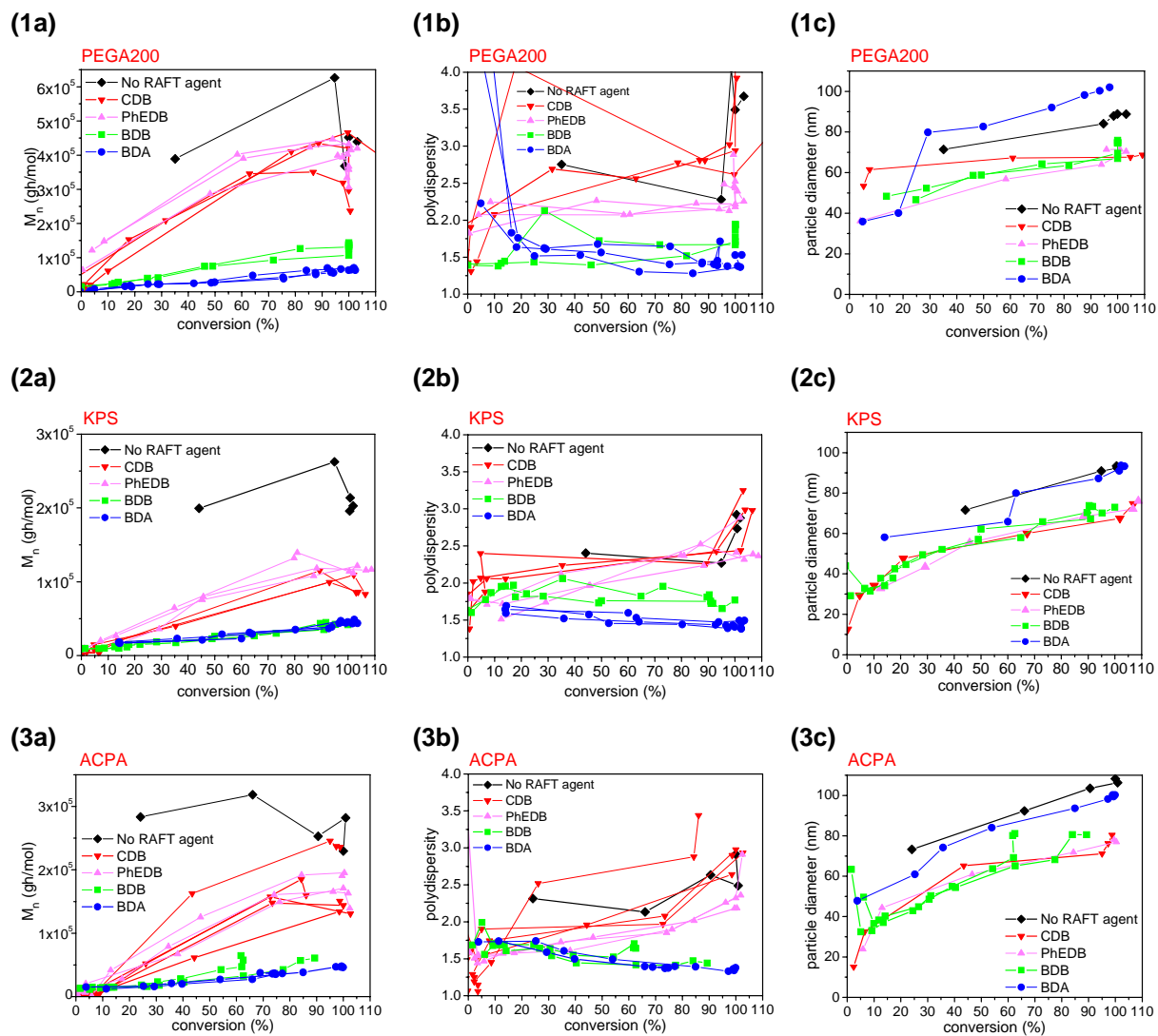


Figure 2. (a) reaction rate profiles by reaction calorimetry, (b) conversion-time plots by reaction calorimetry (c) conversion-time plots by gravimetry

## I.2. Number average molecular weight, polydispersity, particle size

## I.2.A. Organized for each type of initiator



**Figure 3. Evolution of (a) number average molecular weight, (b) polydispersity, and (c) the particle size during the ab-initio emulsion polymerization of styrene at 80°C in presence of various RAFT agents and initiated with (1) PEGA 200 (2) KPS (3) ACPA**

## I.2.B. Organized for each type of RAFT agent

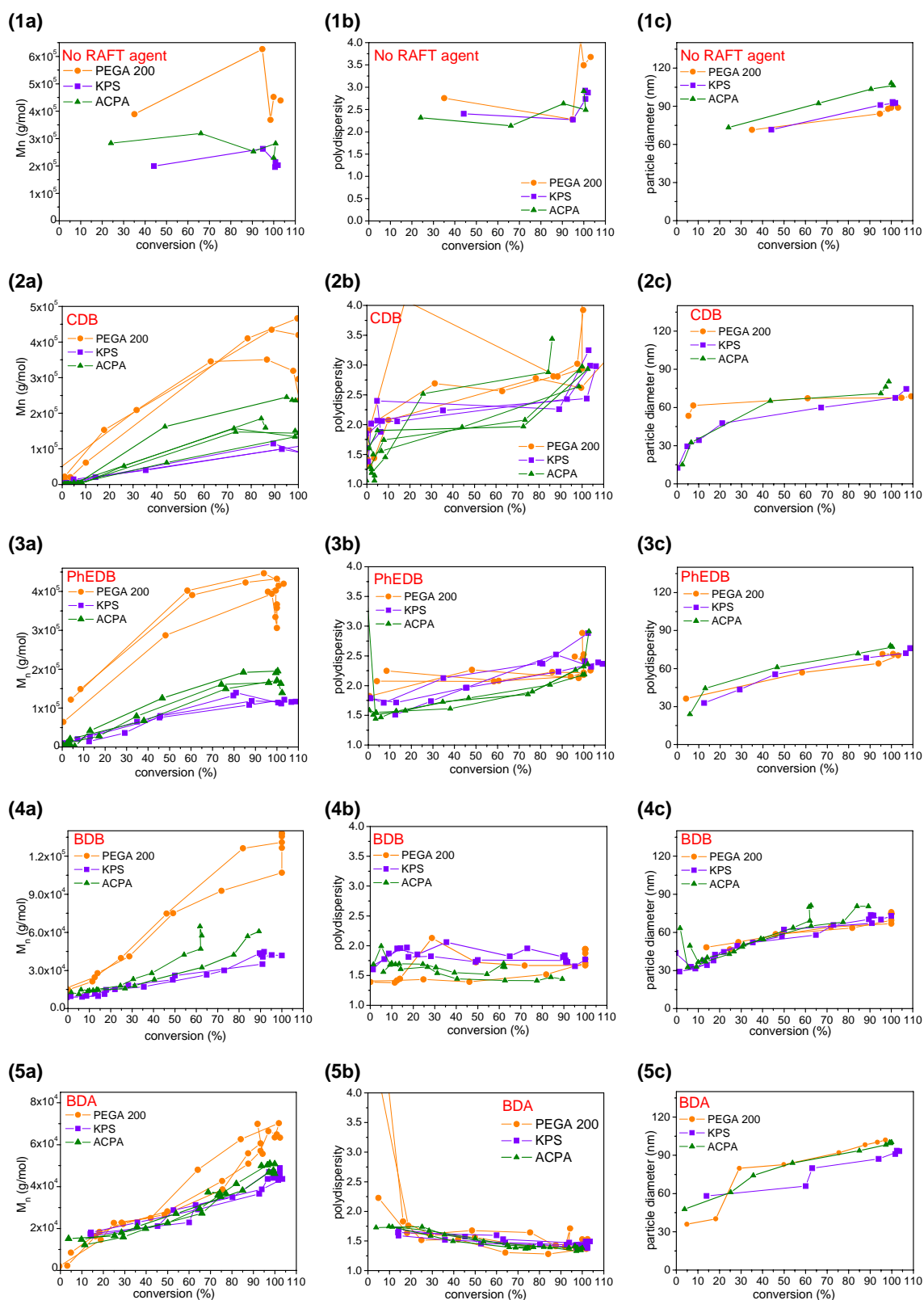
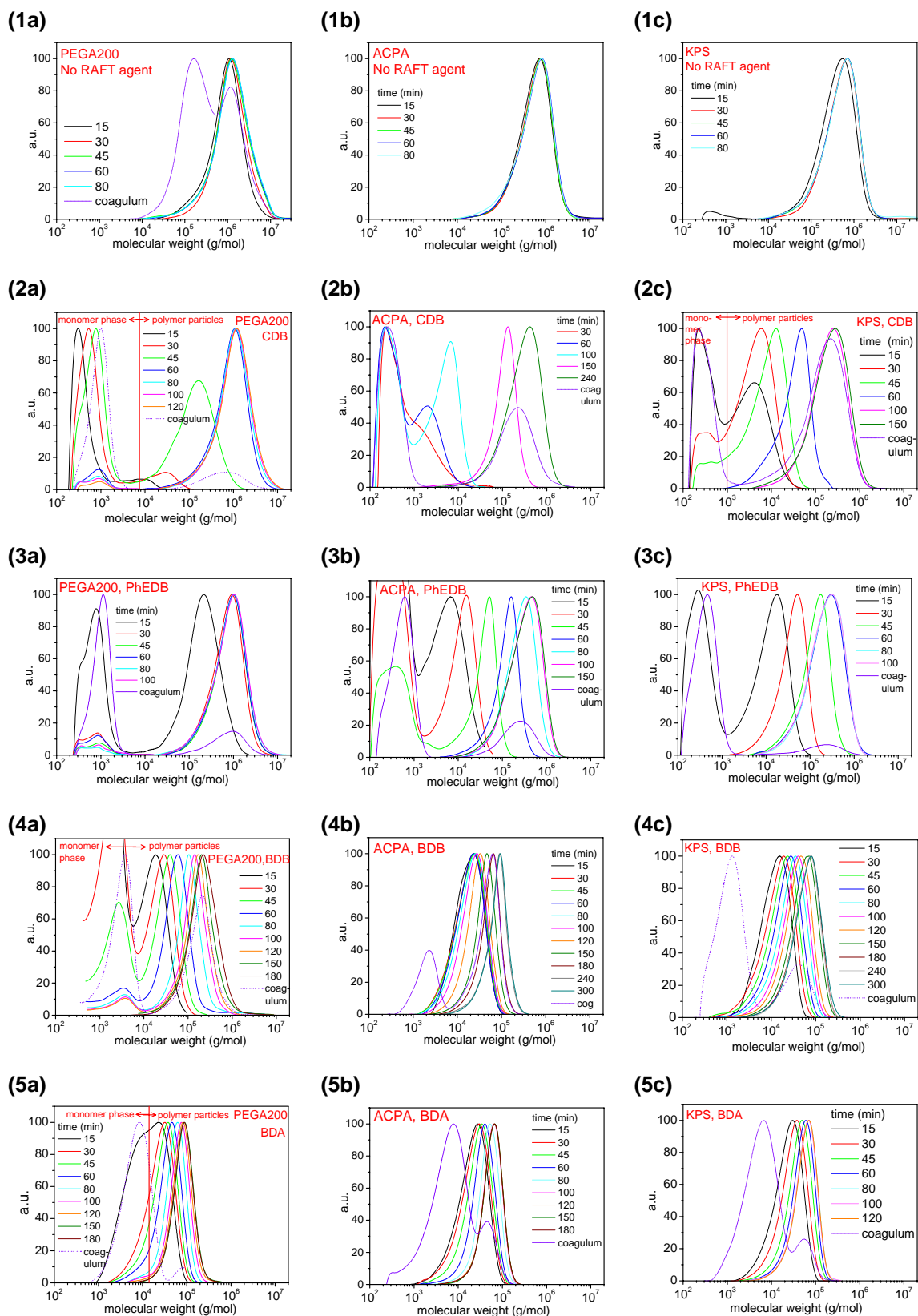


Figure 4. Evolution of (a) number average molecular weight, (b) polydispersity, and (c) the particle size for different type of RAFT agents: (1) none (2) CDB (3) PhEDB (4) BDB (5) BDA

## I.3. Evolution of molecular weight distributions



**Figure 5. Molecular weight distributions for different type of initiators: (a) PEGA200 (b) ACPA (c) KPS, and for different type of RAFT agents: (1) none (2) CDB (3) PhEDB (4) BDB (5) BDA**

## I.4. AIBN

## I.4.A. Molecular weight distributions

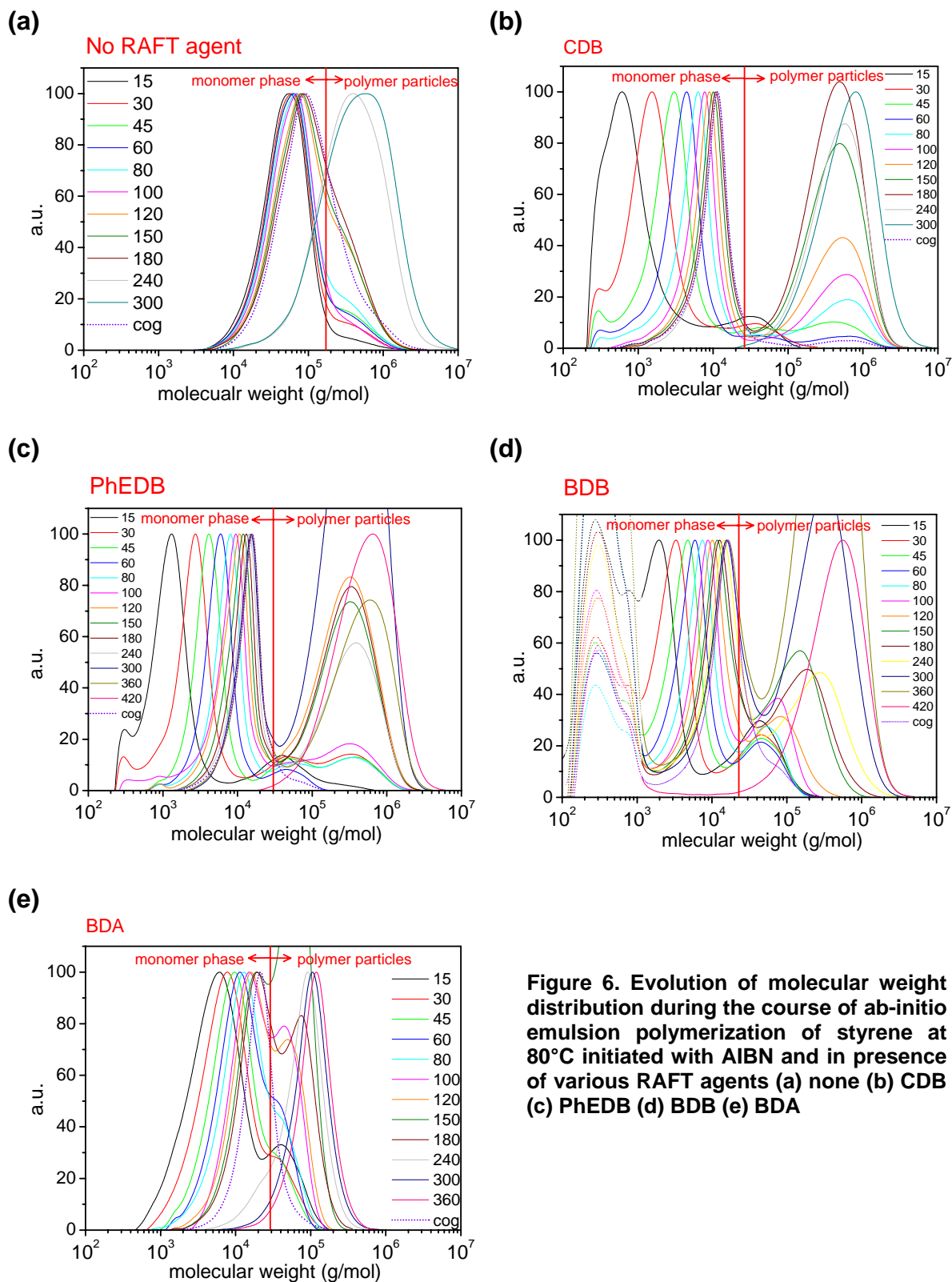


**Figure 6. Evolution of molecular weight distribution during the course of ab-initio emulsion polymerization of styrene at 80°C initiated with AIBN and in presence of various RAFT agents (a) none (b) CDB (c) PhEDB (d) BDB (e) BDA**



## I.4.B. conversion-time and particle size-conversion plots for different RAFT agents

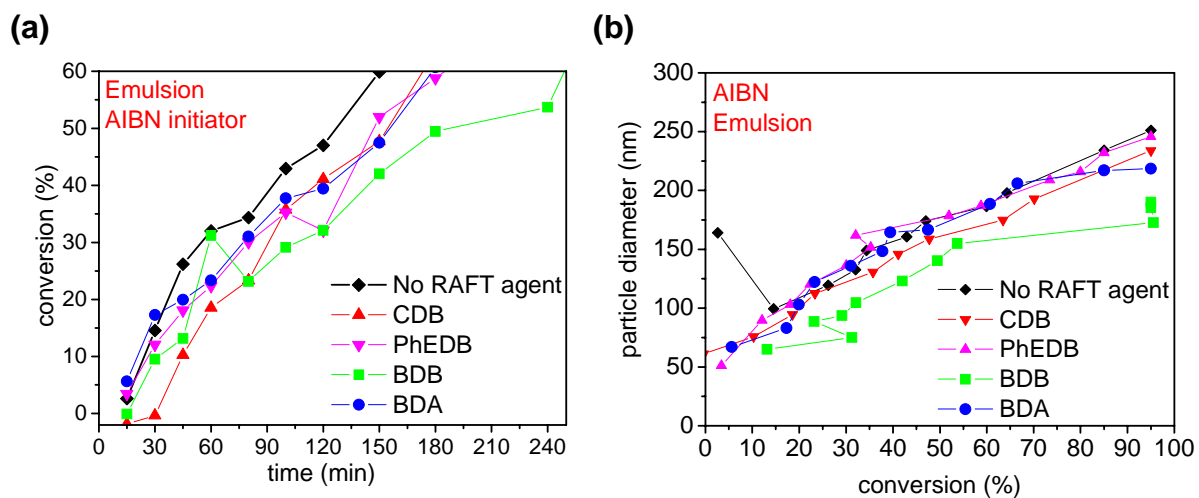


Figure 7. (a) conversion-time plot (b) evolution of particle size with conversion during the course of ab-initio emulsion polymerization of styrene at 80°C initiated with AIBN and in presence of various RAFT agents

## **Appendix II: Experimental Section**

### II.1. The Instruments

### II.2. The Chemicals

### II.3. The Procedures

II.3.A. Bulk, solution, and ab initio emulsion polymerization of styrene

II.3.B. UV-Vis investigation on the Phase transfer of the RAFT agents

II.3.C. Room temperature polymerizations

### **II.1. The Instruments**

#### **Reaction Calorimetry**

The polymerizations were carried out isothermally in a pre-calibrated reaction calorimeter CPA 200 from ChemiSens (Lund, Sweden) with a 200 ml reactor equipped with a stainless steel stirrer and a heating facility through the reactor bottom.

#### **Rotational Thermostat**

The room temperature polymerizations were carried out in the rotational thermostat VLM20 (VLM GmbH, Leopoldshöhe, Germany).

#### **Gravimetric Measurements**

The latexes were characterized regarding solids content with a HR73 Halogen Moisture Analyzer (Mettler Toledo).

### **Gel Permeation Chromatography (GPC)**

Molecular weight distributions were determined by gel permeation chromatography (GPC) and used to calculate weight and number average molecular weights ( $M_w$ ,  $M_n$ ). GPC was carried out by injecting 100  $\mu$ l of about 0.15 wt.-% polymer solutions (solvent tetrahydrofuran) through a Teflon-filter with a mesh size of 450 nm into a Thermo Separation Products set-up being equipped with ultra violet (UV) (TSP UV1000) and refractive index (RI) (Shodex RI-71) detectors in THF at 30 °C with a flow rate of 1 ml per minute. A column set was employed consisting of three 300 x 8 mm columns filled with a MZ-SDplus spherical polystyrene gel (average particle size 5  $\mu$ m) having a pore size of  $10^3$ ,  $10^5$ , and  $10^6$  Å, respectively. This column set allows a resolution down to molecular weights less than 500 g mol<sup>-1</sup>. Molecular weights and molecular weight distributions were calculated based on polystyrene standards (between 500 and 2·10<sup>6</sup> g mol<sup>-1</sup> from PSS, Mainz, Germany).

### **Dynamic Light Scattering**

The average particle size (intensity weighted diameter) was characterized by dynamic light scattering. A Nicomp particle sizer (model 370, PSS Santa Barbara, USA) at a fixed scattering angle of 90° was used.

### **Ultra-Violet/Visible (UV-Vis) Spectroscopy**

A special port for a UV-Vis immersion probe from Hellma (Müllheim / Baden, Germany) with an optical path length of 10 mm connected with a glass fiber optics to a UV-Vis spectrometer Specord 30 (Analytik Jena GmbH, Germany) was used for all the measurements regarding the phase transfer.

## Fluorescence Spectroscopy

Steady state fluorescence spectra were recorded on a Perkin-Elmer LS50B luminescence spectrometer. Emission spectra were recorded in the range of 320 to 560 nm with an excitation wavelength  $\lambda_{\text{exc}} = 290$  nm. The excitation and emission bandwidths were both 4 nm.

## Nuclear Magnetic Resonance (NMR)

NMR was used for characterization of the synthesized RAFT agents. The spectra were recorded on a Bruker DPX-400 Spectrometer at 400MHz.

## Elemental Analysis

Elemental analyses (C, H, N, S) were performed on a Vario EL Elementar (Elementar Analysen-systeme, Hanau, Germany).

## II.2. The Chemicals

- Water was taken from a Seral purification system (PURELAB Plus™) with a conductivity of  $0.06 \mu\text{S cm}^{-1}$  and degassed prior to use
- Styrene, methyl methacrylate, and ethyl benzene were distilled under reduced pressure
- Petrol ether, methanol, Dimethylformamide (DMF), Amoniak solution, 4,4'-azobis (4-cyanopentanoic acid) (ACPA), potassium peroxodisulfate (KPS), sodium dodecyl sulfate (SDS) were used as received.
- AIBN was recrystallized from methanol before use.
- PEGA200 had been synthesized as described elsewhere<sup>110</sup>.

- All the RAFT agents: benzyl dithioacetate (BDA), benzyl dithiobenzoate (BDB), phenyl ethyl dithiobenzoate (PhEDB), and cumyl dithiobenzoate (CDB) were synthesized and purified as described elsewhere<sup>9</sup>.
- Polystyrene nanoparticles (~34 nm diameter) had been synthesized as described elsewhere<sup>111</sup> by another PhD candidate<sup>101</sup>.

### **II.3. The Procedures**

#### **II.3.A. Bulk, solution, and ab initio emulsion polymerization of styrene**

All the polymerizations were carried out under similar conditions regarding temperature (80°C), stirring speed (300 rpm), amount of styrene (20 g), initiator ( $3.41 \times 10^{-4}$  mol), and RAFT agent ( $4.26 \times 10^{-4}$  mol).

#### **Polymerizations in Bulk**

The polymerizations were carried out in 100 ml three-neck reaction flasks equipped with nitrogen inlet, condenser, cooling thermostat, and oil bath. The temperature of the oil bath was maintained at 80°C using heating plate, and contact thermometer. Magnetic stirrer was used for stirring.

A solution of the RAFT agent in 15 g of styrene was charged into the reaction vessel. It was stirred for 20 min while purging nitrogen and then it was heated to 80°C. After few minutes of thermal equilibration the solution of AIBN initiator in 5g of styrene was added and the reaction started. The Nitrogen flow, the 80°C temperature, and 300 rpm stirring were maintained for the whole period of polymerization until the conversion above 50% was achieved and the reaction was stopped.

Samples were taken at specific intervals. A portion of the samples was dropped into excess amount of Methanol to precipitate. After separation and drying the

polymer, it was prepared for GPC analysis. The other portion of the samples was analyzed for the solid content by the moisture analyzer.

### **Polymerizations in solution**

The solution polymerizations were carried out in exactly same setup as for bulk polymerizations. All the polymerization and sample preparation procedure was also same except that at the beginning of the polymerization all the 20 g of styrene was charged into the reactor and the initiator was dissolved in 10g DMF prior addition to the reaction mixture.

Since KPS does not dissolve in DMF, a complex of KPS with CTAB was used instead. The complex was prepared by mixing the two aqueous solutions of KPS and CTAB together, and then filtering and drying the precipitate in a vacuum oven. The correct chemical composition was ensured by elemental analysis.

### **Ab initio emulsion polymerization of styrene**

#### **(a) In all-glass reactors**

Ab initio emulsion polymerizations in all glass reactors were carried out in four-neck double jacketed reactors equipped with nitrogen inlet, condenser, mechanical stirrer, and heating and cooling thermostat.

70 g water and 4 g aqueous solution of SDS (5 wt. %) were charged into the reaction vessel. This solution was stirred and heated to 80°C for 30 min while purging nitrogen and then the solution of RAFT agent in styrene was added. After 5 min of thermal equilibration, the solution of initiator in 10 g of water was added and the reaction started. The Nitrogen flow, the 80°C temperature, and the 300 rpm stirring speed were maintained for the whole course of polymerization

reaction until the gravimetric measurements indicated the full conversion. The product was collected for the further analysis.

Samples were taken at specific intervals. A portion of the sample was analyzed for the solids content by the moisture analyzer. A drop of the sample was poured into DLS vials for particle size measurement. And another portion of each sample was dropped into excess amount of petroleum ether to precipitate. After separation of polymer and drying it in the oven, it was prepared for GPC analysis.

### **(b) In calorimeter reactor**

70 g water and 4 g aqueous solution of SDS (5 wt. %) were charged into the reaction vessel. Nitrogen was purged in this solution for about 30 min outside of the heating bath. Then the solution of RAFT agent in 20 g of styrene monomer was added and the reactor top was closed. The reactor was weighed at this time and slowly located in the heating bath and while stirring at 300 rpm it was heated to 80°C. Before the power temperature arrived to zero and the reference temperature to 80°C the solution of initiator in 10 g of water was charged into a long needle syringe and was located in the heating bath for temperature equilibration. After 15 min it was inserted into the reactor. The time was recorded and the reaction started. The 80°C temperature and the 300 rpm stirring speed were maintained for the whole reaction period. When the reaction ended the reaction vessel was weighed again\* and the product was collected for further analysis.

\* The reactor was weighed before and after the reaction to ensure no water was leaked into the reactor from the heating bath.

### **II.3.B. UV-Vis investigation on the Phase transfer of the RAFT agents**

The investigation was carried out in an especially built reactor equipped with condenser, mechanical stirrer, and heating and cooling jacket. An extra neck on the side of the reactor allowed placing the special port for the UV-vis immersion probe.

The reactor was filled with 200 g of polystyrene dispersion containing polystyrene nanoparticles with solids content of 0.425 wt.-% (or 0.85 g of PS-seed in total) corresponding to a total seed particle number of  $3.6 \cdot 10^{16}$  or  $1.8 \cdot 10^{14}$  per  $\text{cm}^3$  of water. This combination of size and concentration of the seed particles causes a turbidity in the reactor, which turned out to be optimum for absorption measurements. To achieve a complete uptake of the organic phase during the sorption experiments a solution of  $2 \cdot 10^{-4}$  moles of RAFT agent in 0.74 g of styrene (or 0.71 g ethyl benzene, or 0.77g MMA) was placed on top of the dispersion inside the reactor. Before depositing the solution the dispersion was heated to 70 °C and the absorption baseline was measured after thermal equilibration. This procedure makes sure that almost all changes measured are due to the sorption process. The stirrer speed was adjusted to about 50 rpm, which is just enough to sufficiently mix the seed particles but not to disperse the organic phase. During the experiment the absorption was measured every 5 (or 10) minutes in the wavelength range between 300 and 800 nm.

After all the RAFT agent solution was absorbed into the polymer particles and no solution was left on top, and after a period of equilibrium, 2 g aqueous solution of KPS (79.63 mM) was added to the dispersion in order to start and study the polymerization.



### II.3.C. Room temperature polymerizations

All ingredients were added in the following order: 10 g of water (0.556 mol), 100 mg of SDS ( $3.47 \times 10^{-4}$  mol), a solution of 0.028g RAFT agent BDA ( $1.536 \times 10^{-4}$  mol) in 635 mg or 670  $\mu$ l styrene monomer ( $6.1 \times 10^{-3}$  mol), and  $1.22 \times 10^{-4}$  mol initiator (AIBN or KPS) into glass vials (Duran glass, Schott, Germany) of about 15 ml volume (i.d. 12 mm, o.d. 16 mm, height 160 mm). Then the glass vial was screw closed with a Teflon sealing and placed in the rotation thermostat at temperature of 25 °C, and the rotation speed was set to about 15 rpm. In the rotation thermostat 24 vials could be placed simultaneously. After certain time intervals the rotation thermostat was stopped, and a vial was withdrawn for analytics.

#### Temperature variation:

Exactly same procedure was repeated for reaction temperatures of 30, 35, and 40 °C.

#### Initiator concentration variation:

Exactly same procedure was repeated for Initiator concentrations of:  $2.44 \times 10^{-4}$ ,  $6.1 \times 10^{-5}$ , and  $3.05 \times 10^{-5}$ .

### Appendix III: References

1. Staudinger, H. *Berichte der Deutschen Chemischen Gesellschaft* **1920**, 1073-1085.
2. Moad, G.; Solomon, D. H. *The Chemistry of Free Radical Polymerization*; Pergamon: New York, 1995.
3. Veregin, R. P. N.; Georges, M. K.; Kazmaier, P. M.; Hamer, G. K. *Macromolecules* **1993**, 26, 5316-5320.
4. Georges, M. K.; Veregin, R. P. N.; Kazmaier, P. M.; Hamer, G. M. *Macromolecules* **1993**, 26, 2987-2988.
5. Solomon, D. H.; Rizzardo, E.; Cacioli, P. *European Patent 135280A2 (1985) US Patent 4581429*, 1985.
6. Kato, M.; Kamigaito, M.; Sawamoto, M.; Hifashimura, T. *Macromolecules* **1995**, 28, 1721-1723.
7. Wang, J. S.; Matyjaszewski, K. *Macromolecules* **1995**, 28, 7901.
8. Matyjaszewski, K.; Patten, T. E.; Xia, J. *Journal of American Chemical Society* **1997**, 119, 674-680.
9. Le, T. P. T.; Moad, G.; Rizzardo, E.; Thang, S. H. *PCT International Application WO 9801478 A1 980115; Chem Abstr* **1998**, 115390.
10. Chiefari, J.; Chong, Y. K.; Ercole, F.; Krstina, J.; Jeffery, J.; Le, T. P. T.; Mayadunne, R. T. A.; Meijs, G. F.; Moad, C. L.; Moad, G.; Rizzardo, E.; Thang, S. H. *Macromolecules* **1998**, 31, 5559-5562.
11. Chiefari, J.; Mayadunne, R.; Moad, G.; Rizzardo, E.; Thang, S. H. *WO 99/31144* **1999**.
12. Mayadunne, R. T. A.; Rizzardo, E.; Chiefari, J.; Chong, Y. K.; Moad, G.; Thang, S. H. *Macromolecules* **1999**, 32, 6977-6980.
13. Cowie, J. M. G. *Polymers: Chemistry and Physics of Modern Materials*; Intertext Books: Aylesbury, 1973.
14. Odian, G. *Principles of Polymerization*; John Wiley & Sons, Inc.: New York, 1991.

15. Rempp, P.; Merrill, E. W. *Polymer Synthesis*, 2nd ed.; Heuthig & Wepf: Basel, Heidelberg, New York, 1991.
16. Bolland, J. L.; Melville, H. W. *Oesterreichische Chemiker-Zeitung* **1939**, *2*, 201-215.
17. Goto, A.; Fukuda, T. *Prog Polym Sci* **2004**, *29*, 329-385.
18. Fischer, H., "Criteria for Livingness and Control in Nitroxide-Mediated and Related Radical Polymerizations". In *Acs Sym Ser*; Matyjaszewski, K., Ed.: Washington D.C., 2003; Vol. 854, pp 10-23.
19. Krstina, J.; Moad, G.; Rizzardo, E.; Winzor, C. L. *Macromolecules* **1995**, *28*, 5381-5385.
20. Krstina, J.; Moad, C. L.; Moad, G.; Rizzardo, E. *Macromol Symp* **1996**, *111*, 13-23.
21. Moad, G.; Moad, C. L.; Rizzardo, E.; Thang, S. *Macromolecules* **1996**, *29*, 7717-7726.
22. Mayadunne, R. T. A.; Rizzardo, E.; Chiefari, J.; Krstina, J.; Moad, G.; Postma, A.; Thang, S. H. *Macromolecules* **2000**, *33*, 243-245.
23. Chong, Y. K.; Le, T. P. T.; Moad, G.; Rizzardo, E.; Thang, S. H. *Macromolecules* **1999**, *32*, 2071-2074.
24. Rizzardo, E.; Chiefari, J.; Chong, B. Y. K.; Ercole, F.; Krstina, J.; Jeffery, J.; Le, T. P. T.; Mayadunne, R. T. A.; Meijs, G. F.; Moad, C. L.; Moad, G.; Thang, S. H. *Macromol Symp* **1999**, *143*, 291-307.
25. Rizzardo, E.; Chiefari, J.; Mayadunne, R. T. A.; Moad, G.; Thang, S. H., "Synthesis of defined polymers by reversible addition-fragmentation chain transfer: the RAFT process". In *Controlled/living radical polymerization; progress in ATRP, NMP, and RAFT*; American Chemical Society, 2000; pp 278-296.
26. Moad, G.; Chiefari, J.; Chong, Y. K.; Krstina, J.; Mayadunne, R. T. A.; Postma, A.; Rizzardo, E.; Thang, S. H. *Polym Int* **2000**, *49*, 993-1001.
27. Goto, A.; Sato, K.; Tsujii, Y.; Fukuda, T.; Moad, G.; Rizzardo, E.; Thang, S. H. *Macromolecules* **2001**, *34*, 402-408.

28. Barner-Kowollik, C.; Quinn, J. F.; Nguyen, T. L. U.; Heuts, J. P. A.; Davis, T. P. *Macromolecules* **2001**, *34*, 7849-7857.
29. Ladaviere, C.; Dorr, N.; Claverie, J. P. *Macromolecules* **2001**, *34*, 5370-5372.
30. Chiefari, J.; Mayadunne, R. T. A.; Moad, C. L.; Moad, G.; Rizzardo, E.; Postma, A.; Skidmore, M. A.; Thang, S. H. *Macromolecules* **2003**, *36*, 2273-2283.
31. Chong, Y. K.; Krstina, J.; Le, T. P. T.; Moad, G.; Postma, A.; Rizzardo, E.; Thang, S. H. *Macromolecules* **2003**, *36*, 2256-2272.
32. Destarac, M.; Taton, D.; Zard, S. Z.; Saleh, T.; Six, Y. *Acs Sym Ser* **2003**, *854*, 536-550.
33. Davis, T. P.; Barner-Kowollik, C.; Nguyen, T. L. U.; Stenzel, M. H.; Quinn, J. F.; Vana, P. *Acs Sym Ser* **2003**, *854*, 551-569.
34. Adamy, M.; van Herk, A. M.; Destarac, M.; Monteiro, M. J. *Macromolecules* **2003**, *36*, 2293-2301.
35. Boutevin, B. *J Polym Sci Pol Chem* **2000**, *38*, 3235-3243.
36. Monteiro, M. J.; de Brouwer, H. *Macromolecules* **2001**, *34*, 349-352.
37. Coote, M. L. *Macromolecules* **2004**, *37*, 5023-5031.
38. Kwak, Y.; Goto, A.; Komatsu, K.; Sugiura, Y.; Fukuda, T. *Macromolecules* **2004**, *37*, 4434-4440.
39. Kwak, Y.; Goto, A.; Fukuda, T. *Macromolecules* **2004**, *37*, 1219-1225.
40. Toy, A. A.; Vana, P.; Davis, T. P.; Barner-Kowollik, C. *Macromolecules* **2004**, *37*, 744-751.
41. Vana, P.; Davis, T. P.; Barner-Kowollik, C. *Macromol Theor Simul* **2002**, *11*, 823-835.
42. Gilbert, R. G. *Emulsion Polymerization - A mechanistic Approach*; Academic Press: London, 1995.
43. Fitch, R. M. *Polymer Colloids: A Comprehensive Introduction*; Academic Press: San Diego, 1997.
44. Lovell, P. A.; El-Aasser, A. S. *Emulsion Polymerization and Emulsion Polymers*; Wiley: New York, 1997.

45. Tauer, K., "Heterophase polymerization". In *Encyclopedia of Polymer Science and Technology*, Third Edition. Kroschwitz, J. I., Ed.; Wiley-Interscience: New York, 2003.
46. Fitch, R. M.; Tsai, C. H. *Polymer Letters* **1970**, *8*, 703-710.
47. Fitch, R. M.; Tsai, C. H., In *Polymer Colloids*; Fitch, R. M., Ed.; Plenum Press: New York, 1971; pp 73-102.
48. Tauer, K.; Kuhn, I. *Macromolecules* **1995**, *28*, 2236-2239.
49. Tauer, K.; Kuhn, I., "Particle nucleation at the beginning of emulsion polymerization". In *Polymeric Dispersions: Principles and Applications*; Asua, J. M., Ed.; Kluwer Academic Publisher: Dordrecht, 1997; pp 49-65.
50. Harkins, W. D. *Journal of Polymer Science V* **1950**, 217-251.
51. Fitch, R. M.; Tsai, C. H., In *Polymer Colloids*; Fitch, R. M., Ed.; Plenum Press: New York, 1973; pp 73-102.
52. Asua, J. M. *Prog Polym Sci* **2002**, *27*, 1283-1346.
53. Tauer, K.; Kuhn, I.; Kaspar, H. *Prog Polym Sci* **1996**, *101*, 30-37.
54. Tauer, K.; Kaspar, H.; Antonietti, M. *Colloid Polym Sci* **2000**, *278*, 814-820.
55. Antonietti, M.; Kaspar, H.; Tauer, K. *Langmuir* **1996**, *12*, 6211-6217.
56. Morton, M.; Kaizerman, S.; Altier, M. *Journal of Colloid Science* **1954**, *9*, 300-312.
57. Qiu, J.; Charleux, B.; Matyjaszewski, K. *Prog Polym Sci* **2001**, *26*, 2083-2134.
58. Cunningham, M. F. *Prog Polym Sci* **2002**, *27*, 1039-1067.
59. Uzulina, I.; Kanagasabapathy, S.; Claverie, J. *Macromol Symp* **2000**, *150*, 33-38.
60. Monteiro, M. J.; Hodgson, M.; De Brouwer, H. *J Polym Sci Pol Chem* **2000**, *38*, 3864-3874.
61. Prescott, S. W.; Ballard, M. J.; Rizzardo, E.; Gilbert, R. G. *Macromolecules* **2002**, *35*, 5417-5425.
62. Smulders, W.; Gilbert, R. G.; Monteiro, M. J. *Macromolecules* **2003**, *36*, 4309-4318.

63. Smulders, W.; Monteiro, M. J. *Macromolecules* **2004**, *37*, 4474-4483.
64. de Brouwer, H.; Tsavalas, J. G.; Schork, F. J.; Monteiro, M. J. *Macromolecules* **2000**, *33*, 9239-9246.
65. Butte, A.; Storti, G.; Morbidelli, M. *Macromolecules* **2001**, *34*, 5885-5896.
66. Tsavalas, J. G.; Schork, F. J.; de Brouwer, H.; Monteiro, M. J. *Macromolecules* **2001**, *34*, 3938-3946.
67. Lansalot, M.; Davis, T. P.; Heuts, J. P. A. *Macromolecules* **2002**, *35*, 7582-7591.
68. Smulders, W.; Jones, C. W.; Schork, F. J. *AIChE Journal* **2005**, *51*, 1009-1021.
69. Shim, S. E.; Lee, H.; Choe, S. *Macromolecules* **2004**, *37*, 5565-5571.
70. Mcleary, J. B.; Tonge, M. P.; Roos, D. D.; Sanderson, R. D.; Klumperman, B. *J Polym Sci Pol Chem* **2004**, *42*, 960-974.
71. Uzulina, I.; Gaillard, N.; Guyot, A.; Claverie, K. *Cr Chim* **2003**, *6*, 1375-1384.
72. Pham, B. T. T.; Nguyen, D.; Ferguson, C. J.; Hawckett, B. S.; Serelis, A. K.; Such, C. H. *Macromolecules* **2003**, *36*, 8907-8909.
73. Vosloo, J. J.; De Wet-Roos, D.; Tonge, M. P.; Sanderson, R. D. *Macromolecules* **2002**, *35*, 4894-4902.
74. Luo, Y. W.; Tsavalas, J. G.; Schork, F. J. *Macromolecules* **2001**, *34*, 5501-5507.
75. Kanagasabapathy, S.; Claverie, J.; Uzulina, I. *Polymer Preprints* **1999**, *40*, 1080-1081.
76. Monteiro, M. J.; Adamy, M.; Leeuwen, B. J.; van Herk, A. M.; Destarac, M. *Macromolecules* **2005**, *38*, 1538-1541.
77. Monteiro, M. J.; Sjoberg, M.; van der Vlist, J.; Gottgens, C. M. *J Polym Sci Pol Chem* **2000**, *38*, 4206-4217.
78. Monteiro, M. J.; de Barbeyrac, J. *Macromolecules* **2001**, *34*, 4416-4423.
79. Charmot, D.; Corpart, P.; Adam, H.; Zard, S. Z.; Biadatti, T.; Bouhadir, G. *Macromolecular Symposia* **2000**, *150*, 23-32.
80. Shim, S. E.; Shin, Y.; Lee, H.; Choe, S. *Polym Bull* **2003**, *51*, 209-216.

81. Shim, S. E.; Shin, Y.; Lee, H.; Jung, H. J.; Chang, Y. H.; Choe, S. *J Ind Eng Chem* **2003**, *9*, 619-628.
82. Ferguson, C. J.; Hughes, R. J.; Nguyen, D.; Pham, B. T. T.; Gilbert, R. G.; Serelis, A. K.; Such, C. H.; Hawket, B. S. *Macromolecules* **2005**, *38*, 2191-2204.
83. Ferguson, C. J.; Hughes, R. J.; Pham, B. T. T.; Hawket, B. S.; Gilbert, R. G.; Serelis, A. K.; Such, C. H. *Macromolecules* **2002**, *35*, 9243-9245.
84. Grudinina, M. M.; Aleksand'rova, E. M. *Nauchnye Doklady Vysshei Shkoly, Khimiya i Khimicheskaya Tekhnologiya* **1959**, *2*, 354-357.
85. Hergeth, W. D.; Bloss, P.; Biedenweg, F.; Abendroth, P.; Schmutzler, K.; Wartewig, S. *Makromolekulare Chemie-Macromolecular Chemistry and Physics* **1990**, *191*, 2949-2955.
86. Smiley, R. A. *Nitriles*, 3rd ed.; Wiley-Interscience: New York, 1981; Vol. 15.
87. Cheikhalard, T.; Tighzert, L.; Pascault, J. P. *Die Angewandte Makromolekulare Chemie* **1998**, *256*, 49-59.
88. Blachnik, R.; Koritnig, S.; Steinmeier, D.; wilke, A.; Feltz, A.; Reuter, H.; Stieber, E. *D'ans Lax Taschenbuch fuer Chemiker und Physiker*; Springer: Berlin, 1998; Vol. 3.
89. Tauer, K.; Antonietti, M.; Rosengarten, L.; Mueller, H. *Macromol Chem Physic* **1998**, *199*, 897-908.
90. Mertoglu, M., "The synthesis of well-defined functional homo- and block copolymers in aqueous media via reversible addition-fragmentation chain transfer (RAFT) polymerization", University of Potsdam: Faculty of Mathematics and Natural Sciences, 2004
91. Yalkowsky, S. H.; Banerjee, S. *Aqueous solubility - Methods of Estimation for Organic Compounds*; Marcel Dekker Inc.: New York, 1992, 54-61.
92. Coote, M. L.; Radom, L. *J Am Chem Soc* **2003**, *125*, 1490-1491.
93. Barner-Kowollik, C.; Quinn, J. F.; Morsley, D. R.; Davis, T. P. *J Polym Sci Pol Chem* **2001**, *39*, 1353-1365.
94. Moad, G.; Chiefari, J.; Mayadunne, R. T. A.; Moad, C. L.; Postma, A.; Rizzardo, E.; Thang, S. H. *Macromol Symp* **2002**, *182*, 65-80.

95. Kwak, Y.; Goto, A.; Tsujii, Y.; Murata, Y.; Komatsu, K.; Fukuda, T. *Macromolecules* **2002**, *35*, 3026-3029.
96. Barner-Kowollik, C.; Coote, M. L.; Davis, T. P.; Radom, L.; Vana, P. *J Polym Sci Pol Chem* **2003**, *41*, 2828-2832.
97. Wang, A. R.; Zhu, S. P.; Kwak, Y. W.; Goto, A.; Fukuda, T.; Monteiro, M. S. *J Polym Sci Pol Chem* **2003**, *41*, 2833-2839.
98. Tauer, K.; Muller, H.; Schellenberg, C.; Rosengarten, L. *Colloid and Surfaces A: Physicochemical and Engineering Aspects* **1999**, *153*, 143-151.
99. Christian, P.; Giles, M. R.; Howdle, S. M.; Major, R. C.; Hay, J. N. *Polymer* **2000**, *41*, 1251-1256.
100. Tauer, K.; Oz, N. *Macromolecules* **2004**, *37*, 5880-5888.
101. Ali, A. M. I., "PhD Thesis", University of Potsdam: Faculty of Mathematics and Natural Sciences, to be submitted summer 2005
102. Ugelstad, J.; Hansen, F. K. *Rubber Chem Technol* **1976**, *49*, 536-609.
103. Maxwell, I.; Morrison, B. R.; Napper, D. H.; Gilbert, R. G. *Macromolecules* **1991**, *24*, 1629-1640.
104. House, A. D. *House Chem. Rev.* **1962**, *62*, 185.
105. Yalkowsky, S. H.; Banerjee, S. *Aqueous solubility - Methods of Estimation for Organic Compounds*; Marcel Dekker Inc.: New York, 1992, 133.
106. Quinn, J. F.; Rizzardo, E.; Davis, T. P. *Chem Commun* **2001**, *11*, 1044-1045.
107. Barner, L.; Quinn, J. F.; Barner-Kowollik, C.; Vana, P.; Davis, T. P. *Eur Polym J* **2003**, *39*, 449-459.
108. Barner-Kowollik, C.; Vana, P.; Quinn, J. F.; Davis, T. P. *J Polym Sci Pol Chem* **2002**, *40*, 1058-1063.
109. Nozari, S.; Tauer, K. *Polymer* **2005**, *46*, 1033-1043.
110. Walz, R.; Bomer, B.; Heitz, W. *Makromolekulare Chemie-Macromolecular Chemistry and Physics* **1977**, *178*, 2527-2534.
111. Tauer, K.; Schellenberg, C.; Zimmermann, A. *Macromol Symp* **2000**, *150*, 1-12.



## Appendix IV: Symbols and Abbreviations

### Abbreviations

ACPA	4,4'-azobis (4-cyanopentanoic acid)
AIBN	2,2'-azobis-isobutyronitrile (AIBN)
ATRP	Atom Transfer Radical Polymerization
BDA	Benzyl dithioacetate
BDB	Benzyl dithiobenzoate
BPO	dibenzoyl peroxide
CDB	Cumyl dithiobenzoate
CRP	Controlled Radical Polymerization
CTAB	cetyltrimethyl ammoniumbromide
DLS	Dynamic Light Scattering
DMF	dimethyl formamide
DRI	Differential Refractometer
DT	Degenerative Transfer
FRP	Free Radical Polymerization
GPC	Gel Permeation Chromatography
KPS	potassium peroxydisulfate
MALDI-TOF	Matrix Assisted Laser Desorption Ionization Time of Flight
MW	Molecular Weight
MWD	Molecular Weight Distribution
PEGA200	poly(ethylene glycol)-azo-initiator
PDI	Polydispersity Index
PhEDB	Phenyl ethyl dithiobenzoate
RAFT	Reversible Addition-Fragmentation Transfer
SDS	Sodium dodecyl sulfate
SEC	Size Exclusion Chromatography
SFRP	Stable Free Radical Polymerization

TEMPO	2,2,6,6-tetramethylpiperidinyl-1-oxy
UV-Vis	Ultra Violet-Visible

## Symbols

A	activator
A (page 33)	surface area
A (page 40)	Amplitude
AX *	deactivated radical
$C_i$	concentration
$C_{M,P}$	concentration of monomer in the polymer particle
$C_P$	heat capacity
D	dead chain terminated by another growing radical
D (section 3.3)	diffusion coefficient
DP	degree of polymerization
$DP_n$	degree of polymerization
DR	dear chain termination by primary radicals
f	initiator efficiency
g(t)	autocorrelation function
I	initiator
I (section 3.3 & 3.4)	intensity
$(I_{RI})_i$	signal intensity for slice i
$k_a$	activation rate coefficient
$k_{act}$	activation rate coefficient
$k_{ad}$	addition rate coefficient
$k_B$	Boltzman constant
$k_c$ (page 13)	combination rate coefficient
$k_d$	decomposition rate coefficient
$k_d$ (page 13)	dissociation rate coefficient
$k_{da}$	deactivation rate coefficient

---

$k_{\text{deact}}$	deactivation rate coefficient
$k_{\text{ex}}$	exchange rate coefficient
$k_{\text{fr}}$	fragmentation rate coefficient
$k_{\text{GPC}}$	distribution coefficient
$k_i$	Initiation rate coefficient
$K_{\text{OW}}$	octanol-water partition coefficient
$k_p$	propagation rate coefficient
$k_{\text{re-i}}$	re-initiation rate coefficient
$k_t$	termination rate coefficient
$k_{\text{tc}}$	termination rate coefficient by combination
$k_{\text{td}}$	termination rate coefficient by disproportionation
$k_{\text{tr,M}}$	rate coefficient for transfer to monomer
$l$	the length of the light path
L	leaving group
M	monomer
$M_n$	number average molecular weight
$M_w$	weight average molecular weight
n (in section 3.4)	non-bonding orbital
$\bar{n}$	average number of radicals per particle
$N_A$	Avogadro number
$N_p$	Number of polymer particles
P	pressure
$P^*$	growing radicals
$P_1^*$	radical with one monomer unit
$P_n$	dead chain with n repeat units
$P_n^*$	radical with n monomer unit
P-X	dormant chain
P-X-P'^*	intermediate specie
Q	heat of reaction
$\dot{Q}$	heat flow

---

$\dot{Q}_{accu}$	accumulated heat
$\dot{Q}_{cond}$	heat flow by conduction
$\dot{Q}_{stir}$	heat flow by stirring
$\dot{Q}_{loss}$	heat loss
$r$	radius of the swollen particles
$r$ (page 32)	rate of reaction
$R^*$	primary radical
$R_H$	Hydrodynamic radius
$R_i$	rate of initiation
$R_P$	rate of polymerization
$RT$	thermal energy
$R_t$	rate of termination
$R_{tr,M}$	rate of transfer to monomer
$S_W$	water solubility
$t$	time
$T$	absolute temperature
$T_J$	temperature of the jacket
$T_R$	temperature of the reaction mixture
$U$	overall heat transfer coefficient
$V$	volume
$V_e$	elution volume
$V_i$	volume inside the pores
$V_M$	molar volume of monomer
$V_0$	exclusion volume
$V_R$	reaction volume
$X$ (page 34)	conversion
$X^*$	stable free radical
$X-L$	RAFT agent
$Z$	activating group

---

$\Gamma$	cumulant
$\Delta H_R$	change in the internal energy by reaction
$\varepsilon$	extinction coefficient
$\eta_0$	viscosity
$\nu$	kinetic chain length
$\pi$ (in section 3.4)	double-bonding orbital
$\sigma$	interfacial energy
$\sigma$ (in section 3.3)	standard deviation
$\sigma$ (in section 3.4)	single-bonding orbital
$\varphi_P$	volume fraction of polymer
$\chi$	Flory-Huggins polymer-solvent interaction parameter
$\omega$	frequency

## Acknowledgements

I would like to thank all the people whose contribution to this work was valuable:

My supervisor, Dr. sc. Klaus Tauer, for his continuous support and helpful comments all the way during this work; for providing me great opportunities to explore and learn together with him or by myself not only in the lab in Golm but also abroad.

Prof. Dr. Michael Cunningham, for the numerous discussions, the useful suggestions, and his hospitality during my stay in his research group at Queen's University, Kingston, Canada and for his permission to use the PREDICI simulation software.

Prof. Dr. Markus Antonietti, for the opportunity to do both my master and PhD thesis here and use the facilities of the Institute. In addition, I am especially thankful for his constructive comments on my thesis.

Mrs. Marlies Gräwert for an enormous number of GPC measurements, without which this work would not have been possible.

Özlem Sel not only for her help for synthesizing the RAFT agents and supplying me with the data I needed while I was writing my thesis at home, but also for her friendship and concern all the time.

Ursula Lubahn for teaching me how to work with the calorimeter and improving my German language skills through patient instruction. Silvia Pirok for measuring the particle size of many of my samples and the German lessons as well. Thanks to both of you for the support in the lab and for the flowers.

Theodora Krasia, and Murat Mertoglu for their useful tips on synthesis and purification of the RAFT agents.

Steffen Kozempel for introducing me to UV-Vis spectroscopy, translating the summary of my thesis to German on his birthday, and the most important than all, I appreciate him for bringing good mood to our office all the time.

Olaf Niemeyer, Rona Pitschke, and Antje Völkel for NMR, TEM, and preparative ultracentrifuge measurements.

Dr. Charl Faul, Dr. Helmut Schlaad, and Dr. Helmut Cölfen, for answering my questions.

In Canada, Prof. Robin Hutchinson, Marcelo Kaminski Lenzi, David Ng, Catherine Buragina, Martina Osti, Sarah McCarthy, Ryan Simms, Flora Lo, and Ben Kenney. I would like to especially thank Dave for his time introducing me to PREDICI.

A. M. Imroz Ali for producing polystyrene seed particles and Dingding He for the polymerizations at room temperature.

Ines Below and Irina Shekova for lending me laboratory glassware and Cliff Janiszewski for fixing all the glassware that I broke in the lab.

I would like to thank Özlem Sel, Nadine Nassif, Nicole Gehrke, Rumiana Dimova, Christopher Haluska, and Miles Page for their welcome distractions during the final writing of this thesis and of course, for their friendship all the time.

For their help and the good time we spent together, I would like to thank Liliana Ramirez, Cornelia Sinn, Matthieu Barrere, Rivelino Montenegro, Atul Deshpandeh, Christian Holtze, Mattijs Ten Carte, Annette Pape, Katharina Zesch

Hans Börner, Reinhard Sigel, Justyna Justynska, Matthijs Gronewolt, Mathias Meyer, Julien Polleux, Georg Garnweitner, Saroj Kumar Bhattacharyya, Hartmut Rettig, Doreen Eckhardt, Rebecca Voss, Ba Jianhua, Carlo Sarnthein, Cecile Huin, Emre Yagci, Magdalena Titirici, Helena Kaper, Philip Adelhelm.

The financial support by the German Research Society (DFG) and the Max-Planck Society (MPG) is gratefully acknowledged.

I am indebted to my parents for their encouragement and support. And finally to Sven Siefken who proofread my entire thesis, and was extremely helpful and comforting at the time of stress. I cannot thank you enough.